ABSTRACT

KIEKEBUSCH, ELSITA MARIA. Effects of Temperature, Phenology, and Geography on Butterfly Population Dynamics under Climate Change. (Under the direction of Dr. Nicholas M. Haddad.)

Global climate change caused by anthropogenic greenhouse gas emissions is increasing the risk of species extinctions worldwide. Ectotherms are likely to be particularly vulnerable because their basic physiological functions such as development and reproduction are strongly influenced by external temperature. To discern the potential magnitude of future species declines, it is thus vitally important to gain a mechanistic understanding of how temperature determines population responses.

Some of these mechanisms include the effects of temperature on survival and reproduction, the effects of temperature on developmental rates, and geographical variation in temperature. I chose two butterfly species, the Appalachian Brown (*Satyrodes appalachia*) and the Saint Francis' Satyr (*Neonympha mitchellii francisci*) to answer the following questions: 1) How will projected warming affect population growth rates of *S. appalachia*? 2) How will temperature and phenology combine to affect growth rates of *S. appalachia*? 3) How do *S. appalachia* survival rate responses to warming compare across a mid-latitude species' range? 4) How can machine learning be used to optimize models to predict phenology of *N. mitchellii francisci* under different emissions scenarios?

I carried out field warming experiments at all annual life stages of *S. appalachia* to fit functions describing survival and reproductive rates under a range of increased temperatures. I developed a population model based on these vital rate responses and downscaled climate datasets to project future population growth rates under the RCP 8.5 "business as usual" emissions scenario. The model projected that annual growth rates will shift from growing to

shrinking in the 2060s, and when predation was incorporated into the model, shrinking occurred by the late 2020s. My findings suggest population declines for a non-rare species under a higher emissions scenario.

I carried out field experiments to evaluate the timing of annual life stages relative to the critical photoperiod triggering the onset of winter diapause. I combined these measures with downscaled climate datasets to project annual ratios of *S. appalachia* individuals developing directly into a third generation versus going into diapause. Incorporation of these into the above population model revealed that the indirect effect of temperature on phenology had a positive effect on population growth that behaved antagonistically to the negative direct effects of temperature. Under RCP 8.5, the model projected that the annual growth rate will remain above one before 2020, but as temperatures continue to increase throughout the 21st Century, the negative direct effects of temperature outweigh the positive indirect effects and the population growth rates shift from growing to shrinking.

I evaluated juvenile survival rate responses to temperature of *S. appalachia* populations from northern and southern range limits. I compared these responses to future projected temperatures at both locations. I found no difference between the survival rates of individuals from the two populations. Comparison of projected survival rates suggested that southern populations have already surpassed optima for thermal demographic response, while northern populations may surpass optima by the middle of the century under RCP 8.5.

I used machine learning algorithms to optimize degree day models predicting the annual emergence of *N. mitchellii francisci*. I validated the use of several algorithms and identified the RandomForest algorithm as the best classifier. Using downscaled climate data, RandomForest

projected a decreasing mean date of annual first emergence, with projected advances of approximately 1.4 and 2.1 days per decade for RCP 4.5 and RCP 8.5 respectively.

My findings suggest that mechanistic field-based approaches are imperative to predict future effects of climate change. My methods are applicable to a wide range of ectothermic organisms with complex lifecycles. Under higher emissions, my results highlight a critical window of time in the early 21st Century for conservation action.

Effects of Temperature, Phenology, and Geography on Butterfly Population Dynamics under Climate Change

by
Elsita Maria Kiekebusch

A dissertation submitted to the Graduate Faculty of
North Carolina State University
in partial fulfillment of the
requirements for the degree of
Doctor of Philosophy

Biology

Raleigh, North Carolina
2020

APPROVED BY:

_____	_____
Nicholas M. Haddad Committee Chair	William F. Morris
_____	_____
Adam Terando	Steven Frank

DEDICATION

I dedicate this dissertation to my late father, Dr. Bernd Dieter Kiekebusch-Steinitz. He always encouraged me to love nature and mathematics, and I am so grateful he got the chance to see butterflies and my field warming experiments at Fort Bragg.

BIOGRAPHY

After spending my early childhood in Columbia, MD, I moved with my family to Namibia. There, my interest in ecology was inspired by the vast outdoors, beautiful landscapes and iconic wildlife. After returning to the US to attend Swarthmore College, PA, I worked abroad for several years. I worked in El Salvador for a year assisting a grass-roots NGO to develop and train farmers in the use of sustainable agriculture techniques. I moved back to Namibia to satisfy my interest in the ecology of arid environments by working as a technician at the Gobabeb Training and Research Centre, located in the Namib Desert. I then completed a master's degree in Desert Ecology at Ben Gurion University of the Negev in Israel. Through a mutual connection, I was hired to work at the Corridor Project where Nick Haddad was one of 7 PIs evaluating seed dispersal in fragmented landscapes. Nick hired me onwards to work as his field crew leader for a summer at Fort Bragg, and from then onwards I was hooked on butterfly research. I worked on a few other short-term research positions in Tucson, AZ and Bihar, India, before returning to the Haddad Lab, and ultimately deciding to undertake a lifelong ambition of obtaining a PhD.

ACKNOWLEDGMENTS

Biggest thank you to my advisor Nick Haddad for believing in me, for being optimistic, teaching me how to "Science", how to incite competition and for being an all-around fantastic mentor. Thank you also to my committee members Bill Morris, Adam Terando and Steve Frank for imparting their knowledge and skills. I was continually inspired and encouraged by the graduate students who studied butterfly population dynamics before me: Erica Henry and Tyson Wepprich, who I am proud to have as collaborators. I thank all the other graduate students in the Haddad Lab who have been an integral part of my learning experience including Johnny Wilson, Chris Hawn, Yu-Hsian Liu, Sean Griffin, Alice Puchalsky, and especially Lindsey Kemmerling who aided me over the course of two summers during which we travelled through North Carolina, South Carolina, Michigan and back to carry out experiments. I thank Erik Aschehoug and Frances Sivakoff for research results that paved the way for the Appalachian Brown population models in this dissertation. I thank Ben Pluer for spending three productive summers with me at Fort Bragg, for always staying positive, for helping me to remember things, for working hard under any conditions and for all the inside jokes. I thank Victoria Amaral for being a fearless crew leader and collecting invaluable Appalachian Brown survey data through an entire growing season. I thank Heather Cayton and all Fort Bragg undergraduate crew members from 2012-19 who carried out restoration and conservation for Saint Francis' Satyrs, and without whom this research would not have been possible. I thank Brian Ball and the Endangered Species Branch for enabling us to carry out our research at Fort Bragg.

I thank all of my collaborators on the Non-Analogue Environments (aka "Brave New World") SERDP grant for all the helpful feedback and for being so easy to work alongside. I especially appreciate the dedicated effort and time from Allison Louthan and Brian Hudgens in

going over statistics, model selection, mark-recapture code etc. I thank my faculty mentors at NC State, in particular Martha Reiskind for adopting me in her lab when Nick moved to Michigan, Ben Reading for teaching me about machine learning, and Seema Sheth for the chapter feedback and fun Shoot the Science sessions. I also could not have carried out my research without the help of Ashley Colewick, Mark Vukovich, Nate Fuller, Mark Hammond and Doug Aubrey who enabled my use of greenhouses at the MSU Kellogg Biological Station and at the UGA Savannah River Ecology Laboratory, and female butterfly collection at the Savannah River Site and on land managed by the Southwest Michigan Land Conservancy.

I thank my "PhD Buddy" Eugene Cheung for sharing the grad school journey with me, for commiserating and celebrating and for being a true friend. I thank the grad students in my cohort, in the Reiskind Lab, in the Department of Applied Ecology and in the DCL 208 office.

Thank you to my family. I could not have made it this far without the enduring support of my mother Lucy Steinitz and my brother Sergio Kiekebusch-Steinitz. I thank my in-laws: the Hourn family, the Hernandez family, and the Huoy families. And finally, thank you to my wife Sokun Hourn, for making my life better every day.

This research was funded by a grant from the DOD Strategic Environmental Research and Development Program (RCSON15-01) awarded through the Institute for Wildlife Studies, a graduate research fellowship from the DOI Southeast Climate Adaptation Science Center awarded to Elsita Kiekebusch, DOD Fort Bragg Endangered Species Branch contract funding to Nick Haddad, a Teaching Assistantship from NC State University and a Porter Graduate Fellowship for Summer Research from the MSU Kellogg Biological Station.

TABLE OF CONTENTS

LIST OF TABLES

LIST OF FIGURES

CHAPTER 1: Tipping points in vital rate responses to temperature across the annual lifecycle of a butterfly

ABSTRACT

Due to their dependence on environmental temperatures, ectothermic animals are likely to be particularly sensitive to global climate change. Accurate prediction of ectotherm population responses to climate change requires a mechanistic understanding of effects of increased temperatures on survival and reproduction. Yet, despite organismal development through distinct life stages that may differ in sensitivity to temperature, most studies measure effects on a single vital rate. Using a combination of greenhouse and large field experiments, I measured the effects of temperature increases on fecundity, and survival at all annual life stages, of the multivoltine butterfly *Satyrodes appalachia*. I found that maximum temperature over each life stage time period was the most important temperature variable explaining changes in vital rates with temperature. I used the vital rate – temperature relationships to develop a population model parameterized with 1) increased temperatures relative to observed field temperatures and 2) downscaled global climate model data.

I found that population growth rates dropped below one at a temperature increases of approximately 4°C or greater. When I incorporated predation into the model, populations began shrinking at +1.5°C. In sensitivity analyses, I found that larval survival rates, particularly during summer generations, were the vital rates to which growth rates were most sensitive. My population model predicted that *S. appalachia* annual growth rates will go from growing to shrinking in the 2060s under the RCP 8.5 scenario. When predation was incorporated, shrinking occurred in the late 2020s. My findings demonstrate the need for conservation strategies for

ectotherms that target specific vulnerable life stages and consider differing effects of climate variables.

INTRODUCTION

Global climate change is predicted to be a major anthropogenic driver of changes in biodiversity in the 21st century (Sala et al. 2000, Urban 2015). Changes in critical climate variables such as temperature have already been observed to alter species persistence, distributions, and phenology (Parmesan & Yohe 2003, Root et al. 2003). Because environmental temperatures strongly influence their body temperature, growth, and development, ectothermic animals may be more sensitive to temperature changes than endotherms. As over 7 million animals are ectotherms (Stork 2018), understanding the mechanisms of their response to shifting temperature regimes will be necessary to ascertain the potential magnitude of population loss and the path toward conservation. In this paper, I take a mechanistic approach that directly links the effects of temperature-derived variables on population vital rates. First, I estimate the responses of survival and fecundity to these environmental drivers, and second, I use these estimates to parameterize models to predict effects on future population growth.

My approach contrasts with most studies of climate effects on ectothermic animals that tend to examine synthetic responses by correlating geographic distributions with climate (Araujo & Guisan 2006). Such studies overlook the determinants of these responses, such as effects of specific climate variables on survival or reproduction (Buckley et al. 2010). Due to this, non-mechanistic methods are limited in their ability to predict future species responses and therefore provide little guidance for tailoring conservation strategies towards climate regimes with no current analog (Urban et al. 2016, Fordham et al. 2013, Williams & Jackson 2007).

Climate change induced shifts in environmental variables vary spatially and over time (Alexander et al. 2006, Liu et al. 2004, Karl et al. 1993). For example, mean winter temperatures are increasing to a higher degree than mean summer temperatures for the continental United States (Hansen et al. 2012). As populations do not respond to mean global temperatures, identification of the most important temperature variables at relevant spatial and temporal scales is paramount to understanding species responses to climate change (Walther et al. 2002).

In organisms with complex life cycles that have distinct life stages that differ in their responses and sensitivity to temperature, data requirements are high for building population models (Kingsolver et al. 2011, Jackson et al. 2009). Most studies of ectotherm demography focus on a single life stage rather than measuring vital rates at multiple life stages (Radchuk et al. 2013, Schultz et al. 2019), despite differential contributions of each life stage to individual lifetime fitness (Kingsolver et al. 2011). Studies that do not evaluate all life stages may fail to identify the life stages to which population growth is most sensitive and may also fail to detect when more than one life stage is sensitive to climate change. Efficient conservation strategies will therefore benefit from identification of the most sensitive life stages. To address these limitations, I developed multiple field and greenhouse experiments in order to measure vital rates across all annual life stages of a multivoltine butterfly.

Research on butterflies has demonstrated the crucial role that demographic traits play in climate change responses (Crozier & Dwyer 2006, McLaughlin et al. 2002). Butterflies have long been used as model ectothermic species to investigate impacts of climate change due to their sensitivity to abiotic variables (Shreeve 1984, Schtickzelle & Baguette 2004, Altermatt 2010). Some studies have identified critical life stages whose response to changing climate determines population persistence. For example, Radchuk et al. (2013) found that population

growth of the Bog Fritillary (Boloria eunomia) was most sensitive to winter larval survival that was negatively affected by warming. Crozier (2004) demonstrated that winter temperature effects on larval survival of the Sachem Skipper (Atalopedes campestris) enabled its northern range expansion. Monarch (Danaus plexippus) population models have incorporated climate effects on multiple life stages and annual generations. Using a perturbation analysis, Flockhart et al. (2015) established that monarch population growth was most sensitive to vital rates at breeding grounds along the annual migratory route. Zipkin et al. (2012) found that complex interactions between climate variables governed monarch population growth, with different suites of climate variables influencing the first and second annual migratory generations in the US. These studies evaluate climate effects on vital rates through either mechanistic or correlative approaches but fail to combine empirically derived relationships with projected environmental conditions to predict future population dynamics.

I aimed first to quantify the relationship between temperature and demography through empirical identification of the key temperature variables that significantly impact vital rates. Second, I used the established relationships to model population dynamics under future climate change scenarios. To this end, I carried out warming experiments across the entire annual life cycle of the Appalachian Brown butterfly (*Satyrodes appalachia*). I estimated survival at separate life stages over three annual generations as well as fecundity under a range of increased temperatures created through artificial warming arenas and habitat restoration treatments. I created a population model by multiplying together my measured vital rates to estimate annual growth rates. I parameterized the model using a range of increased temperatures matching increases of up to +5°C that are projected to occur in the Southeastern US over the course of the 21st century under the highest IPCC emissions scenario, RCP 8.5 (Sillmann et al. 2013). I carried

out a second model run parameterized with downscaled climate data for the years 2016-2099 under RCP 8.5 to project future annual growth rates. I sought to answer the following questions: 1) What temperature variables have the strongest effects on vital rates? 2) To which life stages is population growth most sensitive under increased temperatures? 3) How will projected warming affect future growth rates?

METHODS

Study species and site

Satyrodes appalachia is a satyrine butterfly occurring in forested wetlands throughout the eastern United States. *S. appalachia* has been observed to complete at least 2 generations per year in the southeastern US and to overwinter as a diapaused early-instar larva (Figure 1.1). I carried out the research at the US Army installation at Fort Bragg, NC where *S. appalachia* is locally rare in wetland areas. A combination of land-use change, fire suppression, and beaver extirpation at Fort Bragg have altered wetland habitat and reduced the number of early successional *Carex* species (Bartel et al. 2010), including *Carex mitchelliana* that is a known host plant for *S. appalachia* (Kuefler et al. 2008).

Experimental setup of restoration plots

Field temperatures were altered as a by-product of experimental habitat restoration implemented in 2011 to increase the abundance of host plants (sedges in the genus *Carex*) and the abundance of butterflies, including *S. appalachia* and the federally endangered Saint Francis' Satyr (*Neonympha mitchellii francisci*, methods in Aschehoug et al. 2015). Restoration treatments that included hardwood removal ("Cut") and dam installation ("Dam") were

implemented in a factorial design resulting in four 30 m x 30 m plots at each of three field sites. To increase the restoration areas, four additional plots were added over the time period of 2013-16 for a total of sixteen plots (Figure 1.2). These included two plots with a Cut treatment and two plots with Cut and Dam treatments.

Immature survival

I measured temperature effects on survival at egg and larval life stages at my field restoration sites. Temperature was manipulated at the scale of 30 x 30m plots via habitat restoration treatments, and within each plot via warming/cooling arenas. During this experiment, I used each of the three restoration sites as a block. I selected three plots per block, including one Cut plot and two Cut and Dam plots (Figure 1.2). I ignored uncut plots because the warming arenas relied on solar warming to increase temperatures.

To manipulate temperatures, I created three experimental arenas within each of the plots. Each arena consisted of 208 L polyethylene drums cut into rings of 37 cm in height and 57 cm in diameter. I established arenas around naturally occurring wetland plants including *C. mitchelliana* by burying them 10 cm deep in the ground. I planted extra sedges where necessary to maintain a similar amount of live sedge within each arena. I removed all visible predators from inside the arenas and excluded predators by enclosing arenas within no-see-um netting (Skeeta©). Inside each arena, I placed a Maxim iButton temperature logger within the foliage of *C. mitchelliana*, away from direct sunlight and at an approximate height of 30cm above the ground, locations that approximate those where I have observed naturally occurring eggs and larvae. To protect iButtons from any additional solar radiation, I shielded them using a cup covered in reflective foil. I recorded temperature every hour. Within each plot, I randomly

assigned each arena to one of three treatments: 1) Control, 2) Shade and 3) Open-top warming. I shaded arenas by covering them with Coolaroo© shade fabric (84-90% UV Block) cut into 1.8 x 1.8 m squares and hung by the corners from PVC pipes at 1.5 m above the ground, such that the arena was centered beneath the shade fabric. I constructed open-top warming chambers using Sun-Lite© pre-fabricated solar glazing panels (Solar Components Corporation, New Hampshire USA). I cut the panels into 2.4 m x 0.9 m rectangles, rolled them into cylinders and fastened them with screws. The resulting cylinders were 0.9 m high with a circumference of 2.1 m, and each was placed over one arena per plot.

To measure egg survival, I collected eggs from wild-caught *S. appalachia* females. Females were brought to the greenhouse and placed in a 15 cm high by 10 cm diameter 'oviposition chamber' consisting of a single potted host plant (*Carex mitchelliana*) enclosed within mesh netting. After 48 hours, I removed the netting, released the butterfly and counted the number of eggs laid. I placed entire potted plants with known number of eggs into each experimental arena for approximately 48 hours. Afterwards, I removed the plant and counted the remaining viable eggs. Non-viable eggs were identified by their altered color, shape and/or size. This allowed me to estimate daily egg survival. I carried out the egg survival experiments during three generations (first: 5/3 – 6/9/17, second: 7/20-8/12/16, and third: 8/31-9/29/16, Figure 1.1).

I estimated larval survival using the larvae that hatched from these eggs. I allowed the eggs to hatch at ambient temperatures in the greenhouse. As soon as all larvae hatched, I counted them and placed them back into the experimental arenas from which they originated in the egg survival experiments. Once I noticed formation of pupae, I checked the arenas daily for emerged adults. I carried out the larval survival experiments over all three annual generations (first: 5/19 – 7/10/17, second: 7/27-9/25/16, and third: 9/7/16-5/31/17, Figure 1.1).

To evaluate the effect of arena temperatures on egg and larval survival rates, I carried out generalized linear mixed effects models using R statistical software (R Core Team, 2016). I used binomial regression analyses to evaluate effects of temperature variables on egg and larval survival. I used the amount of time that an individual spent in each life stage in each arena. By design, this was two days for the eggs, after which they were removed, allowed to hatch, and then placed back into the arenas. I then used the average amount of time that an individual spent in the entire larval life stage. I measured 1) the average temperature (mean), 2) the average of the daily maximum temperatures and 3) the average of the daily minimum temperatures recorded by the iButtons over these time periods for the analyses. I compared a suite of models that included fixed effects of these three temperature variables, where only one temperature variable was included in a model at one time. Each model included one of all possible combinations of the temperature variables and additional fixed effects of warming treatment (Control, Shade, Open-top warming), restoration treatment (Dam or No Dam), generation (first, second, third) and/or the interactions between generation and each of the 3 temperature variables. All models included a nested random effect of plot in site (block). I ranked models using corrected Akaike's Information Criterion (AICc, Hurvich & Tsai 1989) and used the best-supported model in all subsequent analyses.

Adult survival

To estimate adult survival rates and lifespan, I carried out mark-recapture surveys over a three-week period comprising the second adult flight period of 2017 (7/14-8/3). I carried out surveys along transects established within a total of fifteen plots across three restoration sites (Figure 1.2). I followed methods for marking butterflies, walking surveys and establishing

transects as described in Haddad et al. (2008). I carried out surveys on every weekday throughout the flight period. Over the same time, I placed shielded iButtons into each plot and recorded hourly temperatures. I analyzed the data via a multistate mark-recapture model using the package RMark (Laake, 2013) in R to run the program MARK (White & Burnham 1999). In order to test for effects of temperature on dispersal, I compared five models using covariates of probability of transition (Psi) between plots that included maximum, minimum, and mean temperatures, distance between plots, and constant dispersal across sites and time. I ranked all models using corrected Akaike's Information Criterion (AICc) and selected the best covariate for use in subsequent analyses. In order to evaluate possible effects on detection, I carried out a second round of model selection and compared two covariates of detection probability (p) that were linked to detection in a prior study (Sivakoff et al. 2016). I tested for plot and restoration (Cut) effects on detection, while holding survival probability (Phi) constant across sites and time. I selected the highest ranked covariate as above for further use. In order to test for effects of temperature on adult survival probability, I carried out a third round of model selection. I ranked seven models using AICc to compare survival probability covariates that included mean, max, and min temperature, field site, plot, Dam treatment and constant survival across sites and time. I selected the best supported model for further analyses.

Daily fecundity

I estimated fecundity by measuring oviposition in artificially warmed enclosures at a greenhouse located at the Fort Bragg Endangered Species Branch. I carried out the experiment from 7/12 – 8/31/17. I caught wild females, placed them in oviposition chambers for 40-42 hours, and then counted the number of eggs laid. I manipulated temperature during oviposition

by placing chambers under infrared lamps. I used a single iButton placed inside each chamber to record temperatures. To evaluate temperature effects on daily fecundity, I regressed number of eggs laid per day against temperature variables using a quasipoisson generalized linear model to account for overdispersion. I compared a suite of 6 fecundity models to evaluate effects of mean temperature, average daily maximum temperature, average daily minimum temperature, and the quadratic effects of these variables. I defined the average daily minimum and maximum temperatures as the mean of the daily minima and maxima over the 40-42 hour period that each female was in an artificial warming chamber. I carried out QAICc model ranking using the R package MuMIn (Bartoń 2017) to assess support for each temperature variable. To calculate daily fecundity, I accounted for propagation of females by assuming a 1:1 sex ratio and halving the number of eggs laid per day as fitted by the highest ranked temperature model.

Population model

I brought together all the model fits from the highest ranked models in the above experiments and used them to build a simple population model. I started by using the lowest temperatures observed in the field during the immature survival experiments. These were found by) selecting the lowest of the averages of the highest ranked temperature variable from each arena during each experiment (each life stage per generation). I used these temperatures to parameterize the model fits. I then multiplied the resulting vital rates together to estimate annual population growth rate. I built the model using the following equation:

$$\frac{N_t}{N_{t+1}} = af_1(T_{e_1}) \times e_1(T_{e_1}) \times l_1(T_{l_1}) \times af_2(T_{e_2}) \times e_2(T_{e_2}) \times l_2(T_{l_2}) \times af_3(T_{e_3}) \times e_3(T_{e_3}) \times l_3(T_{l_3})$$

where a indicates adult lifespan, f indicates daily fecundity, e indicates egg survival, and l

indicates larval survival (Figure 1.1), and where e, l, and f (but not a) are functions of the temperatures experienced during the respective life stages over the course of the field experiments (T_e, T_l). N_t represents the number of adults in the first flight period in year t. The left side of the equation thus represents the annual population growth rate. Subscripts indicate generation with 1, 2 and 3 representing first, second, and third respectively. I estimated egg survival by exponentiating daily egg survival rates from the field experiment by the average egg longevity of 7 days that I observed through the course of the experiments and assumed to be temperature independent. I estimated fecundity (af(T)) by multiplying the daily fecundity from the greenhouse experiment with the adult lifespan. I estimated mean adult lifespan using adult daily survival from mark recapture based on the following formula (Mayfield 1961):

$$a = 1/(1 - \text{Adult Daily Survival})$$

I limited the fecundity based on known total numbers of oocytes previously found in S. appalachia (Sivakoff et al. 2016) occurring in Cut plots. I assumed that there was no separate effect of generation on adult survival and therefore adult lifespan. I also assumed that there was no additive or interacting effect of generation on the temperature effect on daily fecundity. Fecundity varied by generation solely due to differences in seasonal temperatures that were measured during the egg survival field experiments during each corresponding generation of the egg life stage (T_{e1}, T_{e2}, and T_{e3}).

Once I evaluated the highest ranked temperature variable for each experiment, I used the lowest recorded value of this variable (one per life stage per generation) to parameterize my model. I incrementally increased these temperatures by 0.1 °C until I reached increases of +5 °C and evaluated the effect of each temperature increase on annual growth rates. I incorporated uncertainty into the model by randomly sampling from a normal distribution described by the

standard error of each temperature fit for each vital rate. I bootstrapped the model in this way 1000 times, and then estimated 95% Confidence Intervals based on the results. I carried out this process for each increased temperature increment. I ran the model a second time with an adjustment that incorporated estimates of larval predation. I decreased larval survival in all generations using the proportion of larvae that survived in arenas where predators were excluded versus not excluded at Cut plots based on Aschehoug et al. (2015).

I measured sensitivity and elasticity of each generations' growth to each vital rate by carrying out a perturbation analysis. For this analysis, I divided up the vital rates by generation to separately estimate the growth rate (lambda) for each generation. I used the lowest temperatures recorded in the field (as previously described) to calculate the vital rates for use in the analysis. I individually reduced and increased the values of each vital rate by exactly 5% following Morris and Doak (2002) in order to calculate the average sensitivity of the generational lambdas to the relevant vital rates.

Climate model

To determine how future temperatures could affect *S. appalachia* future population growth, I used the Multivariate Adapted Constructed Analogs (MACA) downscaled climate dataset (Abatzoglou & Brown 2012). I extracted daily temperatures from nine 4-km grid cells known to contain *S. appalachia* populations at Fort Bragg for the years 2016-2099. I did this for 20 Global Climate Models (GCMs) parameterized by the RCP 8.5 emissions scenario. I determined which temperature variables to extract based on the model-rankings. I manipulated the extracted temperatures for further use via a three-step process. First, I calculated the mean of the extracted MACA temperatures across the nine grid-cells resulting in daily values over the

2016-2099 time period for each of the 20 GCMs. Second, I divided the data by known dates that each life stage was present per generation (i.e. 'season'). I calculated the mean of the daily temperatures within that time period resulting in one annual value per GCM for each life stage per generation. Finally, I calculated the median, the 5th, and the 95th percentiles across the 20 GCM values per year.

I defined the seasonal timing of each generation based on my experimental findings of egg, larval, and adult longevity (Table 1.1) I assumed that all individual larvae of the 2nd generation developed into adults in a 3rd generation that overwinters as a diapaused larva. As I were able to extract temperatures that would be experienced by adult females, I updated the population model such that the fecundity was calculated using these temperatures (rather than measured field temperatures experienced by eggs as done previously).

$$\frac{N_t}{N_{t+1}} = af_1(T_{af_1}) \times e_1(T_{e_1}) \times l_1(T_{l_1}) \times af_2(T_{af_2}) \times e_2(T_{e_2}) \times l_2(T_{l_1}) \times af_3(T_{af_3}) \times e_3(T_{e_3}) \times l_3(T_{l_3})$$

I accounted for iButton bias (Terando et al. 2017) and/or micro-climate differences by creating a regression of daily iButton data against daily interpolated climate data from the METDATA dataset (Abatzoglou 2011). I used the daily maximum temperatures from one arena iButton at each of two of the field sites which corresponded to METDATA (and MACA) data from two 4-km grid cells over a time period of approximately 6 months of uninterrupted data logging during 2016-17. (My third field site was within the same grid-cell as one of the others). I extracted the daily maximum temperatures from each METDATA grid cell over the same time period. I regressed the METDATA values against the iButton values. Finally, I estimated future iButton temperatures in order to parameterize the climate model. I did this by converting the extracted seasonal MACA data to predicted future iButton data using the formula from the

regression. The future egg and larval survival rates were estimated using this future iButton data as the warming experiments were carried out in the field. As the fecundity warming experiments were not carried out in the field, the future fecundities were estimated using MACA data directly. I created a second round of annual growth rate estimates by adjusting larval survival rates for predation as was done previously for the population model.

RESULTS

Immature survival

During the egg survival experiments, average arena temperatures were 18.4-24.3ºC in the first generation, 24.9-28.8ºC in the second and 22.1-25.9ºC in the third. The highest ranked model included a marginally significant negative effect of maximum temperature on egg daily survival (Table 1.2). This model also included a fixed effect of generation (Table 1.2, Figure 1.3) and a random effect of plot nested within site. Several other egg-temperature models were close in AICc ranking to the highest model. An ANOVA comparison of the maximum temperatures used to fit the egg daily survival model revealed a significant effect of warming treatment on maximum temperature ($F(2,62) = 3.51$, $p = 0.036$). A Tukey test showed that OTW treatments were significantly warmer than Shade treatments ($p=0.027$).

During the larval survival experiments, average arena temperatures were 23.4-24.9ºC, 24.3-26.7ºC and 12.1-13.9ºC during the first, second and third annual generation respectively. The highest ranked model included a significant negative effect of maximum temperature (Table 1.2). The model also included a significant effect of generation (Table 1.2, Figure 1.3) as well as a random effect of plot nested in site. The negative effect of the third generation was significantly different from the first ($p=0.001$) and second generation ($p<0.001$). The effects of

the first and second generations did not significantly differ. An ANOVA comparison of the maximum temperatures used to fit the larval survival model did not show a significant effect of treatment on maximum temperature (see Appendix Figure 1.A1).

During the summer generations, I increased average temperatures by up to 4ºC in the arenas. Due to decreased sunlight, I was limited by the ability to warm the arenas during the winter months when average temperatures increased by 2ºC. The lower value corresponds to predictions for temperature increases in the Southeastern United States under lower emissions scenarios over the 21st Century (Girvetz et al. 2009). My solar-warmed open-top warming design was also limited in function at night. These findings highlight the need for greenhouse experiments to complement field experiments when locations such as wetland habitats make difficult the use of electricity.

Adult survival

Plot temperatures varied from 23.6 to 26.7ºC on average over the time period during which I conducted mark-recapture studies. I found that distance was the most important covariate determining transition probability. In the second round of model selection, I found that the Cut treatment was the most important covariate determining detection probability. The third round of model selection revealed that survival remained constant across plots and time in the highest ranked model (Table 1.3), though several other models had AICc values close to this. Model output from this survival model revealed daily adult survival of 0.915, which translated to an average adult lifespan of 11.7 days.

Daily fecundity

Average temperature ranged from 23.2-32.4 ºC in the fecundity experiments. The highest ranked model included effects of maximum temperature and maximum temperature squared (Table 1.2, Figure 1.4). At lower temperatures, increasing maximum temperatures increased eggs laid per day, but at higher temperatures this effect was reversed.

Population model

My population model predicted that predation-free *S. appalachia* population growth decreases with increasing temperatures (Figure 1.5a). The model suggests that at approximate maximum temperature increases of 4.4°C, the annual growth rate shifts from growing to shrinking. I observed very high annual growth rates at low temperatures. When I created a more realistic model that incorporated larval predation (Aschehoug, et al. 2015), I found that annual growth rates decreased such that population shrinking began at approximate maximum temperature increases of 1.5°C (Figure 1.5b). I also found that the size of the confidence intervals decreased with increasing temperature suggesting that at higher temperatures there is a higher certainty of population decline.

I found a high sensitivity of the annual growth rate to larval survival rates particularly during the first and second generations (Table 1.4). I evaluated sensitivities at both low (+0C) and high (+4C) temperatures. At higher temperatures, the sensitivities to all vital rates decreased, and annual growth rate became more sensitive to winter larval survival. Elasticities of all vital rates were equal except for adult longevity as this appeared in the formula for annual growth rate as a^3.

Climate model

As I found that maximum temperature was consistently the most important temperature variable across warming experiments, I used this variable to parameterize my climate model. I therefore extracted the seasonal MACA temperatures from 20 GCMs by taking the average of the daily maxima over the time period of presence of each life stage per generation (Table 1.1). I found that the METDATA daily maximum temperatures were significantly correlated with the iButton daily maximum temperatures (R^2=0.95, $F(1,426) = 8730$, $p < 0.001$). I used the regression formula to convert the future MACA temperatures to future iButton temperatures, which I used to estimate annual egg and larval survival for each generation.

Annual growth rates were very high during the early years of the 21st century (Figure 1.6). The climate model predicted that populations would begin to shrink in the year 2061. When I adjusted the model to include larval predation, I found that growth rates first dropped below one in 2019, and this occurred at the latest in the year 2061 for 95% of the GCMs.

DISCUSSION

While *S. appalachia* demographic response to warming temperatures varied by life stage, the full life cycle response to projected future temperatures demonstrated a decreasing trend in vital rates, and therefore annual population growth rates over time. By incorporating a predation adjustment previously measured at the site (Aschehoug et al. 2015), I was able to identify temperature thresholds beyond which growth rates dropped below one. My results suggest that under a higher emissions scenario, *S. appalachia* will experience population declines by the late 2020's. During my experiments, immature survival was measured without predation and independent of density. Female butterflies laid eggs in lab settings which may have been

advantageous compared to field environments. Under these ideal conditions, climate warming still leads to population declines by the 2060's.

My series of experiments in natural and greenhouse settings enabled me to compare responses across the entire annual life cycle of *S. appalachia*. While adult survival was not affected by temperature increases, larvae experienced highly significant negative effects of warmer temperatures. Compounding this vulnerability, the sensitivity analysis revealed that population growth rate was most sensitive to larval survival, particularly during summer generations. Studies of other ectothermic taxa have revealed sensitivity to temperature at juvenile life stages including for loggerhead sea turtles (Matsuzawa et al. 2002), common wall lizards (Van Damme et al. 1992), and white shrimp (Ponce-Palafox et al. 1997). While these results for *S. appalachia* are dire, my findings suggest that conservation strategies will benefit by protecting the species' most vulnerable life stage(s) as the positive effects will amplify to the growth rate.

The average of daily maximum temperatures over life-stage relevant time periods consistently emerged as the significant predictor variable determining vital rate responses. This could have particularly strong effects as predicted increases in short-duration extreme high temperature episodes (Easterling et al. 2000) over critical time periods could dramatically affect annual population growth rates. Research on climate extremes is less common than on climate means and their effects on ecological processes (Smith 2011). Buckley and Kingsolver (2012) found that egg viability in two Colias butterfly species decreased with increase in extreme high temperatures, and that this reduced positive effects on growth rates of mean temperatures due to increased available flight period time. Roland and Matter (2013) found that extreme winter conditions (including both warm and cold temperature extremes) strongly predicted population declines of *Parnassius smitheus* due to sensitivity of eggs and early-instar larvae. My findings

add to the growing body of evidence from butterflies and other ectothermic taxa of the importance of considering climate extremes to predict population responses to climate change.

Despite that temperatures were lower during the winter, increased maximum temperatures still had a negative effect on larval survival (Figure 1.3). One explanation for this is that low temperatures aid the conservation of metabolic resources. Studies have shown that higher temperatures increase the use of insect energy stores needed for winter survival, leading to increased larval mortality (Han & Bauce 1997) and decreased fecundity in emergent adults (Irwin & Lee 2003). Additionally, as temperature is associated with insect developmental time (Gray et al. 2001, Regniere 1990), lower temperatures allow for synchronization of individual life cycles with that of host-plants necessary for herbivory post-diapause (Bale et al. 2002, MacLean 1983).

Differing effects of temperature variables on vital rates and dispersal as well as temperature thresholds beyond which populations will decline suggest routes for habitat conservation and restoration. An ideal approach would be to identify habitats for conservation and restoration that will provide climates that are projected to remain below critical maximum temperatures in the future. This could be novel habitat (for example, cooler northern locations) or currently occupied habitat is more strongly buffered against climate change (e.g. climate refugia). In the case of the former, connectivity could be established to allow dispersal to cooler areas. I found limited effects of temperature on dispersal suggesting that enabling movement - even through warmer areas - could be a successful conservation method. In the latter case, refugia habitat would be prioritized for conservation, a strategy that is gaining traction (Keppel et al. 2011). The experimental restoration actions were tailored towards providing host plants for butterflies, and these ultimately resulted in higher temperature plots due to hardwood removal

that increased sunlight penetration. It is imperative to consider trade-offs inherent in the goals of restoration, for example provision of resources versus availability of suitable micro-climates.

My result suggests that critical tipping points exist within the projected temperature trajectories of high emissions scenarios this century. If CO_2 emissions are not constrained, a non-threatened species under ideal conditions is predicted to experience population declines at temperature rises of 4.4°C. My findings suggest that conservation strategies will benefit from identifying vulnerable life stages for ectotherms with complex life cycles. Such strategies should consider differing effects of climate variables, particularly at the regional scale and between seasons over time.

TABLES

Table 1.1. Dates that define presence of individuals in each life stage per generation from which temperatures were extracted using the MACA downscaled climate dataset. From my experiments I found that on average individual eggs survived for 7 days, non-diapausing larvae survived for 48 days and adults survived for 11 days. I observed that adults emerged in the springtime around approximately May 1st and that the first adult flight period lasted a month and a half until June 15th. Females emerge later than males. I observed this difference to be 5 days in the experimental arenas.

Life Stage	**Generation**	**'Season' Dates**	**Temperature**
Adult Female	1st	May 6 – June 15	T_{af_1}
Egg	1st	May 6 – June 22	T_{e_1}
Larva	1st	May 13 – August 9	T_{l_1}
Adult Female	2nd	July 4 – August 20	T_{af_2}
Egg	2nd	July 4 – August 27	T_{e_2}
Larva	2nd	July 11 – October 14	T_{l_2}
Adult Female	3rd (winter)	August 28 – October 25	T_{af_3}
Egg	3rd (winter)	September 2 – November 1	T_{e_3}
Larva	3rd (winter)	September 9 – May 1 following year	T_{l_3}

Table 1.2. Highest ranked generalized linear mixed effect models for egg and larval survival (binomial) and daily fecundity (quasipoisson). Bolded values indicate p <0.05.

Experiment	**Fixed Effect**	**Chisq**	**DF**	**p**
Egg Daily Survival	Maximum Temperature	3.2308	1	0.07227
	Generation	5.9118	2	0.05203
Larval Survival	Maximum Temperature	26.468	1	**<0.001**
	Generation	20.807	2	**<0.001**
Eggs Laid Per Day	Maximum Temperature	2.5856	1	0.10784
	Maximum Temperature ^2	3.0760	1	0.07946

Table 1.3. Ranked models comparing covariates of adult survival probability (S).

Variables in Model	**Number of Parameters**	**AICc**	**Delta AICc**	**weight**	**Deviance**
Constant across sites and time	5	387.909895	0	0.33842311	300.43939
Dam	6	389.356389	1.44649317	0.16419427	299.71986
Maximum temperature	6	389.534199	1.62430317	0.15022668	299.89767
Minimum temperature	6	390.044069	2.13417317	0.1164207	300.40754
Site	6	390.056259	2.14636317	0.11571327	300.41973
Mean temperature	6	390.068269	2.15837317	0.11502049	300.43174
Plot	19	412.587232	24.6773364	1.48E-06	291.85048

Table 1.4. Sensitivities and elasticities of annual growth rate to each of the vital rates at two separate temperature increases (+0 °C and +4 °C).

Vital Rate	Generation	Value at +0 °C	Average Sensitivity +0 °C	Average Elasticity +0 °C	Value at +4 °C	Average Sensitivity +4 °C	Average Elasticity +4 °C
Egg Survival (e_1)	First	0.735	1783.994	1.000	0.629	3.685	1.000
Larval Survival (l_1)	First	0.203	6452.924	1.000	0.035	65.869	1.000
Fecundity (af_1)	First	49.445	26.506	1.000	58.457	0.040	1.000
Adult Lifespan (a)	ALL	11.747	576.654	5.169	11.747	0.802	4.064
Egg Survival (e_2)	Second	0.601	2181.567	1.000	0.468	4.958	1.000
Larval Survival (l_2)	Second	0.297	4411.019	1.000	0.057	40.635	1.000
Fecundity (af_2)	Second	58.457	22.420	1.000	23.387	0.099	1.000
Egg Survival (e_3)	Third	0.808	576.654	1.000	0.726	3.196	1.000
Larval Survival (l_3)	Third	0.360	1621.408	1.000	0.075	31.074	1.000
Fecundity (af_3)	Third	58.457	3637.397	1.000	52.986	0.044	1.000

FIGURES

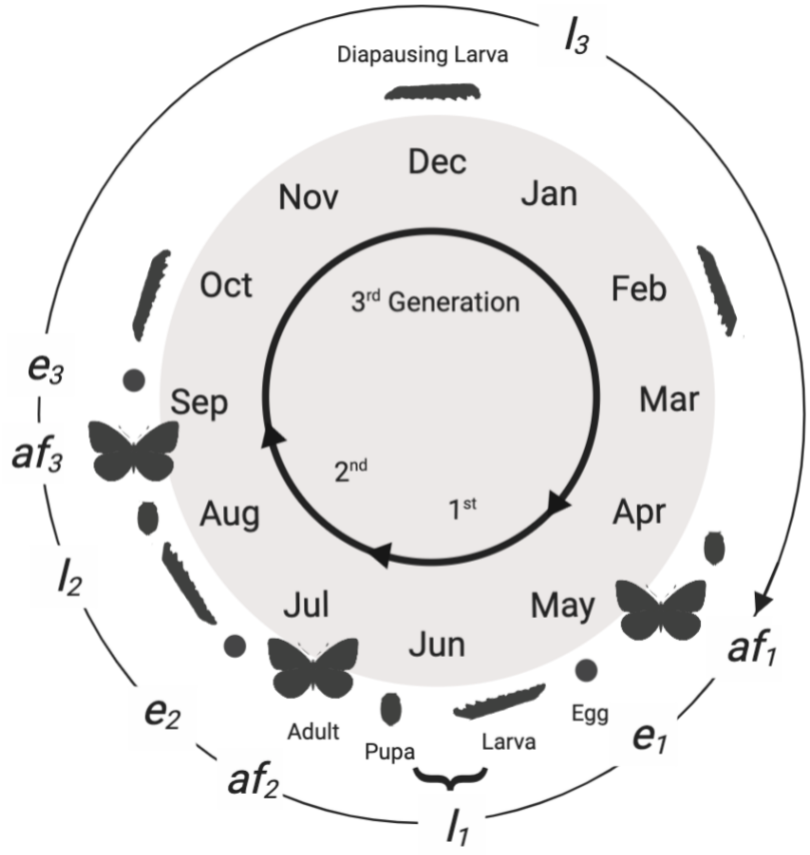

Figure 1.1. Annual lifecycle of *S. appalachia*. Up to three generations consisting of egg, larval, pupal and adult life stages can be completed within one year. Larvae cease developing during winter diapause.

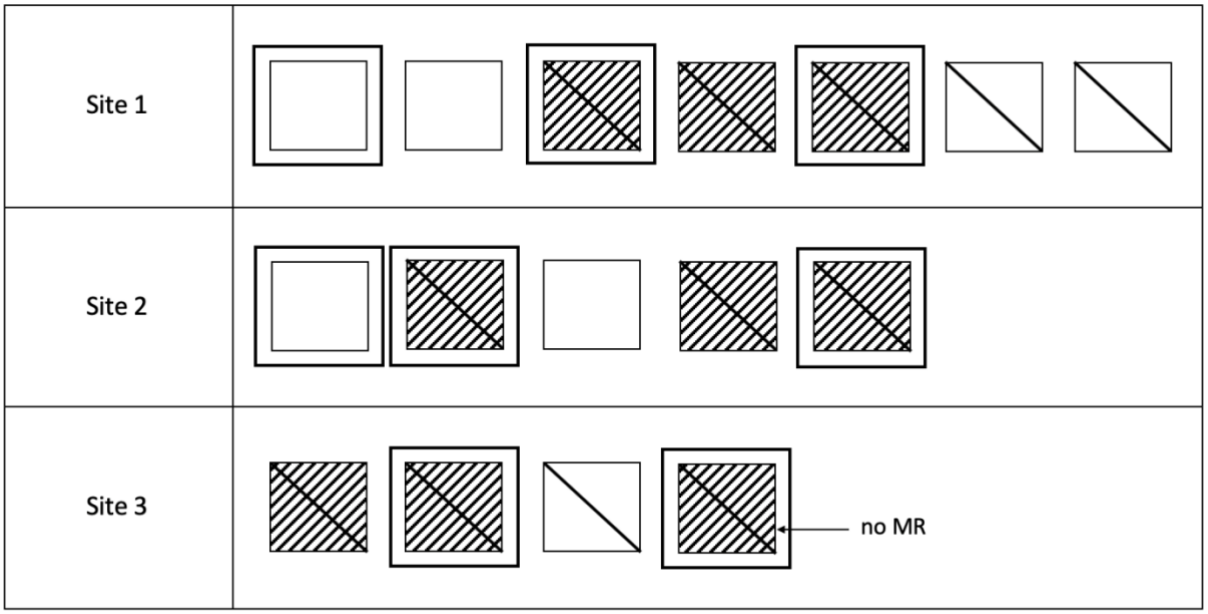

Figure 1.2. Organization of three experimental sites. Each square represents a 30m x 30m plot. Mark-recapture surveys to estimate adult survival occurred at all plots (15) except one at Site 3, labeled “no MR”. Hashed squares represent plots (9) where within-plot warming experiments were conducted to estimate immature (egg and larval) survival. Restoration treatments are represented as follows: Hardwood removed (“Cut”) plots (12) have a single diagonal line from top left to bottom right of the square, artificially dammed (“Dam”) plots (8) have a larger square around the plot square.

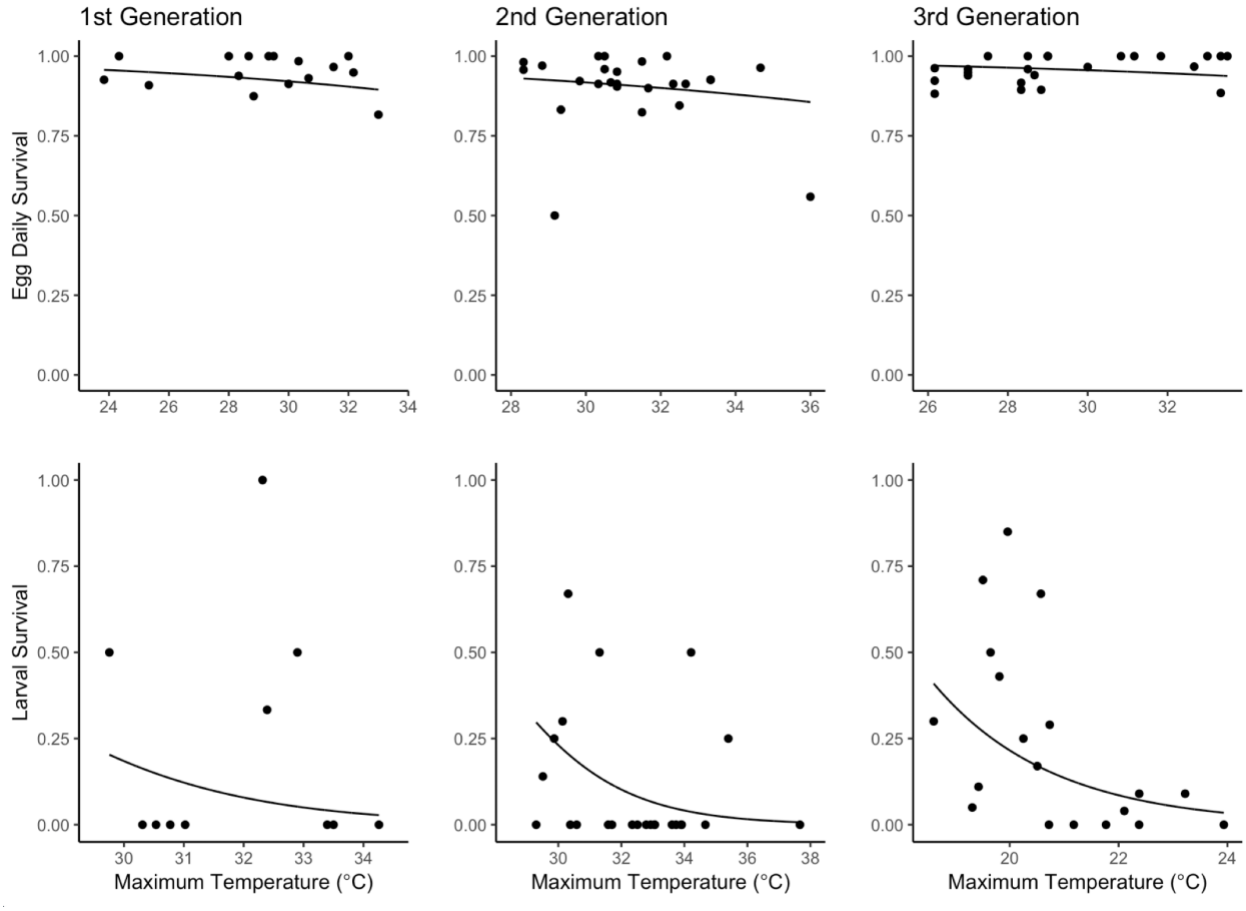

Figure 1.3. Daily egg survival and total larval survival by average of daily maximum temperatures during each generation. Lines represent highest ranked model for each of the annual generations.

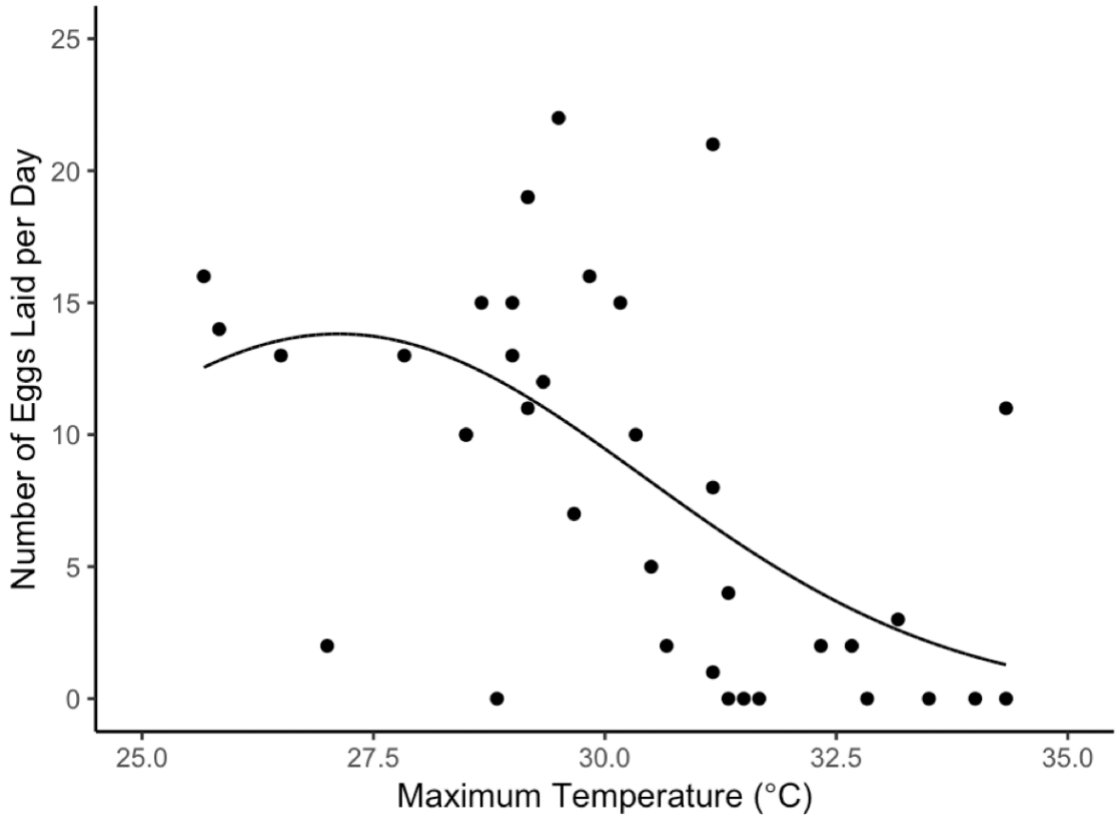

Figure 1.4. Effect of average of daily maximum temperatures in oviposition chambers, on number of eggs laid per day. Line represents a quasipoisson fit of the highest ranked model, which includes the additive effect of maximum temperature and its square.

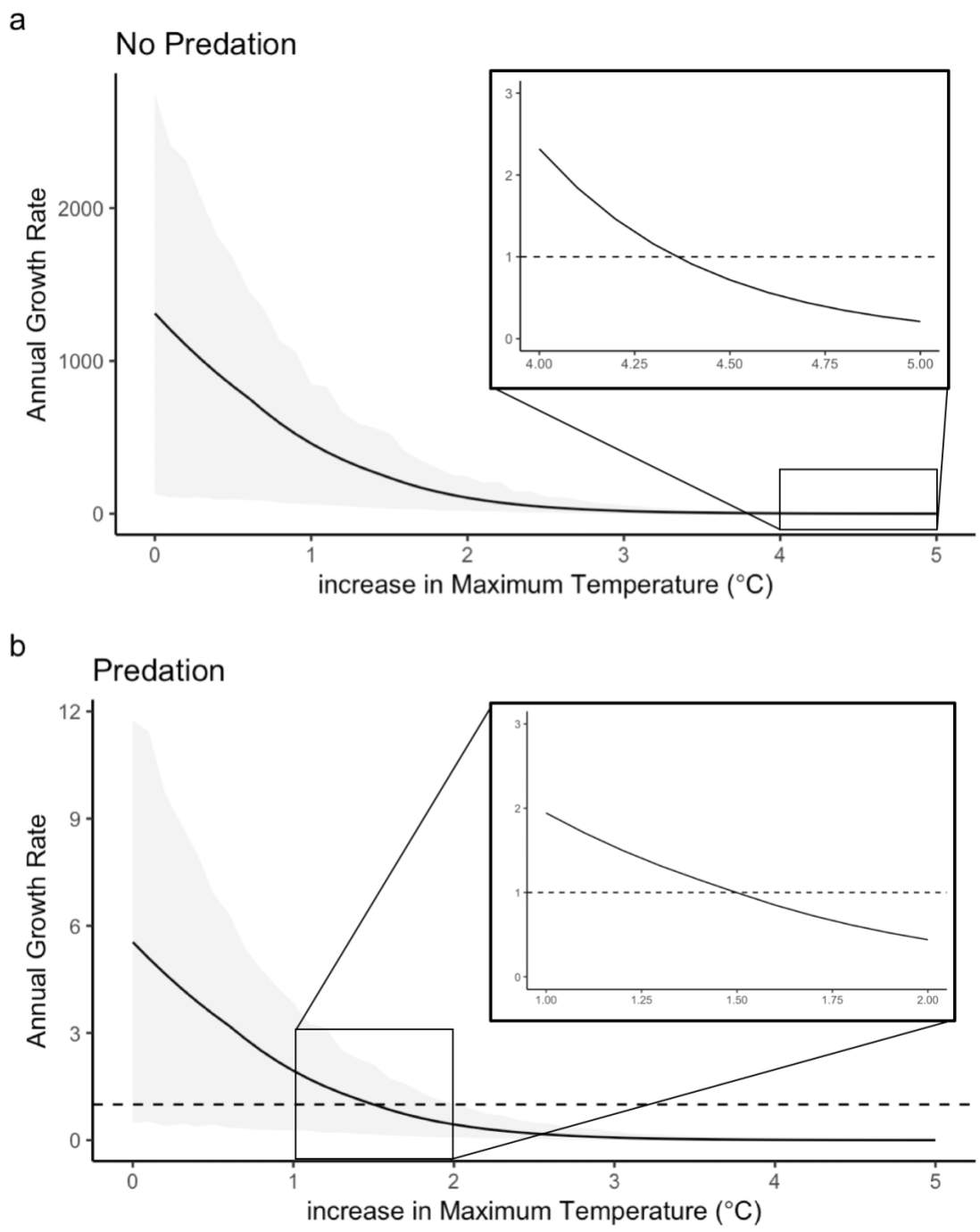

Figure 1.5. Change in annual population growth rate with increase in maximum temperature (°C). Population goes from growing to shrinking (growth rates <1 (dotted line in inset)) at approximate maximum temperature increases of +4.4°C and +1.5°C for models excluding (a) and including (b) predation respectively. Solid line represents model with no uncertainty, shaded area indicates 95% Confidence Intervals.

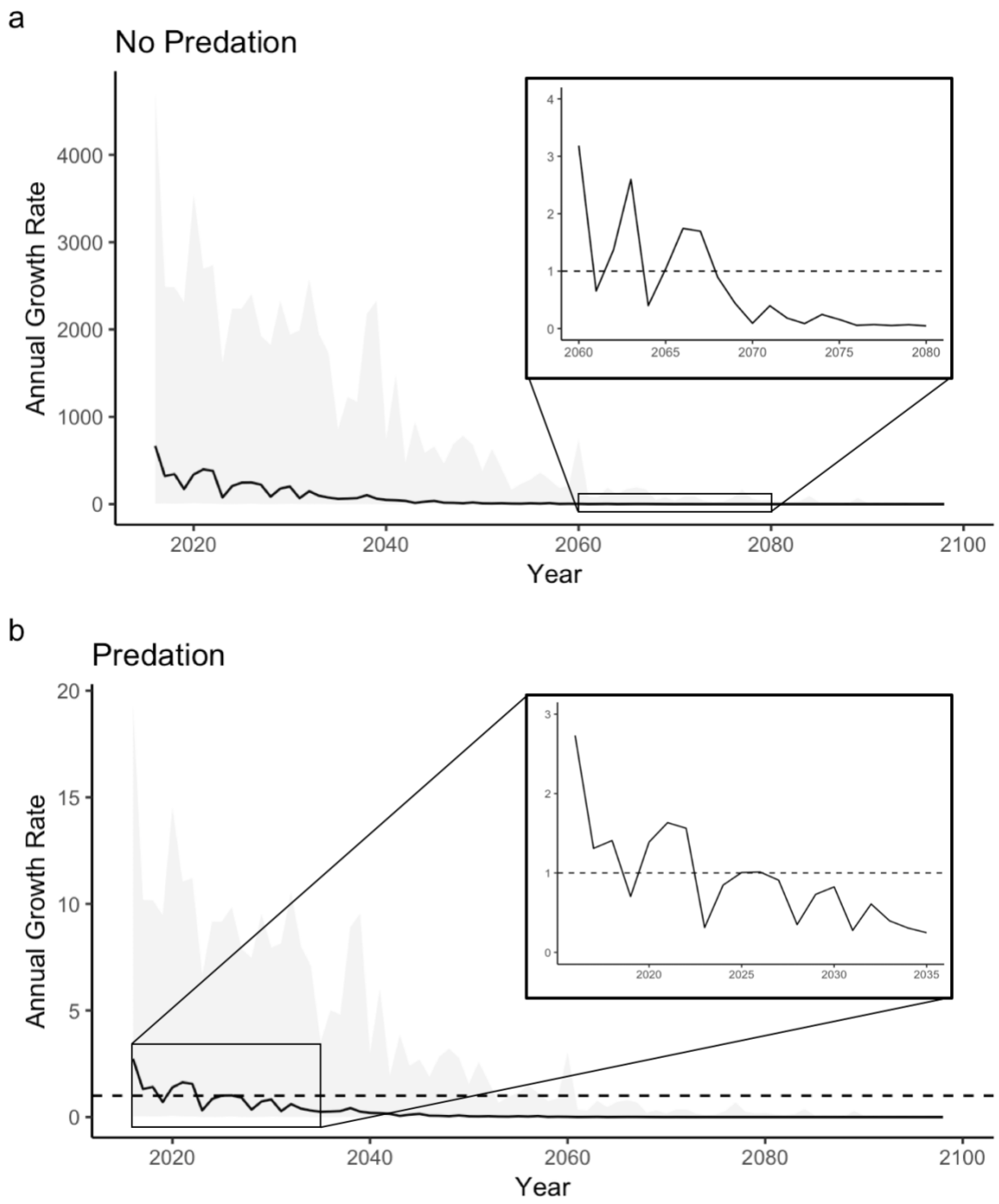

Figure 1.6. Projected annual population growth rates over time. Population begins to shift from growing to shrinking (growth rates <1 (dotted line in inset)) in the year 2061 for models excluding predation (a). For models including predation (b), populations begin shrinking in 2019. Solid line represents the median and shaded area indicates 5th to 95th percentile range from the output of 20 GCMs.

REFERENCES

1. Abatzoglou, J. T. (2011). Development of gridded surface meteorological data for ecological applications and modelling. International Journal of Climatology, 33(1), 121–131.

2. Abatzoglou John T., & Brown Timothy J. (2012). A comparison of statistical downscaling methods suited for wildfire applications. International Journal of Climatology, 32(5), 772–780.

3. Alexander, L. V., Zhang, X., Peterson, T. C., Caesar, J., Gleason, B., Tank, A. M. G. K., … Vazquez-Aguirre, J. L. (2006). Global observed changes in daily climate extremes of temperature and precipitation. Journal of Geophysical Research: Atmospheres, 111(D5).

4. Altermatt, F. (2010). Climatic warming increases voltinism in European butterflies and moths. Proceedings of the Royal Society of London B: Biological Sciences, 277(1685), 1281–1287.

5. Araújo, M. B., & Guisan, A. (2006). Five (or so) challenges for species distribution modelling. Journal of Biogeography, 33(10), 1677–1688.

6. Aschehoug, E. T., Sivakoff, F. S., Cayton, H. L., Morris, W. F., & Haddad, N. M. (2015). Habitat restoration affects immature stages of a wetland butterfly through indirect effects on predation. Ecology, 96(7), 1761–1767.

7. Bale, J. S., Masters, G. J., Hodkinson, I. D., Awmack, C., Bezemer, T. M., Brown, V. K., … Whittaker, J. B. (2002). Herbivory in global climate change research: Direct effects of rising temperature on insect herbivores. Global Change Biology, 8(1), 1–16.

8. Bartel, R. A., Haddad, N. M., & Wright, J. P. (2010). Ecosystem engineers maintain a rare species of butterfly and increase plant diversity. Oikos, 119(5), 883–890.

9. Bartoń, K. (2017). MuMIn: Multi-Model Inference. R package version 1.40.0.

10. Buckley, L. B., & Kingsolver, J. G. (2012). The demographic impacts of shifts in climate means and extremes on alpine butterflies. Functional Ecology, 969–977.

11. Buckley, L. B., Urban, M. C., Angilletta, M. J., Crozier, L. G., Rissler, L. J., & Sears, M. W. (2010). Can mechanism inform species' distribution models? Ecology Letters, 13(8), 1041–1054.

12. Crozier, L. (2004). Warmer Winters Drive Butterfly Range Expansion by Increasing Survivorship. Ecology, 85(1), 231–241.

13. Crozier, L., & Dwyer, G. (2006). Combining Population-Dynamic and Ecophysiological Models to Predict Climate-Induced Insect Range Shifts. The American Naturalist, 167(6), 853–866.

14. Easterling, D. R., Meehl, G. A., Parmesan, C., Changnon, S. A., Karl, T. R., & Mearns, L. O. (2000). Climate Extremes: Observations, Modeling, and Impacts. Science, 289(5487), 2068–2074.

15. Flockhart, D. T. T., Pichancourt, J.-B., Norris, D. R., & Martin, T. G. (2015). Unravelling the annual cycle in a migratory animal: Breeding-season habitat loss drives population declines of monarch butterflies. Journal of Animal Ecology, 84(1), 155–165.

16. Fordham, D. A., Akçakaya, H. R., Araújo, M. B., Keith, D. A., & Brook, B. W. (2013). Tools for integrating range change, extinction risk and climate change information into conservation management. Ecography, 36(9), 956–964.

17. Girvetz, E. H., Zganjar, C., Raber, G. T., Maurer, E. P., Kareiva, P., & Lawler, J. J. (2009). Applied Climate-Change Analysis: The Climate Wizard Tool. PLOS ONE, 4(12), e8320.

18. Gray, D. R., Ravlin, F. W., & Braine, J. A. (2001). Diapause in the gypsy moth: A model of inhibition and development. Journal of Insect Physiology, 47(2), 173–184.

19. Haddad, N. M., Hudgens, B., Damiani, C., Gross, K., Kuefler, D., & Pollock, K. (2008). Determining optimal population monitoring for rare butterflies. Conservation Biology, 22(4), 929–940.

20. Han, E.-N., & Bauce, E. (1997). Effects of Early Temperature Exposure on Diapause Development of Spruce Budworm (Lepidoptera: Tortricidae). Environmental Entomology, 26(2), 307–310.

21. Hansen, J., Sato, M., & Ruedy, R. (2012). Perception of climate change. Proceedings of the National Academy of Sciences, 109(37), E2415–E2423.

22. Hurvich, C. M., & Tsai, C.-L. (1989). Regression and time series model selection in small samples. Biometrika, 76(2), 297–307.

23. Irwin, J. T., & Lee, J., Richard E. (2003). Cold winter microenvironments conserve energy and improve overwintering survival and potential fecundity of the goldenrod gall fly, Eurosta solidaginis. Oikos, 100(1), 71–78.

24. Jackson, S. T., Betancourt, J. L., Booth, R. K., & Gray, S. T. (2009). Ecology and the ratchet of events: Climate variability, niche dimensions, and species distributions. Proceedings of the National Academy of Sciences, pnas.0901644106.

25. Karl, T. R., Jones, P. D., Knight, R. W., Kukla, G., Plummer, N., Razuvayev, V., … Peterson, T. C. (1993). A New Perspective on Recent Global Warming: Asymmetric Trends of Daily Maximum and Minimum Temperature. Bulletin of the American Meteorological Society, 74(6), 1007–1024.

26. Keppel, G., Niel, K. P. V., Wardell-Johnson, G. W., Yates, C. J., Byrne, M., Mucina, L., … Franklin, S. E. (2012). Refugia: Identifying and understanding safe havens for biodiversity under climate change. Global Ecology and Biogeography, 21(4), 393–404.

27. Kingsolver, J. G., Arthur Woods, H., Buckley, L. B., Potter, K. A., MacLean, H. J., & Higgins, J. K. (2011). Complex Life Cycles and the Responses of Insects to Climate Change. Integrative and Comparative Biology, 51(5), 719–732.

28. Kuefler, D., Haddad, N. M., Hall, S., Hudgens, B., Bartel, B., & Hoffman, E. (2008). Distribution, population structure and habitat use of the endangered Saint Francis Satyr butterfly, Neonympha mitchellii francisci. The American Midland Naturalist, 159(2), 298–320.

29. Laake, J.L. (2013). RMark: An R Interface for Analysis of Capture-Recapture Data with MARK. AFSC Processed Rep 2013-01, 25p. Alaska Fish. Sci. Cent., NOAA, Natl. Mar. Fish. Serv., 7600 Sand Point Way NE, Seattle WA 98115.

30. Liu, B., Xu, M., Henderson, M., Qi, Y., & Li, Y. (2004). Taking China's Temperature: Daily Range, Warming Trends, and Regional Variations, 1955–2000. Journal of Climate, 17(22), 4453–4462.

31. MacLean, S. F. (1983). Life Cycles and the Distribution of Psyllids (Homoptera) in Arctic and Subarctic Alaska. Oikos, 40(3), 445–451.

32. Matsuzawa, Y., Sato, K., Sakamoto, W., & Bjorndal, K. (2002). Seasonal fluctuations in sand temperature: Effects on the incubation period and mortality of loggerhead sea turtle (Caretta caretta) pre-emergent hatchlings in Minabe, Japan. Marine Biology, 140(3), 639–646.

33. Mayfield, H. (1961). Nesting Success Calculated from Exposure. The Wilson Bulletin, 73(3), 255–261.

34. McLaughlin, J. F., Hellmann, J. J., Boggs, C. L., & Ehrlich, P. R. (2002). Climate change hastens population extinctions. Proceedings of the National Academy of Sciences, 99(9), 6070–6074.

35. Morris, W. F., & Doak, D. F. (2002). Quantitative conservation biology. Sinauer, Sunderland, Massachusetts, USA.

36. Parmesan, C., & Yohe, G. (2003). A globally coherent fingerprint of climate change impacts across natural systems. Nature, 421(6918), 37–42.

37. Ponce-Palafox, J., Martinez-Palacios, C. A., & Ross, L. G. (1997). The effects of salinity and temperature on the growth and survival rates of juvenile white shrimp, Penaeus vannamei, Boone, 1931. Aquaculture, 157(1), 107–115.

38. Radchuk, V., Turlure, C., & Schtickzelle, N. (2013). Each life stage matters: The importance of assessing the response to climate change over the complete life cycle in butterflies. Journal of Animal Ecology, 82(1), 275–285.

39. Régnière, J. (1990). Diapause termination and changes in thermal responses during postdiapause development in larvae of the spruce budworm, Choristoneura fumiferana. Journal of Insect Physiology, 36(10), 727–735.

40. R Core Team (2016). R: A language and environment for statistical computing. R Foundation for Statistical Computing, Vienna, Austria. URL https://www.R-project.org/.

41. Roland, J., & Matter, S. F. (2013). Variability in winter climate and winter extremes reduces population growth of an alpine butterfly. Ecology, 94(1), 190–199.

42. Root, T. L., Price, J. T., Hall, K. R., Schneider, S. H., Rosenzweig, C., & Pounds, J. A. (2003). Fingerprints of global warming on wild animals and plants. Nature, 421(6918), 57–60.

43. Sala, O. E., Chapin, F. S., Iii, Armesto, J. J., Berlow, E., Bloomfield, J., … Wall, D. H. (2000). Global Biodiversity Scenarios for the Year 2100. Science, 287(5459), 1770–1774.

44. Schtickzelle, N., & Baguette, M. (2004). Metapopulation viability analysis of the bog fritillary butterfly using RAMAS/GIS. Oikos, 104(2), 277–290.

45. Schultz, C. B., Haddad, N. M., Henry, E. H., & Crone, E. E. (2019). Movement and Demography of At-Risk Butterflies: Building Blocks for Conservation. Annual Review of Entomology, 64(1), 167–184.

46. Shreeve, T. G. (1984). Habitat Selection, Mate Location, and Microclimatic Constraints on the Activity of the Speckled Wood Butterfly Pararge Aegeria. Oikos, 42(3), 371–377.

47. Sillmann, J., Kharin, V. V., Zwiers, F. W., Zhang, X., & Bronaugh, D. (2013). Climate extremes indices in the CMIP5 multimodel ensemble: Part 2. Future climate projections. Journal of Geophysical Research: Atmospheres, 118(6), 2473–2493.

48. Sivakoff, F. S., Morris, W. F., Aschehoug, E. T., Hudgens, B. R., & Haddad, N. M. (2016). Habitat restoration alters adult butterfly morphology and potential fecundity through effects on host plant quality. Ecosphere, 7(11), e01522. 10.1002/ecs2.1522.

49. Smith, M. D. (2011). The ecological role of climate extremes: Current understanding and future prospects. Journal of Ecology, 99(3), 651–655.

50. Stork, N. E. (2018). How Many Species of Insects and Other Terrestrial Arthropods Are There on Earth? Annual Review of Entomology, 63(1), 31–45.

51. Terando, A. J., Youngsteadt, E., Meineke, E. K., & Prado, S. G. (2017). Ad hoc instrumentation methods in ecological studies produce highly biased temperature measurements. Ecology and Evolution, 00, 1-15.

52. Urban, M. C., Bocedi, G., Hendry, A. P., Mihoub, J.-B., Pe'er, G., Singer, A., … Travis, J. M. J. (2016). Improving the forecast for biodiversity under climate change. Science, 353(6304), aad8466.

53. Urban, Mark C. (2015). Accelerating extinction risk from climate change. Science, 348(6234), 571–573.

54. Van Damme, R., Bauwens, D., Braña, F., & Verheyen, R. F. (1992). Incubation Temperature Differentially Affects Hatching Time, Egg Survival, and Hatchling Performance in the Lizard Podarcis muralis. Herpetologica, 48(2), 220–228.

55. Walther, G.-R., Post, E., Convey, P., Menzel, A., Parmesan, C., Beebee, T. J. C., … Bairlein, F. (2002). Ecological responses to recent climate change. Nature, 416(6879), 389–395.

56. White, G., & Burnham, K. (n.d.). Program MARK: Survival Estimation from Populations of Marked Animals. Bird Study(46), 120–138.

57. Williams, J. W., & Jackson, S. T. (2007). Novel climates, no-analog communities, and ecological surprises. Frontiers in Ecology and the Environment, 5(9), 475–482.

58. Zipkin, E. F., Ries, L., Reeves, R., Regetz, J., & Oberhauser, K. S. (2012). Tracking climate impacts on the migratory monarch butterfly. Global Change Biology, 18(10), 3039–3049

CHAPTER 2: Antagonistic consequences of climate change on butterfly population dynamics: incorporating effects of increased voltinism

ABSTRACT

Climate change is advancing the spring phenology of ectothermic organisms whose development depends on external temperatures. For many insect species, an earlier first annual emergence date and prolonged growing season may allow sufficient time to produce an additional generation per year. Quantitative measures of the impact of increasing number of generations (voltinism) on population growth are lacking. In particular, the known negative effects of increased temperatures on population vital rates must be considered in the context of indirect effects via increased voltinism. Taken together, these effects may reinforce each other or act antagonistically. To address these knowledge gaps, I carried out a series of experiments on the Appalachian Brown (*Satyrodes appalachia*), a locally rare wetland butterfly that experiences 2-3 annual generations in the Southeast US. I experimentally deduced the timing of the critical photoperiod that cues the onset of diapause to distinguish individuals that develop directly into an additional generation of adults from diapausing individuals that emerge the following year. I used a combination of experiments, transect surveys, and degree day models to understand the timing of annual flight periods. I then projected changes to flight periods under future climates for the years 2016-2099. I found that increased voltinism had a positive effect on annual population growth rates. At low temperature increases relative to observed field conditions, I found that this positive effect surpassed negative direct effects of temperature resulting in increased population growth. However, at higher temperatures (+2°C upwards), the positive effects of voltinism were outweighed by the direct negative effects of temperature on population

vital rates and the annual population growth rate declined relative to the lower temperature increases. The climate-informed population model projected that the annual growth rate would transition from growing to shrinking in the early 2020s. I show the conditions under which two separate consequences of climate change work antagonistically to affect demography, and I discuss the implications for conservation over the course of the 21st century.

INTRODUCTION

Increased temperatures due to anthropogenic climate change have been shown to decrease fitness and performance in a variety of ectothermic taxa (Parmesan 2006, Ma et al. 2015, Kingsolver et al. 2011). These effects of warming have led to direct negative impacts on species demography and population growth (Descimon et al. 2005, Matsuzawa et al. 2002, Oliver et al. 2015). However, the direct effect of temperature on demography is a single avenue of impact and there are others.

Another avenue by which climate may affect demography is by altering species phenology, or the timing of lifecycle events. These phenological shifts have affected numerous plant and animal species (Parmesan & Yohe 2003, Parmesan 2006) with one global meta-analysis showing 80% of 1400 species analyzed shifting in the direction expected due to climate warming (Root et al. 2003). Although much attention has been given to how warming impacts phenology and population dynamics separately, the two effects are often not considered together. These effects could reinforce each other or trade-off against each other. Conceptually, the consequences of climate change could be synergistic and build on each other or they could be antagonistic and reach some balance of effect, possibly producing no overall change (Figure 2.1).

Ectothermic organisms such as butterflies have emerged as important indicators of the effects of climate change on species phenology (Altermatt 2010, Singer & Parmesan 2010). This is because the rate of development of butterfly larvae is highly sensitive to temperature. For temperate species that experience winter larval diapause, increased temperatures can result in the earlier emergence of adult butterflies in spring (Roy & Sparks 2000, Stefanescu et al. 2003, Parmesan 2007) and a longer window of thermal time in which individuals can develop and reproduce (Robinet & Roques 2010).

Photoperiod is another important developmental cue for many temperate-zone insects (Danilevskii 1965, Tauber & Tauber 1976), as it guides individuals to either develop directly into an adult or to enter diapause until the following growing season. Longer daylengths typically foster direct development. As daylengths shorten, the onset of diapause becomes more likely for individuals in the life stage sensitive to cues. With large advances in phenology, the number of generations per year (voltinism) can increase, a phenomenon that has been demonstrated for Lepidoptera (Altermatt 2010, Martin-Vertedor et al. 2010).

The effects of increased voltinism on long-term population viability are multi-faceted. Thomas et al. (2010) demonstrated that faster generation turnover in invertebrates leads to higher rates of molecular evolution. This could increase viability by increasing the likelihood of evolutionary adaption to adverse conditions. Van Dyck et al. (2015) hypothesized that producing an additional generation per year may lead to developmental traps when photoperiod cues, locally adapted to a cooler climate, prove maladaptive in years when autumn conditions are unfavorable for development of individuals in the additional generation. Wepprich (2017) tested this “Lost Generation Hypothesis” and found that for 20 North American butterfly species facultative additional generations tended to increase population growth rates.

Here, I comparatively assess the effect of shifting phenology in response to increased temperatures on population growth rates. I previously developed a population model for the Appalachian Brown butterfly (*Satyrodes appalachia*) and showed that growth rates decrease with increased temperatures (Kiekebusch 2019). I incorporate shifting voltinism into the model to answer the following questions: 1) what is the effect of incorporating an additional generation on population growth? 2) does this effect work synergistically or antagonistically with the direct effects of temperature on population growth? 3) how could population growth rates change over time with projected future temperatures due to climate change?

METHODS

Study Species and Site

I carried out the research at the US Army installation at Fort Bragg, NC where *S. appalachia* occurs in forested wetland areas. *S. appalachia* has been observed to overwinter as a diapaused early-instar larva. Though *S. appalachia* has previously been considered bivoltine at this field location (Aschehoug et al. 2015, Sivakoff et al. 2016), recent field warming experiments (Kiekebusch 2019) revealed that there was sufficient time for a proportion of second generation individuals to develop directly into a third generation (Figure 2.2). Due to a lack of data from previous years, I am unable to conclude that an additional third generation is a new and direct result of climate change.

Critical Photoperiod

I carried out an experiment to determine the timing of the occurrence of the critical photoperiod cueing the onset of diapause in *S. appalachia*. Individuals exposed to this cue during

a sensitive early life stage halt development and initiate diapause through the winter. Warmer temperatures result in earlier annual emergences, shifting the exposure of individuals prior to the critical photoperiod and leading to their direct development into an additional third generation.

Over a ten-week period beginning in mid-July, I caught adult female *S. appalachia* that emerged during the second annual flight period. Each week I caught two females and placed each one into a 15 cm high by 10 cm diameter 'oviposition chamber' consisting of a potted host plant (*Carex mitchelliana*) enclosed within mesh netting. After 48 hours, I removed the netting, released the butterflies and put each potted plant with eggs into a separate netted enclosure. As I couldn't be sure of the exact date that each egg was laid, I defined the date eggs were laid per clutch as the second day of the 48-hour period, when the eggs were placed into the enclosures. I placed all enclosures onto a bench located at a shaded wetland field site and monitored the larval development over a three-month period. I recorded the proportion of surviving offspring within each clutch that developed directly into adults versus those that initiated diapause. I fit a binomial generalized linear model to the resulting data to understand the relationship between the date that eggs were laid and the likelihood that they developed directly into adults. As has been done in previous studies (e.g. Xue et al. 1997), I considered the critical photoperiod to occur at the point at which 50% of individuals developed directly.

First emergence thermal timing

I estimated the timing of annual first emergence of *S. appalachia* in the spring using data from larval warming experiments (Kiekebusch 2019) and a degree-day model. My goal was to quantify *S. appalachia* development as a combination of time and temperature, such that I could later project future emergence ordinal dates using future temperatures. Degree-day models have

long been used in the fields of agriculture, biological control, and species distribution modelling under climate change (Moore & Remais 2014). Cumulative growing degree days (GDD) are a more accurate predictor of butterfly emergence timing than the ordinal date (Cayton et al. 2015).

During my warming experiments, I raised diapausing larvae during the winter in enclosures placed at field sites. I recorded hourly temperatures throughout the winter by placing a single Maxim iButton temperature logger in each enclosure. When I observed the formation of pupae in the spring, I began daily monitoring of all enclosures and recorded the exact date of each butterfly's emergence. For each individual, I extracted daily maximum and minimum temperatures during its larval development from my recorded temperature data. I calculated GDD using a lower threshold of 10°C and an upper threshold of 30°C and applied the single-triangle method to my extracted temperatures. These temperature thresholds have been applied to other Satyrinae (Kuefler et al. 2008) as well as many other butterfly species (Crozier & Dwyer 2006, Cayton et al. 2015, Bryant et al. 2002). I began accumulating degree days on March 1st. I identified the lowest accumulated degree days necessary for emergence and used this for further analyses.

First flight period emergence date projection

To estimate the future annual first emergence dates of *S. appalachia*, I used the Multivariate Adapted Constructed Analogs (MACA) downscaled climate dataset (Abatzoglou & Brown 2012). I extracted daily projected maximum and minimum temperatures from 2016 through 2099 using output from nine 4-km grid cells known to contain *S. appalachia* populations at Fort Bragg. I used downscaled data from 20 Global Climate Models (GCMs, Wilby & Wigley 1997) parameterized by the RCP 8.5 emissions scenario. A projection based on multiple climate

models is thought to outperform a prediction from a single model and is an accepted approach to quantifying uncertainty in future climate change (Knutti et al. 2010).

I calculated GDD for each site per GCM, again following the equation from McMaster & Wilhelm (1997). I used my previously calculated value of lowest GDD of *S. appalachia* emergence to identify the projected ordinal date per year at which this value will be accumulated. I then calculated the average date across sites for each GCM resulting in 20 values per year. I used the median and 5th to 95th percentile range of these values for further analyses.

Second flight period and ratio projection

To determine the date of first emergence and peak abundance of *S. appalachia* in the second flight period, I carried out surveys for adults throughout the entire period that adults were flying during 2018 (April – September). I collected transect counts following methods described by Haddad et al. (2008) at two sites comprising fifteen 0.1 ha plots. I plotted the summed daily counts over time to identify the start and end of the second flight period. I considered the start to occur when counts began to increase for the second time following the first abundance peak (first flight period.) Because second and third generations overlapped, the end of the second flight period was more difficult to distinguish from the beginning of the third flight period. I considered it to occur at the lowest value of transect counts between the second and third peak abundances.

To estimate the ordinal start date of the second flight period, I estimated the number of days between the start of the first and second flight period. I based this on the observed length of the first flight period and the average duration of egg and larval life stages that I measured in my warming experiments (Kiekebusch 2019). I assumed that this duration would remain the same

over years, an approach that is supported by multi-year findings for a related Satyrine butterfly at my study location (Kuefler et al. 2008). I then predicted the timing of the start of future second flight periods by adding my estimated value to each projected future date of first emergence. Using the transect count data, I shifted the ordinal date of each daily count to reflect the shift in start date. For each year, I fit a normal curve to each set of shifted second flight period daily counts using R statistical software (R Core Team, 2018). This method relied on two assumptions. First, I assumed that the observed emergences were neither left nor right-skewed, despite that this has been demonstrated for butterflies (Xue et al. 1997, Brakefield 1982). Second, I did not take into account the effect of changing population sizes on width and amplitude of the flight period curve (Zonneveld 1991) as I did not parameterize my model with actual population sizes. Instead I assumed that the curve remained the same over all years and therefore the ratio was in turn unaffected by population size.

I calculated the area under the curve to the left and right of the critical photoperiod ordinal date in order to estimate the proportion of directly developing and diapausing individuals for each year. From experiments I have observed that females emerge on average 5 days later than males. Because I could not accurately account for differing male and female flight periods during surveys, I assumed that the second flight period estimated from daily adult counts directly translated to the period of time over which second generation eggs were laid.

Integrating voltinism in the population model

I estimated annual growth rates by adapting a population model developed by Kiekebusch (2019) to incorporate shifting voltinism:

$$\frac{N_t}{N_{t+1}} = F_1(T) \times e_1(T) \times l_1(T) \times F_2(T) \times e_2(T) \times (p(l_2(T) \times F_3(T) \times e_3(T) \times l_3(T)) + (1 - p)(l_{2.5}))$$

where F represents fecundity, e represents egg survival, and l represents larval survival as a function of temperature (T). Subscripts indicate within-year generations (Figure 2.2). To account for a changing ratio of developing to diapausing individuals, I used p to indicate the proportion of individuals that develop directly into adults that emerge in the third flight period, and 1-p to indicate the proportion of individuals that initiate diapause and emerge the following year. Second generation larvae are cued by photoperiod to follow one of the two development pathways with l_2 representing the survival of second generation larvae that develop directly into third generation adults and with $l_{2.5}$ representing the survival of larval individuals that initiate diapause.

I estimated winter larval survival ($l_{2.5}$) based on measured winter larval survival of third generation individuals (l_3) from warming experiments (Kiekebusch 2019). I calculated the average duration (in days) of the third generation larval life stage based on the dates that eggs were placed in enclosures and that butterflies emerged. I exponentiated measured larval survival (l_3) by the reciprocal of this duration to estimate daily larval survival over winter. I estimated the average duration of the larval life stage of diapausing second generation individuals by summing 1) the number of days between the critical photoperiod and the average date third generation eggs were placed in enclosures with 2) the duration of the third generation larval life stage. I then subtracted the average egg lifespan of 7 days to account for the larval time period only as critical photoperiod was estimated relative to the ordinal date that second generation eggs were laid. I then exponentiated the calculated daily winter larval survival by the duration of the larval life

stage of diapausing second generation individuals to estimate the overall second generation winter larval survival ($l_{2.5}$).

To compare effects of shifting phenology with direct effects of temperature on vital rates, I parameterized the population model over a range of temperatures and ratios of directly developing vs diapausing second generation individuals. I started with low temperatures measured during field experiments for each life stage per generation and incrementally increased each temperature by up to +5° Celsius. I ran the population model for each increased temperature value over the range of possible values of p. All analyses used in the model incorporated estimates of larval predation as described in Kiekebusch (2019) based on Aschehoug et al. (2015).

Integrating voltinism in the climate model

I parameterized the population model using the MACA daily maximum temperature data (sites, GCMs, RCP as above) in order to project future annual growth rates. I transformed the data in several steps as described in Kiekebusch (2019) to achieve average maximum temperatures over the 'seasonal' time periods that defined each life stage per generation for each year for each GCM. I used the median and 5th to 95th percentile range across the GCMs to parameterize the model following the below formula:

$$\frac{N_t}{N_{t+1}} = F_1(T_{F_1}) \times e_1(T_{e_1}) \times l_1(T_{l_1}) \times F_2(T_{F_2}) \times e_2(T_{e_1}) \times (p(l_2(T_{l_2}) \times F_3(T_{F_3}) \times e_3(T_{e_3}) \times l_3(T_{l_3})) + (1-p)(l_{2.5})$$

with temperature data corresponding to each life stage per generation (T_{F_1}, T_{e_1}, T_{l_1}, T_{F_2}, T_{e_2}, T_{l_2}, T_{F_3}, T_{e_3}, T_{l_3}) and second generation winter larval survival ($l_{2.5}$) calculated as above using third generation winter larval survival (l_3). I defined the seasonal timing of each generation based

on average egg, larval and adult longevity determined from experiments (Table 2.1, Kiekebusch 2019.) I used the projected annual ratios to parameterize the model with values of p and (1 - p). I used the critical photoperiod ordinal date to guide the estimates of the time periods that eggs, adults and larvae were present during the second and third generations. I adjusted the MACA temperature data to account for microclimate differences and potential bias in iButton temperature loggers (see Terando et al. 2017) in the field as described in Kiekebusch (2019).

RESULTS

Critical Photoperiod

I found that within individual clutches, it was possible for individuals to enter different developmental pathways. My observations enabled me to discern a window of time during which the proportion of individuals developing directly into third flight period adults transitioned from one to zero (Figure 2.3). The point at which 50% of individuals went into diapause occurred at ordinal date 216 which I used as the critical photoperiod time point for further analyses.

First emergence thermal timing

I recorded the timing of first emergence in the first flight period for 62 butterflies in experimental warming enclosures during the first annual flight period. I found that *S. appalachia* emerged over a range of GDD from 412 to 913 with the average emergence occurring at 582 GDD. I considered 412 GDD to be the lowest thermal accumulation necessary for emergence, and I used this value to project future first emergence dates.

First flight period emergence date projection

Using the MACA climate dataset I found that ordinal date of first emergence decreased over time (Figure 2.4a). This was an expected outcome because as temperatures increase over time, thermal accumulation occurs at an increased rate, so less days are necessary to achieve emergence.

Second flight period and ratio projection

Transect surveys during 2018 revealed three peaks in the *S. appalachia* abundance curves indicating the presence of three generations and enabling me to distinguish the second flight period abundance curve (Figure 2.5a). I found that there were 60 days between the start of the first and second flight periods. I found that the transect counts did not fit a normal distribution (Shapiro-Wilk $W=0.98$, $p<0.001$), but I fit a normal curve to the data. I shifted the ordinal dates of the transect counts based on the shifting date of first emergence for each year and re-fit a normal curve for each year (see Figure 2.5 for examples). By comparing the area to each side of the critical photoperiod ordinal date under each annual curve, I found an increasing ratio of second flight period offspring developing directly versus initiating diapause over time (Figure 2.4b).

Integrating voltinism in the population model

I found that at low temperature increases (+0°C, +1°C), adding a third generation greatly increased the annual population growth rate (Figure 2.6). However, at temperature increases of +2°C upwards, annual population growth rates remained below 1, revealing conditions under

which negative effects of temperature outweighed positive effects of increasing voltinism on population growth.

I calculated that on average third generation individuals spend 243 days as larvae, and from this I estimated that second generation individuals spend on average 278 days as larvae during the winter. At lowest field temperatures (+0°C), this translated to larval survival of 0.36 (l_3) and 0.31 ($l_{2.5}$) respectively.

Integrating voltinism in the climate model

My climate model projected that by the year 2033, the annual growth rate will shift from growing to shrinking (Figure 2.7). My findings suggest that over the projected temperature ranges in the 21st century, positive effects of increasing voltinism will not outweigh negative effects of temperatures.

DISCUSSION

My research revealed antagonistically operating consequences of warming due to climate change. I found that increasing temperatures led to increased voltinism that had a positive effect on annual growth rates. At lower levels of temperature increases, these positive effects are able to buffer the negative direct effects of increased temperatures on population vital rates. But as temperatures increase, their negative direct effects begin to outweigh the positive indirect effects of voltinism.

The implications of these antagonistic consequences are far reaching. My results suggest that the trajectory of future greenhouse gas emissions levels will determine future population viability. For example, if emissions follow the RCP 4.5 scenario leading to mean global

temperature increases of up to +2°C (Thomson et al. 2011), my model suggests that populations may not experience declines. I expect that the negative effects of relatively lower temperature increases for the next one to two decades will be mitigated by increasing voltinism. If emissions do not lead to stabilizing temperatures in later years, I predict that populations will decline.

The climate-informed population model therefore delineates a short window of time in which to act. Aside from limiting emissions, my findings suggest several possible management strategies that would promote population persistence by targeting undesirable temperature changes. One such strategy would be to identify and conserve climate refugia where environmental conditions will allow population persistence during climate change (Keppel et al. 2012, Keppel et al. 2015, Morelli et al. 2016). Another strategy would be to construct corridors to enable populations to disperse to lower temperature habitats (Beier 2012). Finally, further research on micro-climate differences could assist development of restoration actions that promote cooler habitats (Meyer & Sisk 2001, Weiss et al. 1993).

There is some evidence to suggest that butterflies will be able to adapt to effects of increased temperatures. The model assumes that butterfly photoperiod response remains constant over time, but this may not be the case. There is support for fast evolutionary adaptation to warming in mosquitoes (Bradshaw & Holzapfel 2001) and beetles (Bean et al. 2012), whereby shifting towards shorter critical photoperiods enables populations to take advantage of longer growing seasons. I observed variation within egg clutches to either develop directly or diapause, suggesting that there may be heritable genetic variation in the population for natural selection to act upon. If this is the case, *S. appalachia* could adapt by adding another (fourth) generation. While genetic changes based on seasonality and photoperiodism are possible, there are no known

genetic responses to climate change that have led to higher thermal tolerance or increased thermal optima for performance (Bradshaw & Holzapfel 2008).

My study benefited from my field methodological approach. It can be difficult to extricate emergence phenology and relative daily adult abundance using count surveys alone (Calabrese 2012). My approach enabled me to separately estimate these factors. Furthermore, as compared to laboratory studies, my use of field-derived photoperiod responses provided a realistic estimate of critical photoperiod timing. Most studies do not evaluate critical photoperiod in the field but rather in growth chambers under constant temperatures (Musolin 2012). Variation in temperature due to natural daily fluctuations can affect photoperiod response such that estimates from growth chambers differ from field estimates (Lewis et al. 2003, Bean et al. 2007). My photoperiod response curve also enabled me to estimate proportional voltinism, revealing potential shifts from a partial to near-full generation over the course of a century under 'business as usual' (RCP 8.5).

Ultimately, shifting phenology will determine the seasonal temperatures to which butterflies will be exposed. A future step to improve my model would be to use the measured emergence GDD to project the timing of each life stage per generation. Improving the model in this way would allow for potential future feedback between phenology and temperature. The model also does not take into account possible negative effects of increased voltinism due to developmental traps that arise when unfavorable fall conditions cause high mortality in the additional generation (Van Dyck et al. 2015). I could assess the existence of a developmental trap for *S. appalachia* by determining the GDD necessary for eggs to reach the early-instar point at which diapause occurs and use the downscaled climate dataset to evaluate whether there is sufficient GDD at the end of each annual third egg generation.

My study is more integrative than many others that have attempted to quantify the population growth of temperate insects in the face of anthropogenic climate change. For example, a recent and notable study by Deutsch et al. (2018) used thermal performance curves to predict global crop loss to insects, yet ignored population effects of increased voltinism. Several spatially explicit studies predict increased voltinism of insect pests that are exposed to evolutionarily novel environments but do not directly combine their findings with the demography of their model species (Grevstad & Coop 2015, Lange et al. 2009). On the other hand, Crozier and Dwyer (2006) integrate voltinism into population models as a function of temperature alone and do not include photoperiod response.

The majority of studies that have addressed species phenology by incorporating downscaled climate datasets and/or demographic mechanisms focus on species of economic importance (Logan et al. 2003). These studies include models of the tree-killing mountain pine beetle (Bentz et al. 2016) and the grape berry moth (Tobin et al. 2008) rather than species of conservation concern.

My approach is applicable to other climate-informed population models and species responses that are of interest to a wide range of fields including population ecology, conservation biology, climate change ecology, invasive species ecology and biological control. My findings can inform studies investigating effects of phenological shifts on biological interactions (Ponti et al. 2014, Bartomeus et al. 2011) and potentially resultant mismatches such as those between caterpillars and their host plants (Both et al. 2009) or predator-prey interactions (Visser et al. 2006, van Asch et al. 2007). Ultimately, mechanistic models incorporating multiple biological mechanisms such as demography, phenology, physiology and biological interactions will improve our ability to make realistic projections of species responses to climate change (Urban et

al. 2016). My findings demonstrate the complex interplay between separate direct and indirect consequences of climate change, revealing the conditions where temperature and phenology effects balance each other and where direct temperature effects outweigh positive effects of increased voltinism on population growth rates.

TABLES

Table 2.1. Dates that define presence of individuals in each life stage per generation from which temperatures were extracted from the MACA downscaled climate dataset. Warming experiments revealed that on average individual eggs survived for 7 days, non-diapausing larvae survived for 48 days and adults survived for 11 days. Based on the transect surveys, I found that adults first emerged in the springtime on May 1st and that the first adult flight period lasted a month and a half until June 15th. Separately, I also found that females emerged on average 5 days later than males in the experimental enclosures.

Life Stage	**Generation**	**'Season' Dates**	**Temperature**
Adult Female	1st	May 6 – June 15	T_{F_1}
Egg	1st	May 6 – June 22	T_{e_1}
Larva	1st	May 13 – August 9	T_{l_1}
Adult Female	2nd	July 4 – August 20	T_{F_2}
Egg	2nd	July 4 – August 27	T_{e_2}
Larva	2nd (direct)	July 11 – September 28	T_{l_2}
Larva	2nd (diapause)	August 11 – following year	NA
Adult Female	3rd (winter)	August 28 – October 9	T_{F_3}
Egg	3rd (winter)	September 2 – October 16	T_{e_3}
Larva	3rd (winter)	September 9 – May 1 following year	T_{l_3}

FIGURES

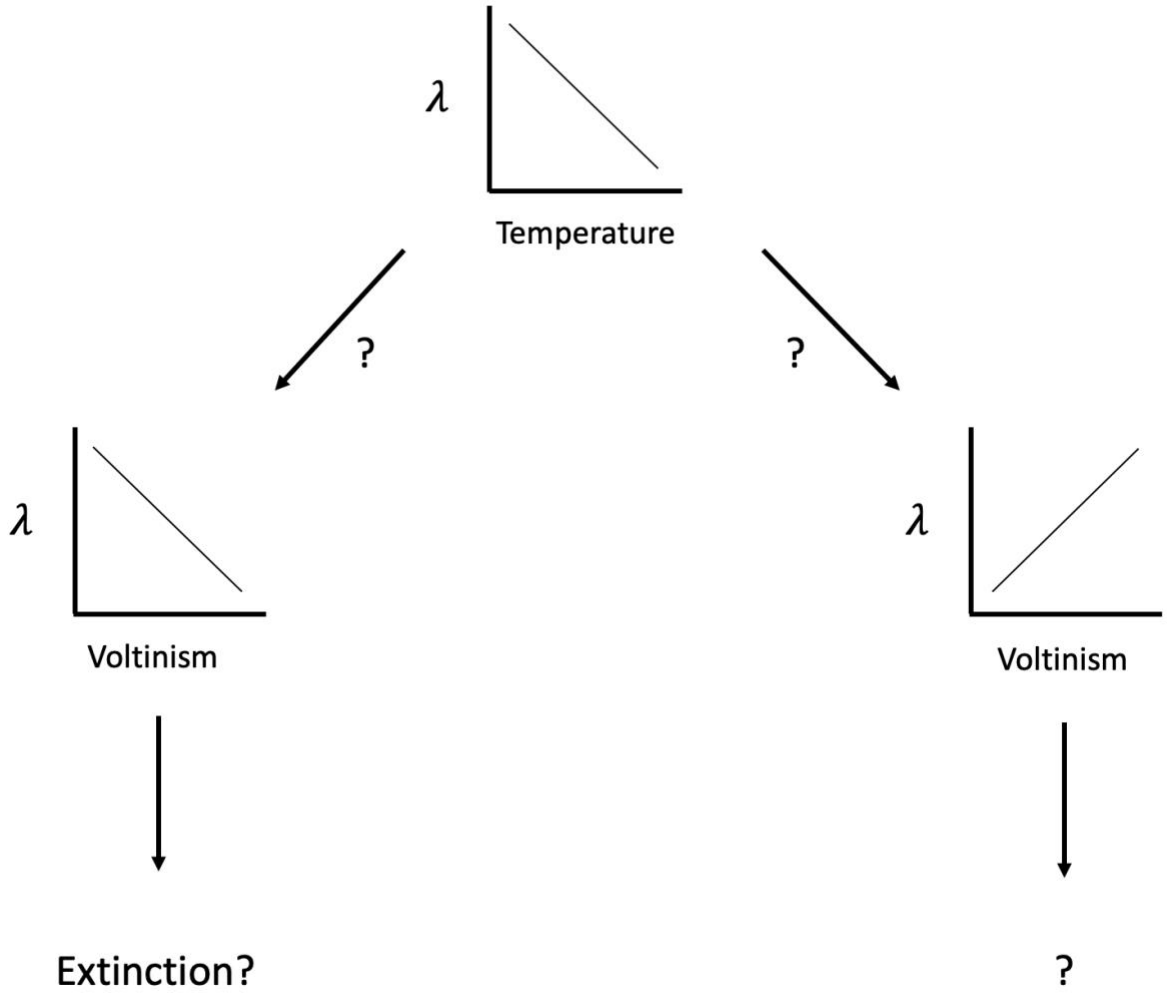

Figure 2.1. Conceptual model illustrating possible consequences of climate change. On the left side, increased voltinism decreases population growth and the effects of temperature and voltinism work synergistically. On the right side, increased voltinism increases population growth and the effects of temperature and voltinism work antagonistically.

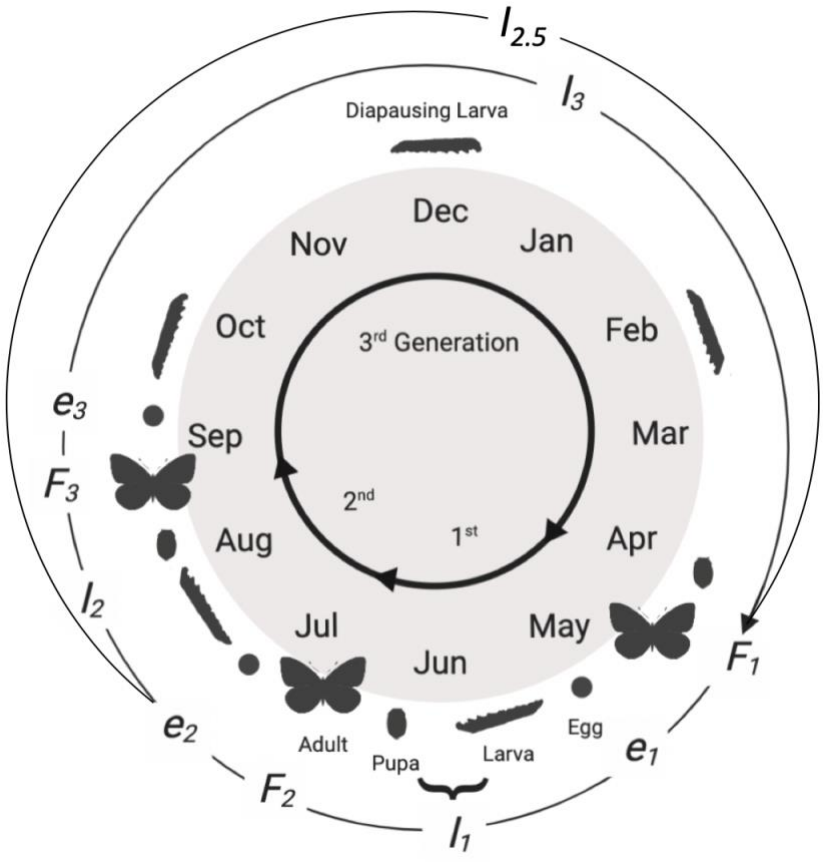

Figure 2.2. Annual lifecycle of *S. appalachia*. Larvae go into diapause during either the second ($l_{2.5}$) or the third generation (l_3).

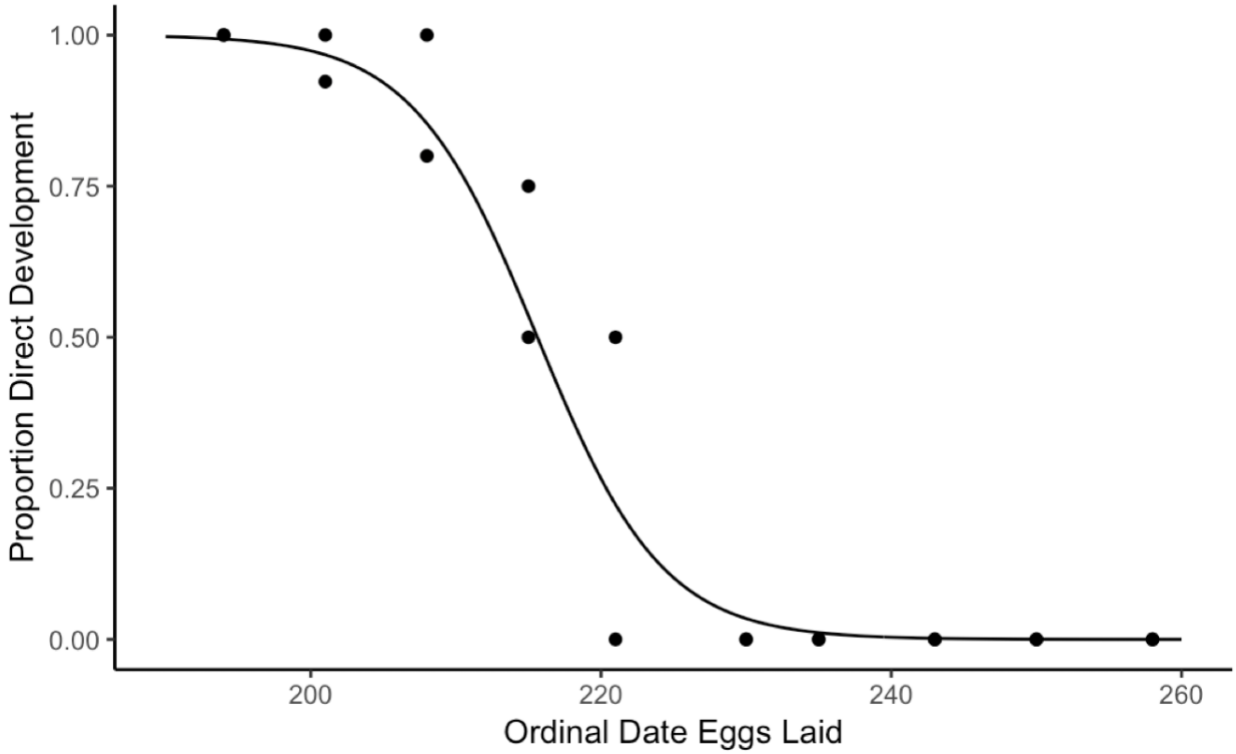

Figure 2.3. Changing proportion of individuals developing directly into third flight period adults by ordinal date that eggs were laid. Points represent 1 or 2 clutches (always 2 clutches per date, so single points on one date represent 2 clutches). Curve represents binomial fit predicting that 50% of eggs laid on the ordinal date of 216 would initiate larval diapause.

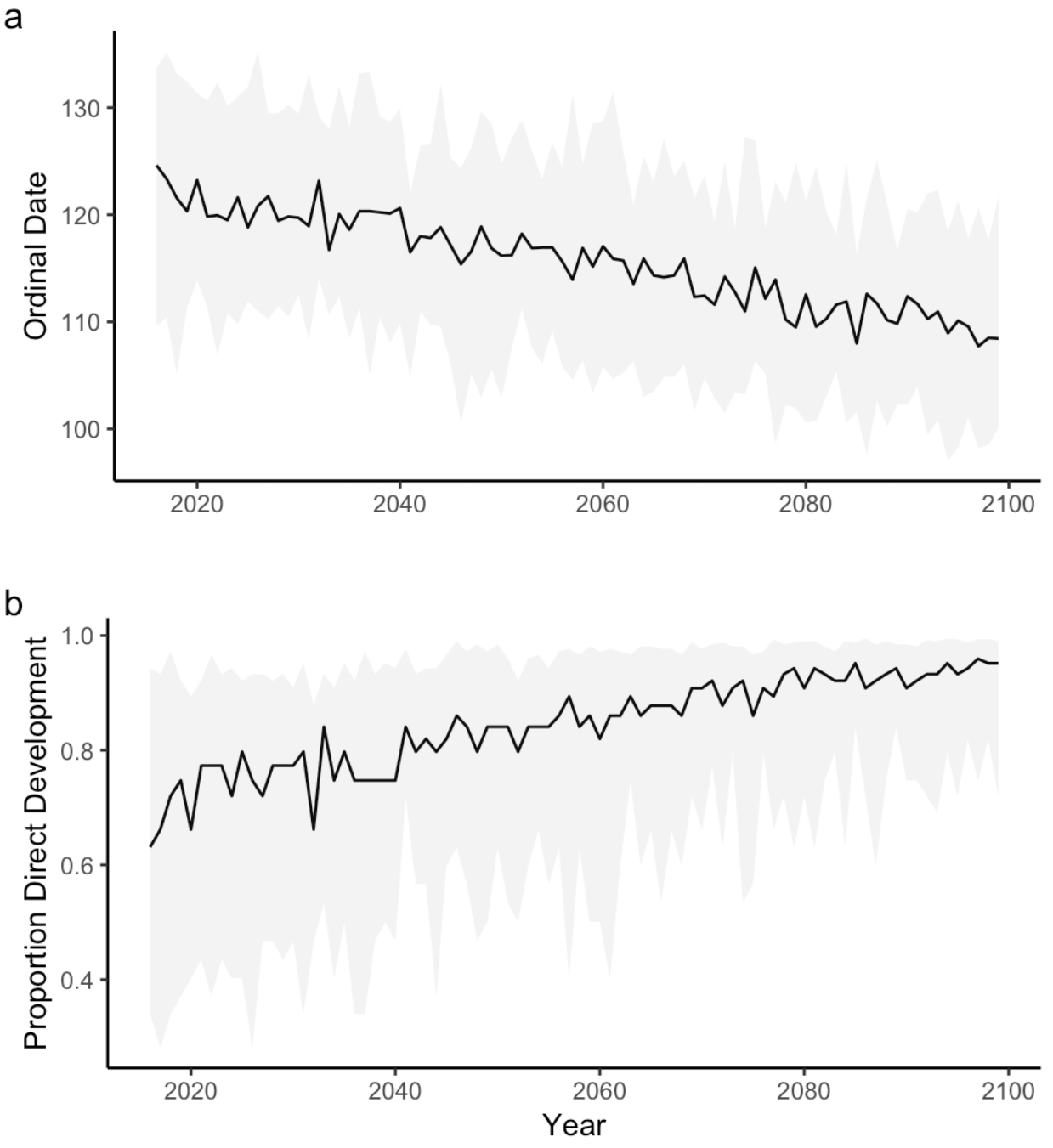

Figure 2.4. Increasing projected temperatures result in a) decreasing ordinal date of first emergence over time for the first flight period and b) increasing ratio of individuals developing directly into third flight period adults versus going into diapause. First emergence occurs at 412 GDD. Line represents median value and grey shading represents 5th to 95th percentile range from 20 GCMs.

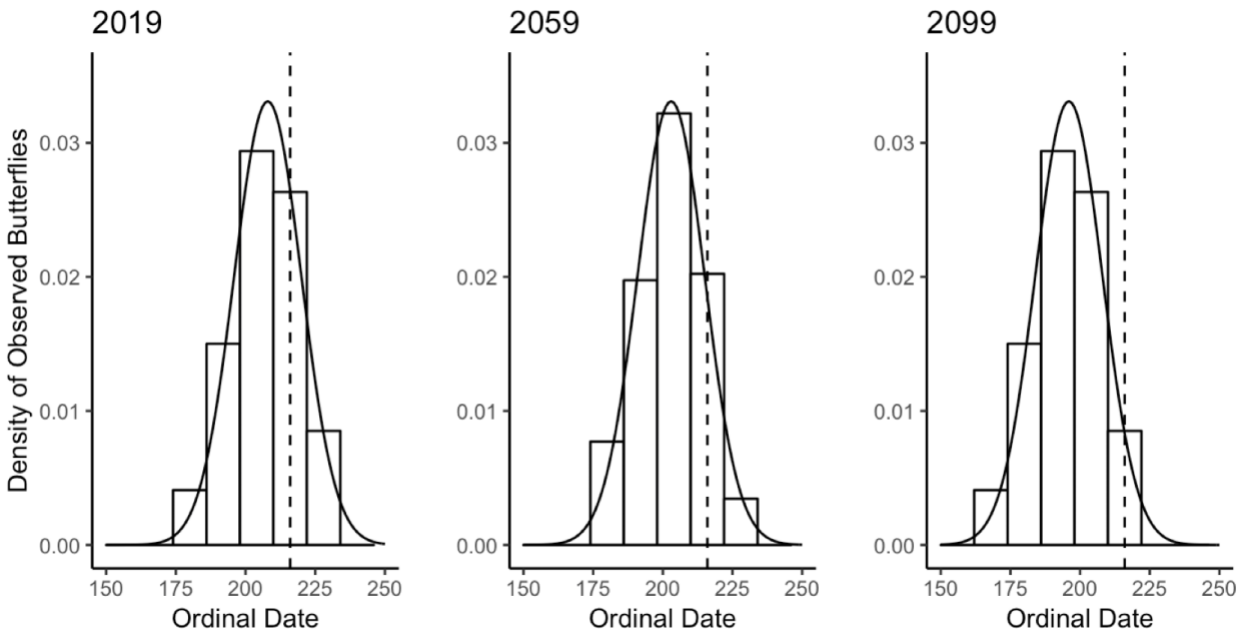

Figure 2.5. Shifted projected transect counts for the years 2019, 2059 and 2099 under the RCP8.5 emissions scenario based on the median value of 20 GCMs. Dashed line represents critical photoperiod occurring at ordinal date 216. Offspring laid by individuals to the left of the line develop directly into third flight period adults, whereas offspring laid by individuals to the right of the line go into diapause. The projected proportion of individuals developing directly is 75%, 86% and 95% for 2019, 2059, and 2099 respectively.

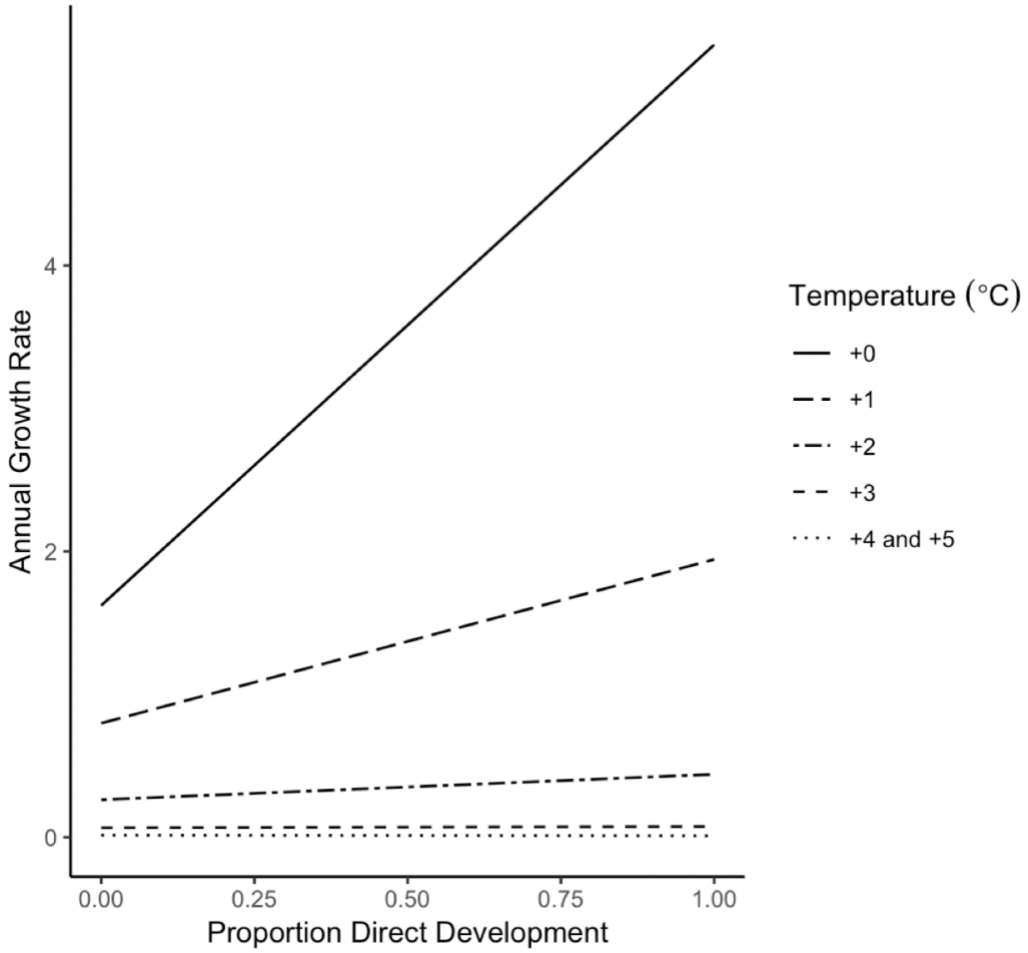

Figure 2.6. Annual growth rate from population model parameterized by a range of temperatures (lowest field temperatures up to +5°C) comparing no direct development (2 generations) to 100% direct development (3 generations). All annual growth rate estimates at temperature increases of +4°C and +5°C were < 0.015. Model incorporated larval predation.

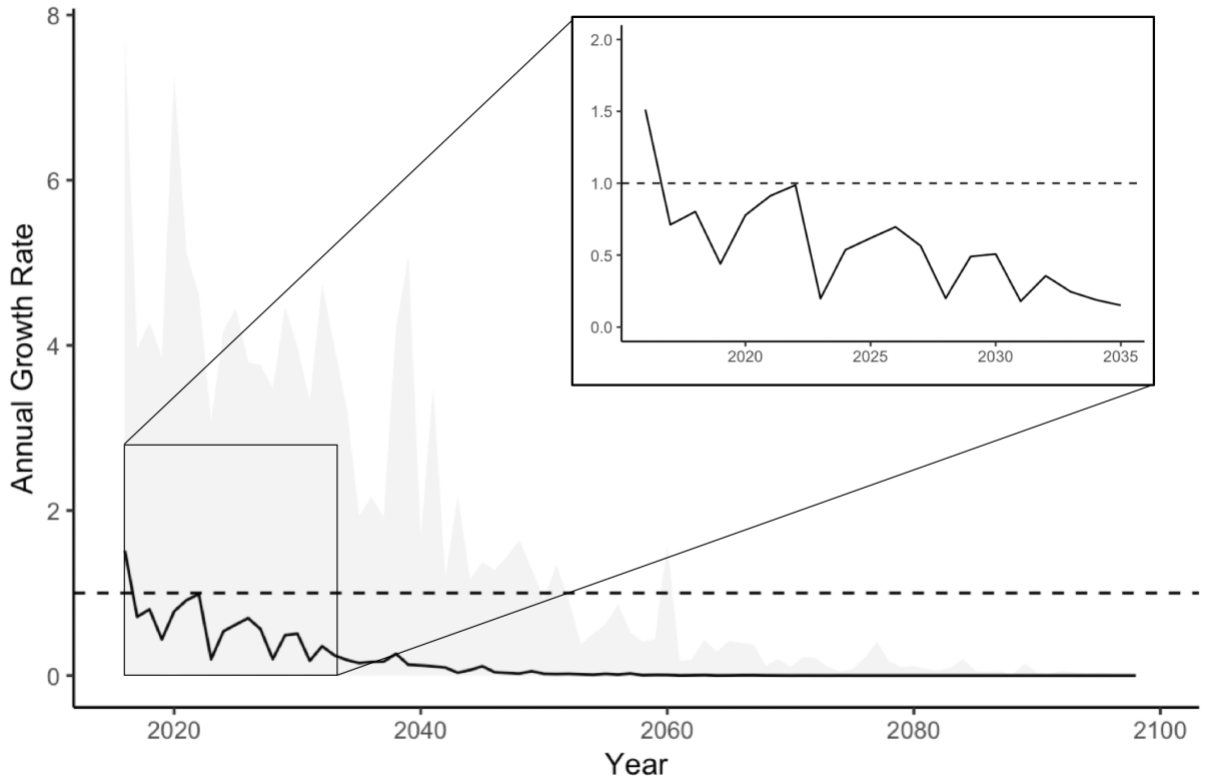

Figure 2.7. Projected annual growth rate from 2016-2099 incorporating shifting voltinism due to increased temperatures throughout the time period. Model incorporated larval predation.

REFERENCES

1. Abatzoglou John T., & Brown Timothy J. (2012). A comparison of statistical downscaling methods suited for wildfire applications. International Journal of Climatology, 32(5), 772–780.

2. Altermatt, F. (2010). Climatic warming increases voltinism in European butterflies and moths. Proceedings of the Royal Society of London B: Biological Sciences, 277(1685), 1281–1287.

3. Aschehoug, E. T., Sivakoff, F. S., Cayton, H. L., Morris, W. F., & Haddad, N. M. (2015). Habitat restoration affects immature stages of a wetland butterfly through indirect effects on predation. Ecology, 96(7), 1761–1767.

4. Bartomeus, I., Ascher, J. S., Wagner, D., Danforth, B. N., Colla, S., Kornbluth, S., & Winfree, R. (2011). Climate-associated phenological advances in bee pollinators and bee-pollinated plants. Proceedings of the National Academy of Sciences, 108(51), 20645–20649.

5. Bean, Dan W., Dalin, P., & Dudley, T. L. (2012). Evolution of critical day length for diapause induction enables range expansion of Diorhabda carinulata, a biological control agent against tamarisk (Tamarix spp.). Evolutionary Applications, 5(5), 511–523.

6. Bean, Daniel W., Wang, T., Bartelt, R. J., & Zilkowski, B. W. (2007). Diapause in the Leaf Beetle Diorhabda elongata (Coleoptera: Chrysomelidae), a Biological Control Agent for Tamarisk (Tamarix spp.). Environmental Entomology, 36(3), 531–540.

7. Beier, P. (2012). Conceptualizing and Designing Corridors for Climate Change. Ecological Restoration, 30(4), 312–319.

8. Bentz, B. J., Duncan, J. P., & Powell, J. A. (2016). Elevational shifts in thermal suitability for mountain pine beetle population growth in a changing climate. Forestry: An International Journal of Forest Research, 89(3), 271–283.

9. Both, C., Asch, M. V., Bijlsma, R. G., Burg, A. B. V. D., & Visser, M. E. (2009). Climate change and unequal phenological changes across four trophic levels: Constraints or adaptations? Journal of Animal Ecology, 78(1), 73–83.

10. Bradshaw, W. E., & Holzapfel, C. M. (2001). Genetic shift in photoperiodic response correlated with global warming. Proceedings of the National Academy of Sciences, 98(25), 14509–14511.

11. Brakefield, P. M. (1982). Ecological Studies on the Butterfly Maniola jurtina in Britain. II. Population Dynamics: The Present Position. The Journal of Animal Ecology, 51(3), 727.

12. Bryant, S. R., Thomas, C. D., & Bale, J. S. (2002). The influence of thermal ecology on the distribution of three nymphalid butterflies. Journal of Applied Ecology, 39(1), 43–55.

13. Calabrese, J. M. (2012). How emergence and death assumptions affect count-based estimates of butterfly abundance and lifespan. Population Ecology, 54(3), 431–442.

14. Cayton, H. L., Haddad, N. M., Gross, K., Diamond, S. E., & Ries, L. (2015). Do growing degree days predict phenology across butterfly species? Ecology, 96(6), 1473–1479.

15. Crozier, L., & Dwyer, G. (2006). Combining Population-Dynamic and Ecophysiological Models to Predict Climate-Induced Insect Range Shifts. The American Naturalist, 167(6), 853–866.

16. Danilevskii, A. S. (1965). Photoperiodism and seasonal development of insects. Photoperiodism and Seasonal Development of Insects.

17. Descimon, H., Bachelard, P., Boitier, E., & Pierrat, V. (2005). Decline and extinction of Parnassius apollo populations in France-continued. Studies on the Ecology and Conservation of Butterflies in Europe, 1, 114-115.

18. Deutsch, C. A., Tewksbury, J. J., Tigchelaar, M., Battisti, D. S., Merrill, S. C., Huey, R. B., & Naylor, R. L. (2018). Increase in crop losses to insect pests in a warming climate. Science, 361(6405), 916–919.

19. Grevstad, F. S., & Coop, L. B. (2015). The consequences of photoperiodism for organisms in new climates. Ecological Applications, 25(6), 1506–1517.

20. Haddad, N. M., Hudgens, B., Damiani, C., Gross, K., Kuefler, D., & Pollock, K. (2008). Determining Optimal Population Monitoring for Rare Butterflies. Conservation Biology, 22(4), 929–940.

21. Keppel, G., Mokany, K., Wardell-Johnson, G. W., Phillips, B. L., Welbergen, J. A., & Reside, A. E. (2015). The capacity of refugia for conservation planning under climate change. Frontiers in Ecology and the Environment, 13(2), 106–112.

22. Keppel, G., Niel, K. P. V., Wardell-Johnson, G. W., Yates, C. J., Byrne, M., Mucina, L., … Franklin, S. E. (2012). Refugia: Identifying and understanding safe havens for biodiversity under climate change. Global Ecology and Biogeography, 21(4), 393–404.

23. Kiekebusch, E. (2019). Effects of temperature, phenology and geography on butterfly population dynamics under climate change. North Carolina State University.

24. Knutti, R., Furrer, R., Tebaldi, C., Cermak, J., & Meehl, G. A. (2009). Challenges in Combining Projections from Multiple Climate Models. Journal of Climate, 23(10), 2739–2758.

25. Kuefler, D., Haddad, N. M., Hall, S., Hudgens, B., Bartel, B., & Hoffman, E. (2008). Distribution, population structure and habitat use of the endangered Saint Francis Satyr

butterfly, Neonympha mitchellii francisci. The American Midland Naturalist, 159(2), 298–320.

26. Lange, H., Økland, B., & Krokene, P. (2006). Thresholds in the life cycle of the spruce bark beetle under climate change. 11.

27. Lewis, P. A., DeLoach, C. J., Knutson, A. E., Tracy, J. L., & Robbins, T. O. (2003). Biology of Diorhabda elongata deserticola (Coleoptera: Chrysomelidae), an Asian leaf beetle for biological control of saltcedars (Tamarix spp.) in the United States. Biological Control, 27(2), 101–116.

28. Logan, J. A., Régnière, J., & Powell, J. A. (2003). Assessing the impacts of global warming on forest pest dynamics. Frontiers in Ecology and the Environment, 1(3), 130–137.

29. Ma, G., Rudolf, V. H. W., & Ma, C. (2015). Extreme temperature events alter demographic rates, relative fitness, and community structure. Global Change Biology, 21(5), 1794–1808.

30. Martín-Vertedor, D., Ferrero-García, J. J., & Torres-Vila, L. M. (2010). Global warming affects phenology and voltinism of Lobesia botrana in Spain. Agricultural and Forest Entomology, 12(2), 169–176.

31. Matsuzawa, Y., Sato, K., Sakamoto, W., & Bjorndal, K. (2002). Seasonal fluctuations in sand temperature: Effects on the incubation period and mortality of loggerhead sea turtle (Caretta caretta) pre-emergent hatchlings in Minabe, Japan. Marine Biology, 140(3), 639–646.

32. McMaster, G. S., & Wilhelm, W. W. (1997). Growing degree-days: One equation, two interpretations. Agricultural and Forest Meteorology, 87(4), 291–300.

33. Meyer, C. L., & Sisk, T. D. (2001). Butterfly Response to Microclimatic Conditions Following Ponderosa Pine Restoration. Restoration Ecology, 9(4), 453–461.

34. Morelli, T., Daly, C., Dobrowski, S., Dulen, D., Ebersole, J., Jackson, S., … Beissinger, S. (2016) Managing Climate Change Refugia for Climate Adaptation. *PLOS ONE* 11(8), e0159909

35. Moore, J. L., & Remais, J. V. (2014). Developmental Models for Estimating Ecological Responses to Environmental Variability: Structural, Parametric, and Experimental Issues. Acta Biotheoretica, 62(1), 69–90.

36. Musolin, D. L. (2012). Surviving winter: Diapause syndrome in the southern green stink bug Nezara viridula in the laboratory, in the field, and under climate change conditions. Physiological Entomology, 37(4), 309–322.

37. Oliver, T. H., Marshall, H. H., Morecroft, M. D., Brereton, T., Prudhomme, C., & Huntingford, C. (2015). Interacting effects of climate change and habitat fragmentation on drought-sensitive butterflies. Nature Climate Change, 5(10), 941–945.

38. Parmesan, C. (2006). Ecological and Evolutionary Responses to Recent Climate Change. Annual Review of Ecology, Evolution, and Systematics, 37(1), 637–669.
39. Parmesan, C., & Yohe, G. (2003). A globally coherent fingerprint of climate change impacts across natural systems. Nature, 421(6918), 37–42.

40. Ponti, L., Gutierrez, A. P., Ruti, P. M., & Dell'Aquila, A. (2014). Fine-scale ecological and economic assessment of climate change on olive in the Mediterranean Basin reveals winners and losers. Proceedings of the National Academy of Sciences, 111(15), 5598–5603.

41. R Core Team (2018). R: A language and environment for statistical computing. R Foundation for Statistical Computing, Vienna, Austria. URL https://www.R-project.org/.

42. Robinet, C., & Roques, A. (2010). Direct impacts of recent climate warming on insect populations. Integrative Zoology, 5(2), 132–142.

43. Root, T. L., Price, J. T., Hall, K. R., Schneider, S. H., Rosenzweig, C., & Pounds, J. A. (2003). Fingerprints of global warming on wild animals and plants. Nature, 421(6918), 57–60.

44. Roy, D. B., & Sparks, T. H. (2000). Phenology of British butterflies and climate change. Global Change Biology, 6(4), 407–416.

45. Singer Michael C., & Parmesan Camille. (2010). Phenological asynchrony between herbivorous insects and their hosts: Signal of climate change or pre-existing adaptive strategy? Philosophical Transactions of the Royal Society B: Biological Sciences, 365(1555), 3161–3176.

46. Sivakoff, F. S., Morris, W. F., Aschehoug, E. T., Hudgens, B. R., & Haddad, N. M. (2016). Habitat restoration alters adult butterfly morphology and potential fecundity through effects on host plant quality. Ecosphere, 7(11), e01522. 10.1002/ecs2.1522.

47. Stefanescu, C., Peñuelas, J., & Filella, I. (2003). Effects of climatic change on the phenology of butterflies in the northwest Mediterranean Basin. Global Change Biology, 9(10), 1494–1506.

48. Tauber, M. J., & Tauber, C. A. (1976). Insect Seasonality: Diapause Maintenance, Termination, and Postdiapause Development. Annual Review of Entomology, 21(1), 81–107.

49. Terando, A. J., Youngsteadt, E., Meineke, E. K., & Prado, S. G. (2017). Ad hoc instrumentation methods in ecological studies produce highly biased temperature measurements. Ecology and Evolution, 00, 1-15.

50. Thomas, J. A., Welch, J. J., Lanfear, R., & Bromham, L. (2010). A Generation Time Effect on the Rate of Molecular Evolution in Invertebrates. Molecular Biology and Evolution, 27(5), 1173–1180.

51. Thomson, A. M., Calvin, K. V., Smith, S. J., Kyle, G. P., Volke, A., Patel, P., … Edmonds, J. A. (2011). RCP4.5: A pathway for stabilization of radiative forcing by 2100. Climatic Change, 109(1), 77.

52. Tobin, P. C., Nagarkatti, S., Loeb, G., & Saunders, M. C. (2008). Historical and projected interactions between climate change and insect voltinism in a multivoltine species. Global Change Biology, 14(5), 951–957.

53. Urban, M. C., Bocedi, G., Hendry, A. P., Mihoub, J.-B., Pe'er, G., Singer, A., … Travis, J. M. J. (2016). Improving the forecast for biodiversity under climate change. Science, 353(6304), aad8466.

54. Van Asch, M., Van Tienderen, P. H., Holleman, L. J. M., & Visser, M. E. (2007). Predicting adaptation of phenology in response to climate change, an insect herbivore example. Global Change Biology, 13(8), 1596–1604.

55. Van Dyck, H., Bonte, D., Puls, R., Gotthard, K., & Maes, D. (2015). The lost generation hypothesis: Could climate change drive ectotherms into a developmental trap? Oikos, 124(1), 54–61.

56. Visser, M. E., Holleman, L. J. M., & Gienapp, P. (2006). Shifts in caterpillar biomass phenology due to climate change and its impact on the breeding biology of an insectivorous bird. Oecologia, 147(1), 164–172.

57. Weiss, S. B., Murphy, D. D., Ehrlich, P. R., & Metzler, C. F. (1993). Adult emergence phenology in checkerspot butterflies: The effects of macroclimate, topoclimate, and population history. Oecologia, 96(2), 261–270.

58. Wepprich, T. (2017) Effects of Climatic Variability on a Statewide Butterfly Community. North Carolina State University.

59. Wilby, R. L., & Wigley, T. M. L. (1997). Downscaling general circulation model output: A review of methods and limitations. Progress in Physical Geography: Earth and Environment, 21(4), 530–548.

60. Xue, F.-S., Kallenborn, H. G., & Wei, H.-Y. (1997). Summer and winter diapause in pupae of the cabbage butterfly, Pieris melete Ménétriés. Journal of Insect Physiology, 43(8), 701–707.

61. Zonneveld, C. (1991). Estimating death rates from transect counts. Ecological Entomology, 16(1), 115–121.

CHAPTER 3: Demographic responses to warming across a mid-latitude species' range

ABSTRACT

The effects of climate change on ectothermic species vary geographically, leading to population demographic changes and range boundary shifts for terrestrial species. Tropical species are likely to be more vulnerable to future warming than their temperate counterparts due to higher relative thermal sensitivity and proximity to temperatures near thermal optima. Response patterns of mid-latitude species are less straightforward due to higher variability among taxa. Using a single species of butterfly (*Satyrodes appalachia*) that inhabits a mid-latitude range in eastern North America, I compared effects of high temperatures on early-life stage survival of individuals from populations at the northern and southern species range boundaries using greenhouse warming experiments. I then evaluated the location of historic and projected future temperatures on the resulting demographic response curves. Using a suite of statistically downscaled global climate models, I compared current, mid-21st century, and end of century temperatures for both northern and southern population locations. I found that increasing temperatures decreased demographic rates across all experiments. I found no difference between the survival of individuals from northern and southern range extremes over the temperatures tested. Comparison of survival curves at observed and projected temperatures suggested that South Carolinian populations have already surpassed optima for thermal demographic response, while Michigan populations may surpass optima by the middle of the century. If emissions trajectories continue, my findings highlight the importance of the early-century window of time for conservation actions necessary to avoid population declines in the northern limits of the species range.

INTRODUCTION

The effects of climate change will vary among ectothermic species particularly due to latitudinal geography. The degree of warming will be greater at higher latitudes (Hansen et al. 2006), and this has already differentially altered species phenology (Root et al. 2003, Parmesan et al. 2007). Warming will shift species range boundaries and increase or decrease abundances (Luoto et al. 2006, Hughes 2000, Thomas & Lennon 1999). Despite these differences across space, the effects of warming on individual species fitness may be less negative at higher latitudes than in the tropics.

Two factors, thermal sensitivity and thermal range, suggest that tropical ectotherms will be particularly vulnerable to climate warming. While temperatures in the tropics are predicted to increase to an absolute level higher than in temperate zones, physiological heat tolerance of ectotherms remains similar across latitude (Diamond et al. 2012, Ghalambor et al. 2006). Tropical ectotherms are currently living closer to the high temperatures beyond which fitness will decline (critical thermal maxima) as compared to their temperate counterparts (Tewksbury et al. 2008). Additionally, ectotherms in the tropics tend to be adapted to temperature ranges that are less variable, while ectotherms in temperate climates may be considered "thermal generalists" as they are adapted to tolerate a broader range of annual temperatures (Addo-Bediako et al. 2000, Sunday et al. 2011). As global temperatures rise due to anthropogenic emissions of greenhouse gases, ectotherm fitness in the tropics will decrease if critical maxima are surpassed, while ectotherm fitness at high latitudes will not decrease with modest warming (Deutsch et al. 2008). Less well-understood is the effect of warming on fitness of mid-latitude species (Pelini et al. 2014, Youngsteadt et al. 2017), which is the focus of my study.

Population demographic rates are a useful measure of fitness as they increase with body temperature until reaching an optimum temperature beyond which they decline (Huey & Berrigan 2001). These thermal performance curves can thus provide a physiological framework to estimate direct effects of temperature on fitness (Frazier et al. 2006). Though a strong latitudinal signal has been demonstrated when comparing performance curves of taxa at the latitudinal extremes, there is less support for a unified response pattern among mid-latitude taxa (Kingsolver et al. 2013).

Consider a species inhabiting a relatively narrow mid-latitude range. Demographic responses to warming of individuals from northern and southern populations may compare in one of several different ways (Figure 3.1). First, northern populations have higher thermal tolerance resulting in higher growth rates at increased temperatures as compared to southern counterparts. Second, there is no difference in response to warming between the two populations. Third, southern populations have higher thermal tolerance than northern populations. In the first scenario, the location of actual future northern and southern temperatures suggests that northern populations will have much higher growth rates than southern populations. In the second scenario, this difference is not as pronounced. In the third scenario, higher thermal tolerance in the southern population partially mitigates the negative effects of increased future temperatures on population growth rates, such that demographic responses across the range are more similar.

To evaluate these scenarios, I compare population responses of a single species of butterfly, the Appalachian Brown (*Satyrodes appalachia*), at northern and southern extremes of its geographic range (Figure 3.2). The range encompasses approximately 15° latitude within a temperate mid-latitude zone. Using greenhouse warming experiments, I tested vital rate responses to warming at high temperature ranges for individuals from populations at northern

and southern locations within the species geographic range (Figure 3.2). I hypothesized that individuals from southern populations would not be more vulnerable to increased temperatures than individuals from northern populations due to the latitudinal narrowness of the species' geographic range and the higher temperatures I tested that placed all individuals closer to thermal maxima.

METHODS

Study species and sites

S. appalachia is a locally rare wetland butterfly. The range of *S. appalachia* encompasses a large portion of eastern North America (Carde et al. 1970) and has been observed as far north as southern Quebec, Canada and as far south as the central Gulf States, with a small isolated population in northern Florida (Opler 1998).

I collected individuals from populations located in South Carolina and Michigan which represented areas located in the northern and southern limits of the species' geographic range (Figure 3.2). In South Carolina, I collected female butterflies in a forested wetland area at the Savannah River Site in Jackson SC located at the approximate latitude of 33°N. I transported individuals to a greenhouse located on site at the Savannah River Ecology Laboratory for the experiment. In Michigan, I caught females at a forested wetland site managed by the Southwest Michigan Land Conservancy at approximately 42°N and transported them to a greenhouse located at the Kellogg Biological Station in Hickory Corners MI. I used the offspring of these females which I raised from eggs to adults.

Collection occurred during the warm summer months (June-August) of 2018 when it was feasible to catch adult female butterflies at both population locations. Experiments continued

through September by which point all experimental individuals (offspring) had emerged as adults.

Geographic range experiment

I compared the vital rate responses to increased temperatures of the offspring of individuals collected from northern and southern parts of *S. appalachia*'s geographic range. I brought all wild-caught females to the greenhouses and placed them into 'oviposition chambers' consisting of a single potted host plant (*Carex* spp.) enclosed within mesh netting. I allowed females to lay eggs for approximately 48 hours before releasing them.

I created warming enclosures using 27 x 27 x 48 "Pop Up Butterfly Terrariums" (Educational Science©). On tables in each greenhouse, I created four rows of three enclosures. I placed 100W 110V infrared ceramic heating lamps (theBlueStone©) inside the enclosures and manipulated the temperatures emitted by connecting the lamps in series to TT-300H-WH plug-in dimmers (Lutron©). I aimed to increase temperatures by up to 5°C above ambient greenhouse temperature. Within each row, I randomly assigned each enclosure to one of three warming treatments: 1) control (no lamps), 2) one lamp set at medium dimmer intensity, 3) two lamps set at high dimmer intensity. I placed two potted host plants inside the enclosure below the lamp(s) and inside plastic water-tubs. The tubs were monitored regularly, and water levels kept constant. I placed a single iButton temperature logger (Maxim©) into each enclosure to record hourly temperatures throughout the experiment.

I removed eggs from oviposition chambers in order to count them. As I could not reattach eggs to plants, I placed 7-12 eggs onto film caps laid on top of the soil of the potted plants within each heated enclosure. To estimate egg survival rates, I recorded the initial number of eggs

placed in each enclosure and the number of eggs that hatched. To estimate larval survival rates, I allowed the larvae to continue to develop until adulthood and counted the number of individuals that eclosed. To estimate the length of time individuals spent in each life stage, I averaged the amount of time it took all individuals within each enclosure to develop from eggs to larvae and from larvae to adults. I used these lengths of time and experimental start dates to define the time periods from which temperatures were extracted for further analysis.

I fit generalized linear mixed effects models using the R statistical software (R Core Team, 2018) to evaluate the effect of temperatures on egg and larval survival rates at the two sites. I combined the data from both sites and used binomial regression analyses to compare a suite of models. The models included fixed effects of the site of population origin (i.e., Michigan or South Carolina), mean, maximum and minimum temperatures as well as interactions between site and temperature variables. I did not combine more than one temperature variable in a single model. I defined maximum and minimum temperature as the average of the daily maximum and minimum temperatures experienced by the individuals in the enclosure. I also included a random effect of the row in which the enclosure was placed as the greenhouses were not equally ventilated. I ranked the models using corrected Akaike's Information Criterion (AICc, Hurvich & Tsai 1989) to identify the model that best explained the data.

Temperature comparison

I compared my fitted egg and larval survival curves to observed and projected climate data for both the Michigan and South Carolina field sites. I employed the temperature variable that emerged as the highest ranked in the model selection process. I used the METDATA interpolated climate data set (Abatzoglou 2011) to estimate temperatures at the time of the

experiment (2018) for further comparison. I extracted daily temperature data from each of the two 4-km grid cells containing the butterfly population sites. These corresponded to approximate dates during which the egg and larval experiments were carried out. I used the same dates for both sites which were time periods during which I knew that juvenile life stages were present in the field. These were June 1 – July 1 for the egg survival experiment and June 15 – September 1 for the larval survival experiment. I used the mean of the daily maximum temperatures over those time periods for further analysis.

I used the Multivariate Adapted Constructed Analogs (MACA) downscaled climate model dataset (Abatzoglou & Brown 2012) to project future temperatures. I extracted data from the same 4-km grid cells over the same time periods as above. I used data from 20 Global Climate Models (GCMs) parameterized by the RCP 8.5 ("higher emissions") scenario for the years 2018 – 2098. For each year, I calculated the mean of the daily maxima for each GCM. From the resulting 20 values, I calculated the median and the 5th to 95th percentile range and used these values to estimate future juvenile survival rates using the fitted juvenile survival curves.

RESULTS

Geographic range experiment

Increasing maximum temperatures reduced egg and larval survival (Table 3.1, Figure 3.3) in the highest ranked models for each experiment (Table 3.2, Table 3.3). Site was not included in the highest ranked models in both sets of analyses, but AICc values were similar for maximum temperature models with and without site effects. I investigated further and found that site did not significantly affect survival rates in both the egg and larval survival experiments (Table 3.1).

During both experiments, mean temperatures were correlated with maximum and minimum temperatures at $R_2 > 0.5$, so mean temperature was not included in candidate models for selection. Maximum and minimum temperatures were not well correlated ($R_2 < 0.5$) so both were included in candidate models.

An ANOVA comparison of the mean enclosure temperatures during the egg survival experiment did not show a significant effect of treatment on mean temperature ($F(2,23) = 0.291$, $p = 0.75$). An ANOVA comparison of the mean enclosure temperatures during the larval survival experiment revealed a significant effect of treatment on mean temperature ($F(2,13) = 5.27$, $p = 0.021$). A Tukey test showed that the high lamp intensity treatment was significantly warmer than control ($p=0.023$) and medium intensity ($p=0.047$). I removed treatment effects from candidate models for comparison.

In the Michigan warming experiment I unexpectedly observed adult emergence in September rather than the following spring. This surprised me as *S. appalachia* in Michigan is considered univoltine (Opler 1998). I could not corroborate my finding with observations in the field during 2018 using data from the Michigan Butterfly Network (available at pollardbase.org). However, a second annual generation was also observed for another Satyrine butterfly species during captive rearing the same year (A. Colewick pers. comm. 2018), possibly due to high summer temperatures and/or ideal conditions in greenhouse environments. This enabled me to directly compare summer larval survival between Michigan and South Carolina populations. It remains to be seen whether *S. appalachia* in Michigan will increase voltinism (number of generations per year) with increasing temperatures in the future, and what effects this could have on population responses (see Kiekebusch 2019).

Temperature comparison

My results demonstrated how population responses to warming depend on the shape of demographic curves and their position relative to regional warming (Figure 3.4). Because I did not find site differences and because projected temperatures were always higher in the southern location, Michigan individuals always had higher survival rates than South Carolinian individuals in any one year. Due to the steepness and location of the larval survival curve for example, projected 2058 temperatures resulted in a large difference in survival rates between Michigan and South Carolina individuals (Figure 3.4d, Figure 3.5d). As the same curve flattened at higher temperatures, this difference between populations decreased in the year 2098.

In Michigan, the greenhouse temperatures tested were higher than those recorded in the field during 2018. I fit a curve to the higher temperature ranges, but I was unable to extrapolate from these responses to the lower (observed) temperature ranges. This is because the location of the thermal optimum could occur at a temperature higher than the Michigan observed 2018 field temperatures but lower than the tested greenhouse temperatures. This would result in a convex curve that the experimental temperatures would be unable to detect.

My analysis revealed that the northern site is projected to experience a higher degree of warming than the southern site. The absolute level of Michigan temperatures remains lower than South Carolina temperatures over the 21st century, matching predictions in the literature (Hansen et al. 2006).

DISCUSSION

Over all experiments for the temperature ranges I tested, I found a negative effect of increasing temperature on early life-stage survival. This result in combination with observed and

projected temperatures suggests that *S. appalachia* populations in South Carolina currently exist at temperatures that surpass critical optima, while populations in Michigan are projected to surpass critical optima by the middle of the 21st century under the RCP8.5 emissions scenario.

My results across a mid-latitude range conform to the pattern of latitudinal differences in thermal performance for ectotherms whereby lower latitude species are more vulnerable to increased temperatures than higher latitude counterparts (Deutsch et al. 2008). These findings also correspond to recorded butterfly range shifts due to southern population extinctions and northern range expansions over similar mid-latitudinal zones (Hill et al. 1999, Parmesan et al. 1999, Parmesan et al. 1996). My findings add to a dearth of data on insect thermal tolerances (Youngsteadt et al. 2017), and support those of published studies that show low geographic variation in upper thermal maxima for insects (Addo-Bediako et al. 2000) as well as other ectotherms (Sunday et al. 2011, Ghalambor et al. 2006). I did not find evidence for adaptation to higher local temperatures among southern population individuals.

I carried out my experiments with two butterfly life stages during the warmest summer months. As such it is difficult to extrapolate solely from these vital rates the effects on annual population growth rates as additional measures such as fecundity, adult survival and differences in voltinism across the species range would need to be incorporated (e.g. Kiekebusch 2019). However, I can expect that the differences in vital rate responses between populations would propagate in a population model if vital rates are multiplied. I found that summer larval survival was the vital rate to which population growth was most sensitive for *S. appalachia* populations in North Carolina (Kiekebusch 2019), which reinforces the importance of my findings for population growth and viability.

Ultimate demographic impact of warming is further confounded by shortened generation time and life span (Huey & Berrigan 2001) and increased voltinism (Altermatt 2010) due to increased temperatures. In temperate zones, climate change is increasing the length of the growing season and allowing species to experience temperatures closer to or even exceeding thermal optima, either on average or through increased frequency of temperature extremes. These effects are occurring at disparate rates at mid-latitude sites with varying impacts on species fitness (Kingsolver et al. 2013), highlighting the need for species-specific physiological information to be incorporated into predictions of species responses to future climate change.

My greenhouse study had limitations that could be overcome if demographic studies were to be carried out in the field. Natural circumstances could not be tested that would normally arise in the field, for example effects of other climate variables and biotic interactions. I was unable to test the full range of 'current' Michigan temperatures that would actually be experienced by wild butterflies in my greenhouse setting. This could have informed the shape of the Michigan population's thermal curve, in particular to locate population thermal optima within the context of current Michigan temperatures.

Measurement of population demographic rates allows direct estimation of temperature effects on fitness in a spatially explicit framework. My findings display the value of comparative experiments that can improve mechanistic understanding of differential population responses to warming (Pelini et al. 2012) which is imperative to predicting future climate impacts on biodiversity (Urban et al. 2016).

My findings suggest critical windows for conservation. My analysis identifies the largest difference between the population vital rates during the middle of the century. Depending on temperature effects on other vital rates, South Carolinian populations may already be in

decline. In 2061 the larval survival rates from the 95th percentile across 20 GCM projections are first projected to drop below 0.25. But there may yet be time to avoid declines in Michigan if emissions are stabilized (e.g. as is inferred by a lower emissions scenario like RCP 4.5) or if conservation actions can be implemented that promote dispersal northwards, such as establishment of corridors (Nuñez et al. 2013) or that preserve climate refugia, locations where temperatures will remain stable (Morelli et al. 2016).

TABLES

Table 3.1. Effects of temperature and site on egg and larval survival from highest ranked generalized linear mixed effect models (binomial).

Range Experiment	**Fixed Effect**	**Chisq**	**DF**	**p**
Egg Survival	Maximum Temperature	11.184	1	**<0.001**
Egg Survival	Maximum Temperature	12.833	1	**<0.001**
	Site	2.366	1	**0.124**
Larval Survival	Maximum Temperature	7.473	1	**0.006**
Larval Survival	Maximum Temperature	8.032	1	**<0.005**
	Site	1.597	1	**0.206**

Table 3.2. Model ranking for models predicting effects of temperature variables, site and their interactions on egg survival.

Fixed Effects	Random Effect	df	logLik	AICc	delta	weight
Maximum Temperature	Row	3	-98.735	204.6	0	0.329
Maximum Temperature + Site	Row	4	-97.53	205	0.4	0.269
Minimum Temperature + Site	Row	4	-97.72	205.3	0.78	0.222
Maximum Temperature + Site + Maximum Temperature * Site	Row	5	-97.139	207.3	2.72	0.085
Minimum Temperature + Site + Minimum Temperature * Site	Row	5	-97.72	208.4	3.88	0.047
Minimum Temperature	Row	3	-100.676	208.4	3.88	0.047
Site	Row	3	-104.27	215.6	11.07	0.001

Table 3.3. Model ranking for models predicting effects of temperature variables and site on larval survival.

Fixed Effects	Random Effect	df	logLik	AICc	delta	weight
Maximum Temperature	Row	3	-19.36	46.7	0	0.734
Maximum Temperature + Site	Row	4	-18.588	48.8	2.09	0.258
Site	Row	3	-24.137	56.3	9.56	0.006
Minimum Temperature	Row	3	-25.483	59	12.25	0.002
Minimum Temperature + Site	Row	4	-24.829	61.3	14.57	0.001

FIGURES

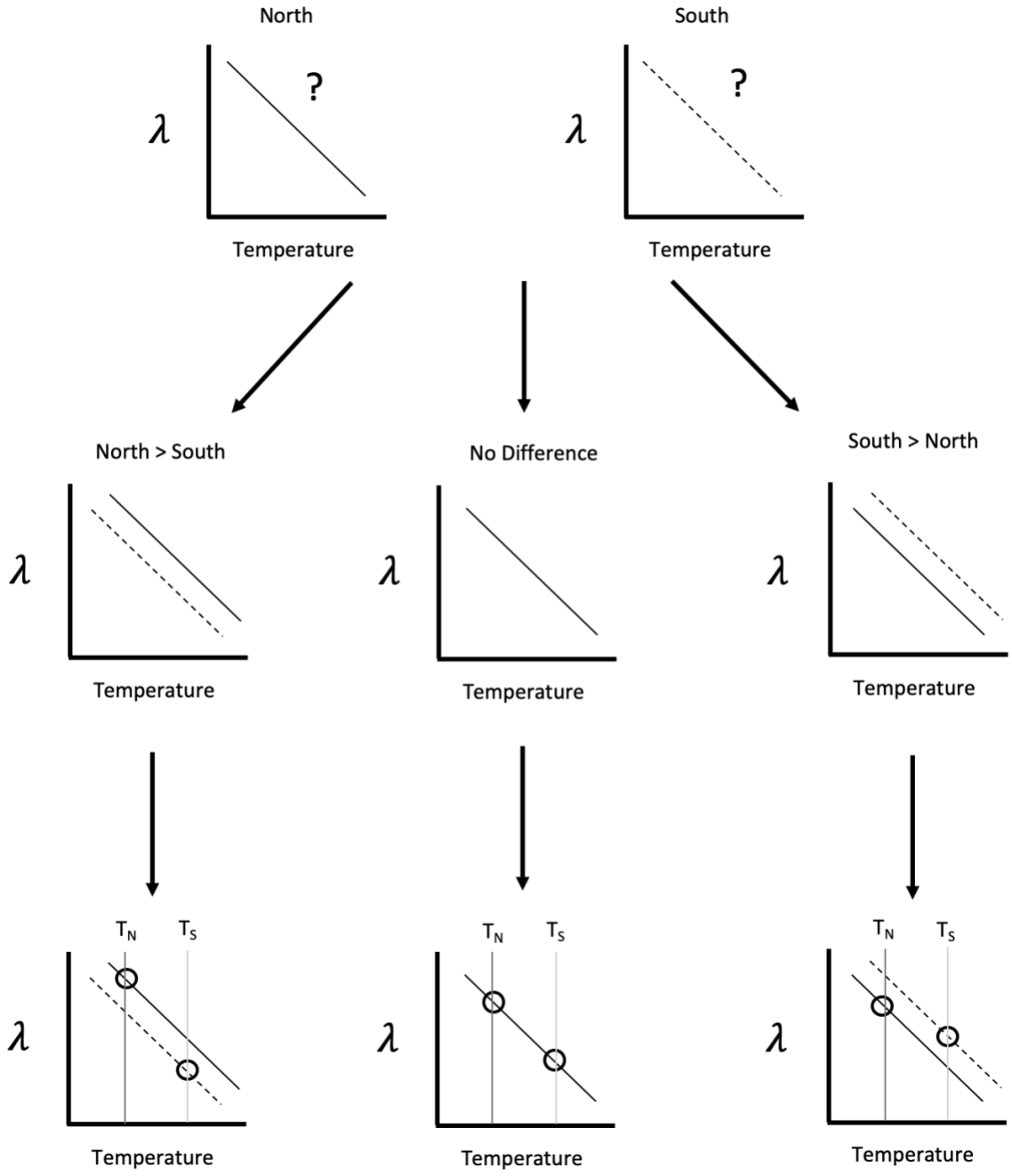

Figure 3.1. Possible demographic responses of northern and southern populations to increasing temperatures in the context of regional differences in temperatures experienced by a northern (T_N) and southern (T_S) population.

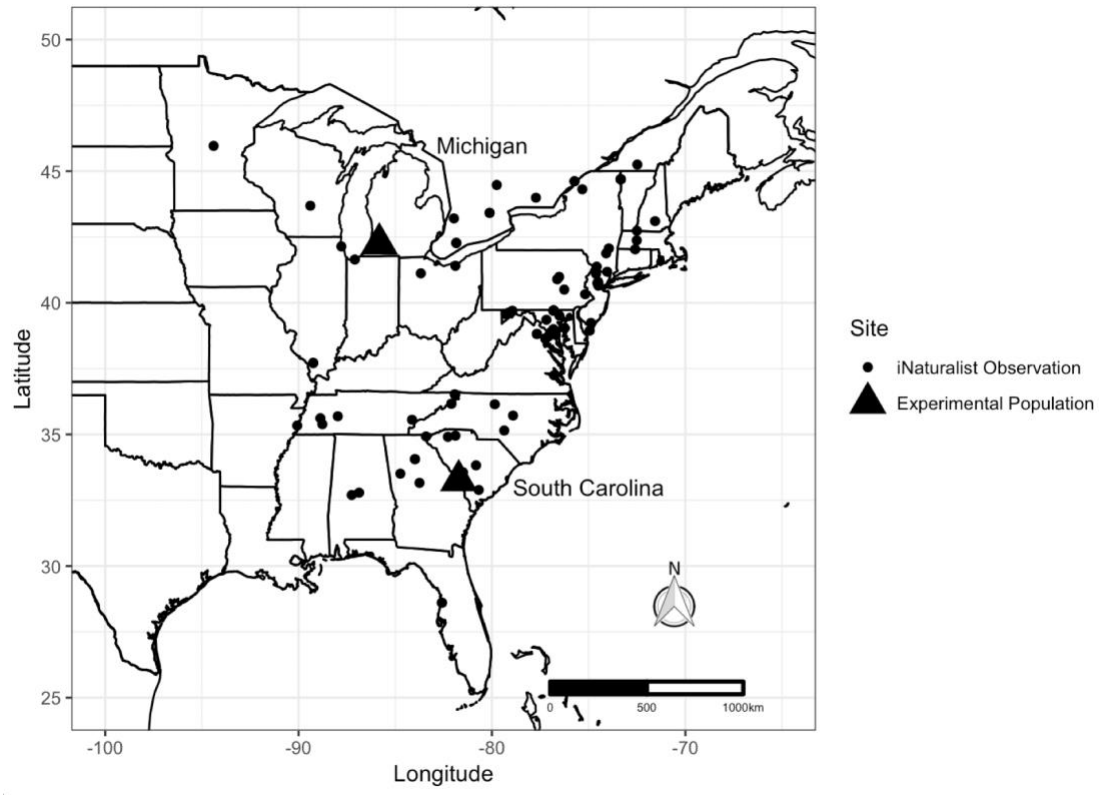

Figure 3.2. Range map for *S. appalachia* with experimental locations. Created using R package "rinat" (Barve & Hart 2017) using only butterfly observations that qualify as research grade (see Wittmann et al. 2019).

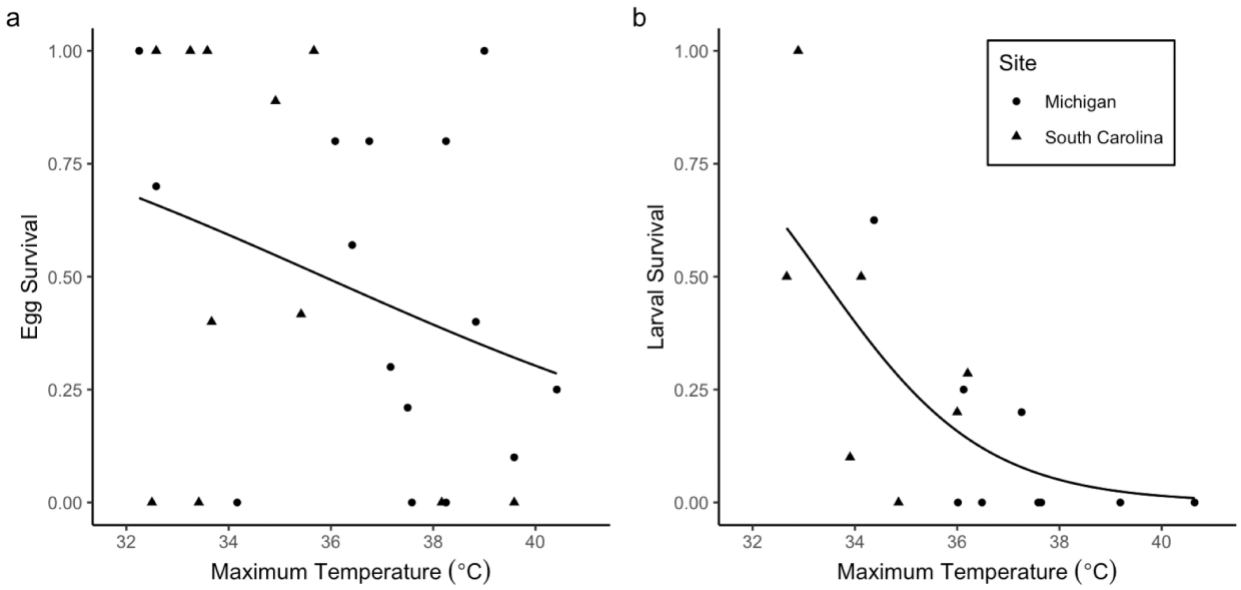

Figure 3.3. Increasing maximum temperature decreases egg (a) and larval (b) survival with no additive effect of population location (Site).

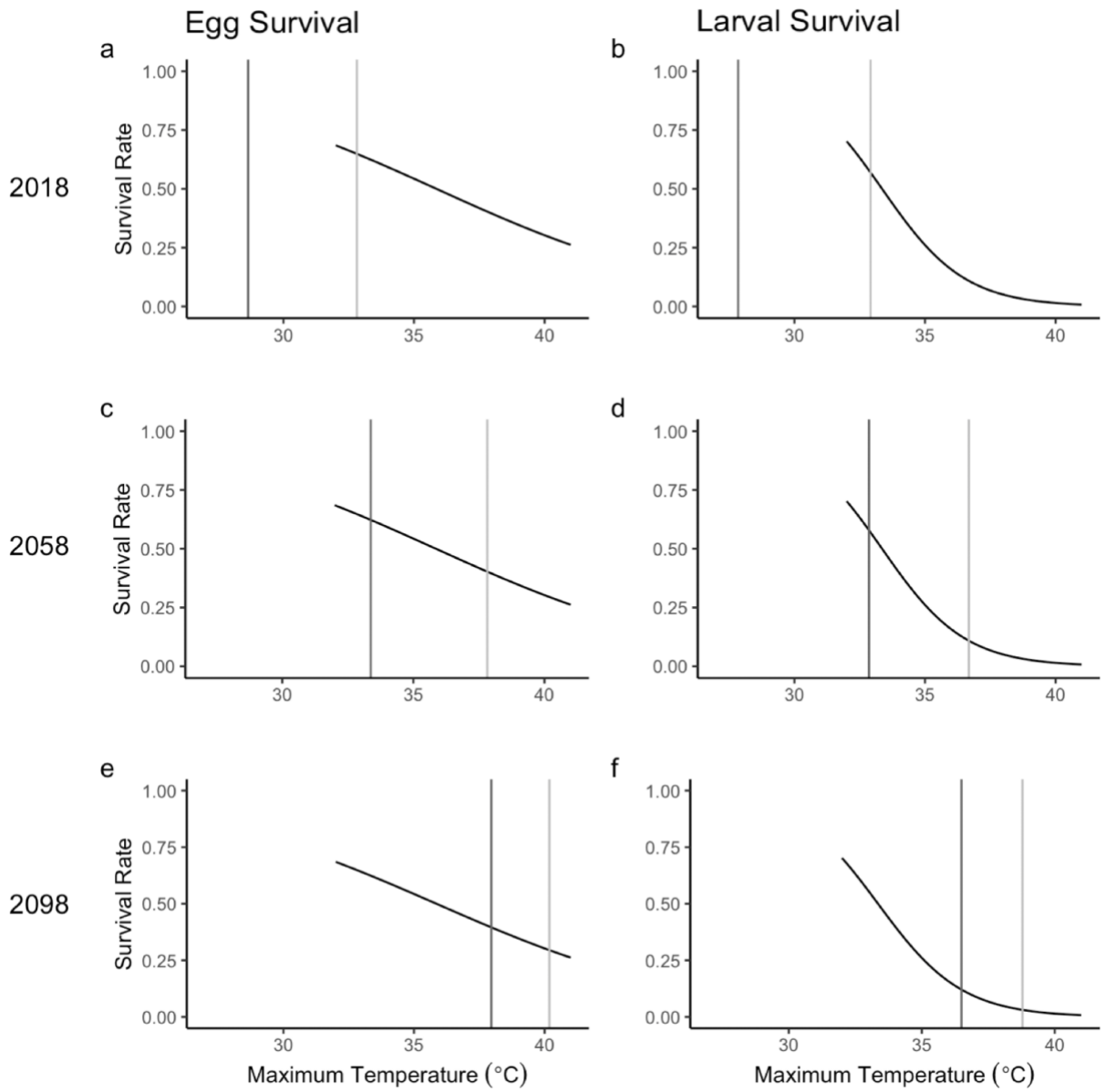

Figure 3.4. Comparing fitted egg and larval survival curves to observed and projected temperatures. Vertical lines represent average daily maximum temperatures over the estimated time periods when the egg and larval life stages occur. Dark grey vertical lines represent Michigan temperatures. Light grey vertical lines represent South Carolina temperatures. I used METDATA to find the temperatures in the year 2018. I used MACA to project the median temperatures across 20 GCMs for 2058 and 2098.

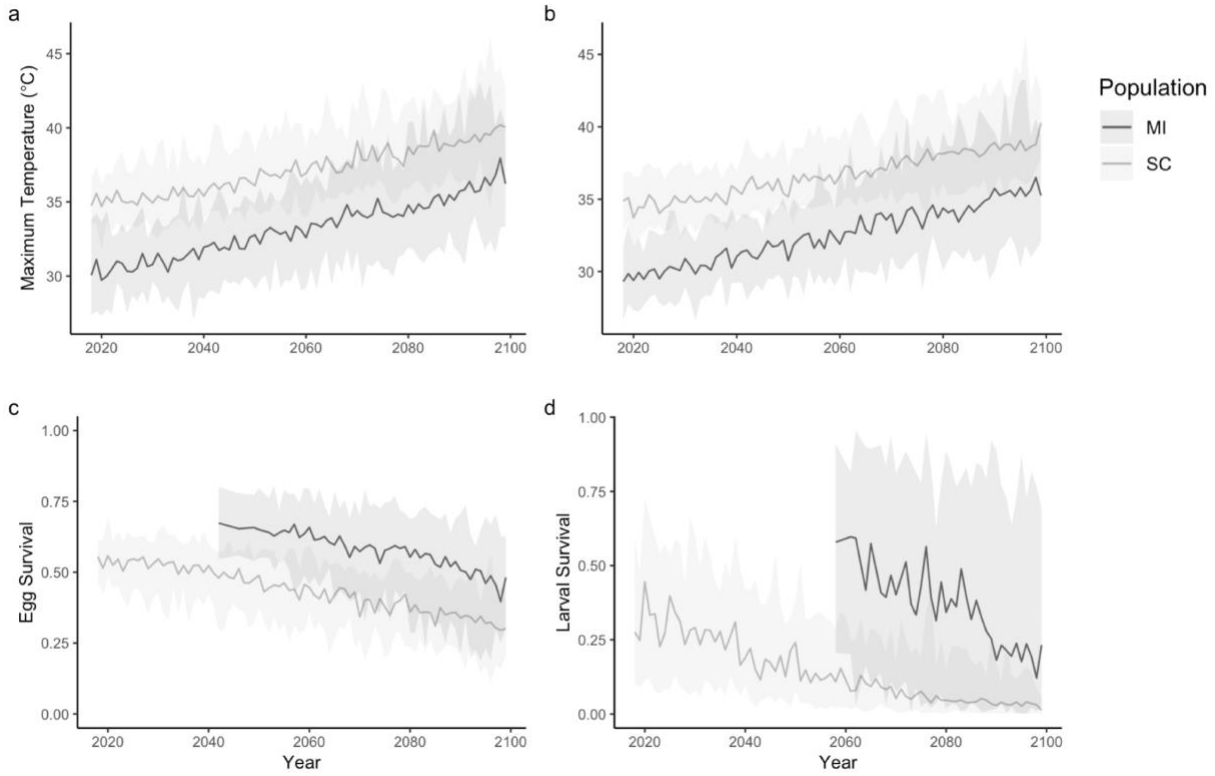

Figure 3.5. Comparative projected temperatures for eggs (a) and larvae (b) with projected vital rates respectively (c, d). Shading represents the 5th to 95th percentile range from 20 GCMs. Michigan projected egg and larval survival rates are truncated as temperatures ranges occurring before 2058 were not tested in my experiments.

REFERENCES

1. Abatzoglou, J. T. (2011). Development of gridded surface meteorological data for ecological applications and modelling. International Journal of Climatology, 33(1), 121–131.

2. Abatzoglou John T., & Brown Timothy J. (2012). A comparison of statistical downscaling methods suited for wildfire applications. International Journal of Climatology, 32(5), 772–780.

3. Addo-Bediako, A., Chown, S. L., & Gaston, K. J. (2000). Thermal tolerance, climatic variability and latitude. Proceedings of the Royal Society of London B: Biological Sciences, 267(1445), 739–745.

4. Altermatt, F. (2010). Climatic warming increases voltinism in European butterflies and moths. Proceedings of the Royal Society of London B: Biological Sciences, 277(1685), 1281–1287.

5. Barve, V., & Hart, E. (2017). rinat: Access iNaturalist Data Through APIs. R package version 0.1.5.

6. Carde, R., Shapiro, A., & Clench, H. (1970). Sibling species in the Eurydice group of Lethe (Lepidoptera: Satyridae). Psyche, 77(1), 70–103.

7. Deutsch, C. A., Tewksbury, J. J., Huey, R. B., Sheldon, K. S., Ghalambor, C. K., Haak, D. C., & Martin, P. R. (2008). Impacts of climate warming on terrestrial ectotherms across latitude. Proceedings of the National Academy of Sciences, 105(18), 6668–6672.

8. Diamond, S. E., Sorger, D. M., Hulcr, J., Pelini, S. L., Toro, I. D., Hirsch, C., … Dunn, R. R. (2012). Who likes it hot? A global analysis of the climatic, ecological, and evolutionary determinants of warming tolerance in ants. Global Change Biology, 18(2), 448–456.

9. Frazier, M. R., Huey, R. B., & Berrigan, D. (2006). Thermodynamics Constrains the Evolution of Insect Population Growth Rates: "Warmer Is Better." The American Naturalist, 168(4), 512–520.

10. Ghalambor, C. K., Huey, R. B., Martin, P. R., Tewksbury, J. J., & Wang, G. (2006). Are mountain passes higher in the tropics? Janzen's hypothesis revisited. Integrative and Comparative Biology, 46(1), 5–17.

11. Hansen, J., Sato, M., Ruedy, R., Lo, K., Lea, D. W., & Medina-Elizade, M. (2006). Global temperature change. Proceedings of the National Academy of Sciences, 103(39), 14288–14293.

12. Hill, J. K., Thomas, C. D., & Huntley, B. (1999). Climate and habitat availability determine 20th century changes in a butterfly's range margin. Proceedings of the Royal Society of London B: Biological Sciences, 266(1425), 1197–1206.

13. Huey, R. B., & Berrigan, D. (2001). Temperature, Demography, and Ectotherm Fitness. The American Naturalist, 158(2), 204–210.

14. Hughes, L. (2000). Biological consequences of global warming: Is the signal already apparent? Trends in Ecology & Evolution, 15(2), 56–61.

15. Hurvich, C. M., & Tsai, C.-L. (1989). Regression and time series model selection in small samples. Biometrika, 76(2), 297–307.

16. Kiekebusch, E. (2019). Effects of temperature, phenology and geography on butterfly population dynamics under climate change. North Carolina State University.

17. Kingsolver, J. G., Diamond, S. E., & Buckley, L. B. (2013). Heat stress and the fitness consequences of climate change for terrestrial ectotherms. Functional Ecology, 27(6), 1415–1423.

18. Luoto, M., Heikkinen, R. K., Pöyry, J., & Saarinen, K. (2006). Determinants of the biogeographical distribution of butterflies in boreal regions. Journal of Biogeography, 33(10), 1764–1778.

19. Morelli, T., Daly, C., Dobrowski, S., Dulen, D., Ebersole, J., Jackson, S., … Beissinger, S. (2016) Managing Climate Change Refugia for Climate Adaptation. *PLOS ONE* 11(8), e0159909

20. Nuñez, T. A., Lawler, J. J., Mcrae, B. H., Pierce, D. J., Krosby, M. B., Kavanagh, D. M., … Tewksbury, J. J. (2013). Connectivity Planning to Address Climate Change. Conservation Biology, 27(2), 407–416.

21. Opler, P. A. (1998). A field guide to eastern butterflies. Houghton Mifflin Company.

22. Parmesan, C. (1996). Climate and species' range. Nature; London, 382(6594), 765–766.

23. Parmesan, C. (2007). Influences of species, latitudes and methodologies on estimates of phenological response to global warming. Global Change Biology, 13(9), 1860–1872.

24. Parmesan, C., Ryrholm, N., Stefanescu, C., Hill, J. K., & others. (1999). Poleward shifts in geographical ranges of butterfly species associated with regional warming. Nature, 399(6736), 579.

25. Pelini, S. L., Diamond, S. E., Nichols, L. M., Stuble, K. L., Ellison, A. M., Sanders, N. J., … Gotelli, N. J. (2014). Geographic differences in effects of experimental warming on ant species diversity and community composition. Ecosphere, 5(10), art125.

26. Pelini, Shannon L., Diamond, S. E., MacLean, H., Ellison, A. M., Gotelli, N. J., Sanders, N. J., & Dunn, R. R. (2012). Common garden experiments reveal uncommon responses across temperatures, locations, and species of ants. Ecology and Evolution, 2(12), 3009–3015.

27. R Core Team (2018). R: A language and environment for statistical computing. R Foundation for Statistical Computing, Vienna, Austria. URL https://www.R-project.org/.

28. Root, T. L., Price, J. T., Hall, K. R., Schneider, S. H., Rosenzweig, C., & Pounds, J. A. (2003). Fingerprints of global warming on wild animals and plants. Nature, 421(6918), 57–60.

29. Sunday, J., Bates, A., & Dulvy, N. (2011). Global analysis of thermal tolerance and latitude in ectotherms. Proceedings of the Royal Society B: Biological Sciences, 278(1713), 1823–1830.

30. Tewksbury, J. J., Huey, R. B., & Deutsch, C. A. (2008). Putting the Heat on Tropical Animals. Science, 320(5881), 1296–1297.

31. Thomas, C. D., & Lennon, J. J. (1999). Birds extend their ranges northwards. Nature, 399(6733), 213.

32. Urban, M. C., Bocedi, G., Hendry, A. P., Mihoub, J.-B., Pe'er, G., Singer, A., … Travis, J. M. J. (2016). Improving the forecast for biodiversity under climate change. Science, 353(6304), aad8466.

33. Wittmann, J., Girman, D., & Crocker, D. (2019). Using iNaturalist in a Coverboard Protocol to Measure Data Quality: Suggestions for Project Design. Citizen Science: Theory and Practice, 4(1), 21.

34. Youngsteadt, E., Ernst, A. F., Dunn, R. R., & Frank, S. D. (2017). Responses of arthropod populations to warming depend on latitude: Evidence from urban heat islands. Global Change Biology, 23(4), 1436–1447.

CHAPTER 4: Predicting butterfly spring emergence phenology in future climates using machine learning

ABSTRACT

Climate change is advancing the phenology of butterflies and other insects, a result of ectotherm developmental dependence on external temperatures. Predicting future spring insect emergences in the face of climate warming is needed to project population and community dynamics. Growing degree days (GDD) have historically been used to predict the timing of spring emergences but thresholds for the GDD formula and accumulation start dates have rarely been measured and have been optimized in different ways for different species. In addition to this, climate variables aside from temperature can also affect insect phenology. I apply a new method to predict phenological emergence: machine learning algorithms that are capable of simultaneously incorporating multiple interacting climate variables and measures of temperature accumulation. I drew on 16 years of daily growing season presence/absence observations of endangered Saint Francis' Satyr (*Neonympha mitchellii francisci*) butterflies to create two historic datasets. The first incorporated daily measurements of climate variables and cumulative GDD, and the second incorporated a range of daily cumulative GDD calculated using combinations of different threshold values. Using the datasets, I identified important variables and classifier algorithms. I used the highest performing classifier to predict adult butterfly annual first emergence dates using downscaled climate projections from two greenhouse gas emissions scenarios. Over the course of the 21st Century, I found a decreasing mean date of first emergence, with advances of approximately 1.4 and 2.1 days per decade for RCP 4.5 and RCP 8.5 respectively. I was able to identify optimal GDD thresholds for Saint Francis' Satyr as 30°C

and 8°C for upper and lower thresholds respectively. My findings demonstrate a case study of the use of machine learning algorithms to optimize degree day models and to predict butterfly phenology under climate change, and I discuss the broader applicability of this method.

INTRODUCTION

Climate variables such as temperature and precipitation are shifting due to global climate change (Girvetz et al. 2009). As many species traits are cued by these variables, the timing of lifecycle events (phenology) such as flowering and migration is being altered for temperate zone animals and plants (Root et al. 2003, Menzel 2000, Lesica & Kittelson 2010). For example, the amount of time that juvenile insects require to develop into adults is dependent on external temperatures. Due to this dependence, insects are shifting to earlier annual spring emergence dates in response to climate warming (Parmesan & Yohe, 2003), with one study estimating the advance of butterfly emergence dates to between 2-10 days per decade (Roy & Sparks 2000). As the climate continues to change, prediction of future phenological shifts will be necessary to anticipate the start and duration of future growing seasons (Kramer et al. 2000), species interactions and potential mismatches (Van Asch et al. 2007, Liu et al. 2011), mitigation of pest outbreaks (Gregory et al. 2009), and the risk of late-season frost events that can negatively affect early emerging species (Inouye 2008). Estimating the magnitude of shifts is made difficult because critical temperatures have not been measured for most species. I investigate the potential of emerging methods in machine learning to identify critical thresholds for development in order to predict phenological responses.

Measures of temperature accumulation such as Growing Degree Days (GDD) are recognized as a successful tool to predict insect developmental timing (Wilson & Barnett 1983,

Bryant et al. 1998). Growing Degree Days are a heuristic to estimate the accumulation of thermal time, the temperature-dependent time period required during which development occurs. They are typically defined by upper and lower thresholds outside of which development does not progress (McMaster & Wilhelm 1997). These developmental thresholds have rarely been optimized for specific insect species besides agricultural pests (e.g. Peterson & Meyer 1995, Davis et al. 1996, Goebel 2006). Instead, temperature thresholds originally developed for crop species such as corn have been used to define the GDD formula for butterflies (Cayton et al. 2015). In some cases, no explanation is given as to how thresholds were chosen (Powney et al. 2010, Crozier & Dwyer 2006, Witter et al. 2012).

In addition to thermal thresholds, the start date from which GDD is accumulated also influences accurate prediction of spring phenological events. Start dates have been modelled based on observations of emergence (McBrien & Judd, 1998) or allowed to vary annually based on temperatures experienced (Augspurger 2013). Traditionally, corn GDD begin accumulating on March 1st, coinciding with the beginning of the historical growing season in the central United States. With climate change leading to an increased length of growing season (see example in Wepprich et al. 2019), start dates may need to be advanced to pick up available thermal time prior to March 1st.

Butterfly development is affected by climate variables other than temperature. Due to larval thermoregulatory behavior, Bryant et al. (2002) demonstrate the critical role played by solar radiation in determining adult emergence for three Nymphalid species. Precipitation can delay butterfly emergence likely by reducing solar insolation levels during months critical to development (Stefanescu et al. 2003). Butterfly developmental sensitivity to temperature can be influenced by variables such as precipitation, humidity and photoperiod (Kharouba et al. 2014).

To predict the future shift in timing of spring butterfly emergence in response to climate change, I use machine learning algorithms. Machine learning originates in the field of artificial intelligence and is capable of identifying structure in large complex datasets (data mining). Machine learning has been touted as an alternative to traditional statistics due to its ability to analyze ecological datasets that are highly dimensional, are non-parametric, contain nonlinear variables that may be correlated or interacting, and have missing values (Cutler et al. 2007, Olden et al. 2008). I chose to use machine learning algorithms to predict phenological responses to climate change for several reasons. First, they are capable of incorporating large numbers of climate variables and temperature accumulation measures at once. Second, the algorithms can be used to rank variables by their predictive value, thus enabling identification of the most important (and unimportant) variables. Finally, by "learning" the patterns inherent in a dataset, the algorithms can create predictions based on a new dataset.

I used a supervised learning approach that enables modelling the relationship between specified inputs (e.g. climate variables, degree days) and known outputs (e.g. adult butterfly presence). I evaluated three separate algorithms that represented each of three machine learning approaches (also known as classifier groups): artificial neural networks (Lek et al. 2006), support vector machines (Drake et al. 2006), and decision trees (De'ath & Fabricius 2000, Prasad et al. 2006). Each approach uses a different technique to identify patterns in the data in order to 'learn' to classify the datapoints (or instances) into the pre-set categories (or classes). In my datasets for analysis, I specified the independent variable (butterfly observation) into one of two classes (presence or absence).

My goal was to identify the best performing algorithm using cross-validation methods to provide metrics of classification strength, and then to use that best algorithm to predict future

emergence based on the most important variables for prediction. I trained and evaluated each algorithm using a historic climate dataset alongside daily butterfly observations for the years 2003-2018. Then I used the best algorithm to predict future butterfly emergence based on downscaled climate datasets from 2 emissions scenarios for the years 2016-2099. I further compared these approaches to predictions that could be made based on GDD alone.

METHODS

Study species and study site

The federally endangered Saint Francis' Satyr (*Neonympha mitchellii francisci*) is a wetland butterfly that occurs only at the US Army installation of Fort Bragg, NC. Individuals overwinter as diapaused early-instar larvae. When temperatures increase in the spring, the larvae resume development and first emerge as adults in May. Historic datasets were created from butterfly observations collected over a 16-year period (2003-2018). During this time, transect surveys were carried out for adult butterflies (methods in Haddad et al. 2008) on a near-daily basis through the growing season to observe the date of first emergence and to track the presence of adult butterflies during flight periods. I classified each data instance representing one day as either 'present' or 'absent' based on whether an adult butterfly was observed on that day. I used this daily presence/absence data as the independent variable within the historic datasets for further analysis.

First historic dataset: comparing climate variables and GDD start dates

To create the first historic dataset, I amassed climate data for every day during the same 2003-18 time period that butterflies were observed. I collected these data from the METDATA gridded

surface meteorological dataset (Abotzoglou, 2011) that maps surface weather variables at ~4km resolution (available at http://clim-engine.appspot.com/#). Alongside the daily presence/absence data, I added daily measures of 7 climate variables. These were daily maximum temperature, daily minimum temperature, daily accumulated precipitation, daily maximum relative humidity, daily minimum relative humidity, mean daily specific humidity, and mean daily downward shortwave radiation.

I included additional variables such as the year, ordinal date and several variables pertaining to the calculation of Growing Degree Days (GDD). To do this, I followed the growing degree day formula outlined in McMaster and Wilhelm (1997) which defines daily growing degree days as follows:

$$\Delta\mathrm{GDD} = \left(\frac{(\mathrm{T_{max}} + \mathrm{T_{min}})}{2}\right) - \mathrm{T_{base}}$$

where T_{max} refers to the daily maximum temperature and T_{min} refers to the daily minimum temperature. T_{base} refers to the base temperature (also known as the lower threshold) below which development does not progress. T_{max} and T_{min} were set equal to T_{base} if they were lower than T_{base} and set equal to an upper threshold if they were greater than the upper threshold prior to any further calculation.

For this analysis, I used the single-triangle calculation method with an upper threshold of 30°C (86°F) and a base (lower threshold) value of 10°C (50°F), which are standards for corn in North America (McMaster & Wilhelm, 1997, Anandhi 2016). There is some justification for the use of corn thresholds as butterflies have evolved alongside their hostplants (Ehrlich & Raven 1964) and the larvae of Nymphalidae: Satyrinae feed exclusively on the monocots Poaceae and Cyperaceae. I created two cumulative GDD variables by using two separate start dates (January 1st and March 1st; see Figure 4.2) to designate where to begin accumulating growing degree days.

I also included the daily growing degree days (ΔGDD), and the threshold-adjusted daily maximum temperatures and threshold-adjusted daily minimum temperatures as variables in the dataset.

Second historic dataset: comparing growing degree day thresholds

To create the second historic dataset, I used the daily maximum and minimum temperatures from METDATA collected as above. I used these temperatures to calculate a range of possible cumulative GDD variables using the above formula and a March 1st start date. I used all combinations of upper threshold values from 25-35°C and lower threshold (T_{base}) values from 5-15°C resulting in 121 cumulative GDD dependent variables. I used additional variables including the daily maximum and daily minimum temperatures, the ordinal date and the year.

Comparison of classifier methods

I conducted machine learning analyses using the Waikato Environment for Knowledge Analysis (WEKA) software version 3.8 (Holmes et al. 1994, Frank et al. 2010). For both historic datasets, I trained the machine via three classifier methods (see workflow, Figure 4.1). The first method is Sequential Minimal Optimization (SMO), which belongs to the group of algorithms known as support vector machines. Support vector machines build a model of the datapoints in multi-dimensional space. The points are mapped such that they can be divided by a hyperplane (line) into the classes. The second classifier I used is the Multilayer Perceptron (MLP), which is a type of artificial neural network. In an artificial neural network, inputs and outputs are connected through layers of connected nodes. The input variables are multiplied iteratively by sets of weights that represent their relative importance. The machine learns by adjusting the

weights to improve accuracy of the results. The third classifier is Random Forest, which belongs in the algorithmic family known as decision trees. Decision trees hierarchically partition the data resulting in decision rules for assigning the data into classes.

In order to evaluate and compare the performance of the above classifier methods, all methods were cross-validated using 66% Split and 10-Fold cross-validation techniques. Here the datasets are divided into training and testing datasets. The machine learns the patterns with the training dataset and then tests itself with the testing dataset. In the first method, 66% of the data is used for training and 33% is used for testing. In the second method, the data is divided into 10 equal sets (or folds). Nine of the folds are used for training and the tenth fold (selected randomly) is used for testing. This procedure is repeated 10 times, and accuracy is assessed as the average of the 10 repetitions.

Several metrics are used to measure model performance. These are the percent correctly classified instances (ie. how many predictions were correct), the Kappa statistic (if greater than 0 the classifier is performing better than random), and the Area Under Receiver Operating Characteristics curve (AUROC, if greater than 0.5 the classifier is performing better than random assignment). For both the Kappa statistic and the AUROC, a value of 1 indicates perfect assignment.

Variable importance and data dimensionality

I carried out a variable (attribute) evaluation process using the InfoGainAttributeEval method provided in WEKA. This is a procedure that ranks all variables based on the information gained with respect to correct classification (Witten et al. 2011). The process does not specify a cutoff beyond which variables are unimportant, but rather indicates the relative importance of

each variable. I used the ranking to evaluate the number of variables necessary to achieve optimal classifier performance for each classifier to ensure that the models were neither overfit nor underfit.

Once I had identified my best performing classifier, I again ranked the variables using the ClassifierAttributeEval method (Witten et al. 2011) to gain a better understanding of the most important variables for the best classifier model.

Predictive analytics

In order to predict Saint Francis' Satyr phenology under future climate scenarios, I used projected climate data for the years 2016-2099 from the MACA statistically downscaled climate dataset (Abatzoglou & Brown, 2012) that I downloaded at https://climate.northwestknowledge.net/MACA/data_csv.php. MACA uses METDATA as a training dataset to remove bias and match spatial patterns. I created 36 future climate datasets using the downscaled data from 18 Global Climate Models (GCMs) parameterized by two Representative Concentration Pathways (RCPs). I excluded two of the possible 20 GCMs available (CCSM4 and NorESM1-M) as these did not have data for maximum and minimum relative humidity. The two emissions scenarios I used were RCP 4.5 where carbon emissions stabilize and global mean temperature increases are limited to +2.4°C (Thomson et al. 2011) and RCP 8.5, where emissions follow current trajectories and global mean temperature increases to +4.9°C (Riahi et al. 2011). Using WEKA, I trained the machine using the first historic climate dataset and the best classifier method. I then used the future climate datasets as test datasets to elicit a prediction from the machine based on each future climate dataset. I used the means and 5^{th} to 95^{th} percentile range across the GCM projections for further comparisons.

Optimized prediction

As described above, I found the best classifier for the second historic dataset, and then I used the ClassifierAttributeEval method to rank the variables by importance to the best classifier model. This allowed me to identify the best GDD thresholds for predicting Saint Francis' Satyr emergence. I used these thresholds with the butterfly presence/absence observations to calculate average cumulative GDD of the observed first emergence dates. I then used the daily maximum and minimum temperatures from the MACA datasets from 20 GCMs for RCP4.5 and RCP8.5 to calculate future cumulative GDD using the best GDD thresholds. I then extracted annual future dates of first emergence based on the dates when the average cumulative GDD was surpassed.

Growing degree day comparison

I compared the machine learning prediction based on the different climate variables and the prediction based on optimized thresholds of future Saint Francis' Satyr first emergence dates with that which could be predicted by using growing degree days with corn thresholds. To do this, I used the historic observations of annual first emergence dates for the years 2003-2018 and the cumulative growing degree days extracted from the METDATA maximum and minimum daily temperatures. I found the mean of the accumulated GDD values corresponding to annual ordinal dates of first emergence using March 1st and January 1st start dates. I applied the mean GDD values to the MACA datasets for all 20 GCMs for both emissions scenarios to extract annual ordinal dates of first emergence for 2016-2099. I compared the mean of the extracted dates to the mean dates predicted by machine learning and by the GDD formula with the optimized thresholds.

RESULTS

Comparison of classifier methods

For the first historic dataset, the Random Forest classifier method had the highest percentage of correctly classified instances, as well as the highest levels of prediction strength based on Kappa Statistic and AUROC values (Table 4.1). I used this classifier method for future predictive analyses.

For the second historic dataset, the Multilayer Perceptron classifier method had the highest percentage of correctly classified instances, as well as the highest levels of prediction strength based on the Kappa Statistic, while Random Forest had higher prediction strength based on AUROC values (Table 4.1). I evaluated the over and underfitting of both models in order to choose one for future predictive analyses.

The historic datasets had a majority of days with adult butterfly absence throughout each annual cycle. Cross-validation for both datasets revealed that SMO was the weakest classifier. It was unable to distinguish between butterfly presence and absence, which was supported by the poor Kappa Statistic and AUROC values.

Variable performance and data dimensionality

Using InfoGainAttributeEval, I ranked the variables in both datasets and used them to evaluate whether the models were overfit or underfit. For the first historic dataset, I found that for the Random Forest classifier using all 14 climate variables resulted in highest classification performance (see Appendix Figure 4.A1). Inspection of the Random Forest curves demonstrated a limited drop-off in performance at lower numbers of variables suggesting very minimal underfitting and no overfitting. I proceeded with the Random Forest algorithm and all variables

for further analysis. Using WEKA's ClassifierAttributeEval ranking method, I found that for Random Forest, the most important variables were cumulative GDD beginning March 1st, cumulative GDD beginning January 1st, and ordinal date (Table 4.2). The other variables were less important but their inclusion increased classification performance.

For the second historic dataset, I found that for the Multilayer Perceptron using all 121 GDD variables resulted in highest classification performance (see Appendix Figure 4.A2). Inspection of the curves showed a large jump in performance increasing from 10 to 20 GDD variables. In contrast to this, inspection of the Random Forest curves demonstrated a limited drop-off in performance at lower numbers of variables. This suggested that a single best GDD variable could be used to make predictions of SFS emergence with 94-95% accuracy.

Predictive analytics

I used the Random Forest classifier to project daily adult butterfly presence and absence for the years 2016-2099. The output showed plausible results including adult flight periods (groupings of daily adult presence as was observed in the field historically). I averaged the annual first emergence dates across the 18 output projections for each RCP scenario. Figure 4.3 shows the observed (historic) annual first emergence ordinal date alongside the mean projected annual ordinal date of first emergence for both emissions scenarios. This was the first day per year where the model predicted presence of butterflies. The results show a clear trend towards advancing spring emergence over time with a more pronounced decrease in emergence dates for the higher emissions scenario (RCP 8.5).

Optimized prediction

Using WEKA's ClassifierAttributeEval ranking method, I found that for Random Forest the most important variable for classification was GDD calculated with an upper threshold of 30°C and a lower threshold (T_{base}) of 8°C (Table 4.3). In contrast to this, the ClassifierAttributeEval used with the Multilayer Perceptron ranked all variables at the same value (p=0, not shown). Due to this, I decided to proceed with the GDD variable (and thresholds) identified by Random Forest for further predictions.

Using the upper and lower threshold values that were the highest ranked by Random Forest and the historic dataset, I calculated average growing degree days (upper threshold = 30°C, lower threshold = 8°C, start date of March 1st) at annual first emergence to be 710.8.

Growing degree day comparison

Using the historic data set I calculated the average growing degree days (upper threshold = 30°C, lower threshold = 10°C) at annual first emergence to be 588.9 (March 1st start date) and 715.9 (January 1st start date).

Projected first emergence dates using GDD methods and Random Forest showed agreement in decreasing spring emergence dates over time for both climate scenarios. Comparison of the two methods revealed that Random Forest tended to strike a middle ground between January 1st and March 1st start date GDD predictions over the earlier half of the 21st Century, whereas Random Forest more closely matched March 1st predictions over the period 2050 onwards for both emissions scenarios (Figure 4.4).

Comparison of the projected first emergence dates using the differing GDD thresholds showed decreasing spring emergence dates over time for both climate scenarios (Figure 4.5). For

the RCP 4.5 scenario, the optimized GDD thresholds decreased the date of first emergence as compared to the corn thresholds. For RCP 8.5, the predictions matched very closely.

DISCUSSION

Machine learning algorithms successfully classified butterfly presence and absence when given cumulative GDD and climate variables. When paired with downscaled climate data, these algorithms can be used to project future butterfly flight periods that revealed trends in phenological advances that matched the degree of CO_2 emissions scenarios. Comparing the observed average ordinal date of emergence from 2003-2012 to the projected average from 2090-2099, I found that the Random Forest algorithm estimated mean phenological advancement of 14.1 ± 1.96 days and 21.4 ± 1.89 days for RCP 4.5 and RCP 8.5 respectively over the 21st Century (mean ± standard error). This translates to a respective shift of approximately 1.4 and 2.1 days per decade.

The machine learning predictions are lower than average findings in the literature for butterfly shifts in the past century. For example, Roy & Sparks (2000) found advances of 2-10 days per decade and Parmesan (2007) found advances of 3.7 days per decade. Root et al. (2003) estimated average phenological shifts for invertebrates between 5 and 6 days per decade. This discrepancy may reflect the prioritization by the Random Forest algorithm of March 1st start dates over January 1st, a pattern that holds in the past and that was used to train the models, but which may change in the future. The Saint Francis' Satyr may also be a species that will experience a relatively low degree of spring phenological shift, pointing towards the value of considering other species.

When comparing the projected and observed data over the three years where the datasets overlapped (2016-18, see Figure 4.3), I found that the mean Random Forest predictions were in most cases not accurate to the exact day. They were off by up to 14 days in 2017 when butterflies emerged extremely early. However, this value was still within the range (5^{th} to 95^{th} percentile) for RCP 8.5. The findings suggest that the median dates can be taken as a trend over time, whereas there may be much higher variation in actual future emergence dates. This variation could occur in future due to increased frequency of extreme weather events (Alexander et al. 2006, Easterling et al. 2000).

Consistent with other studies (Olden et al. 2008, Prasad et al. 2006), Random Forest emerged as the best classifier algorithm for the first historic dataset that evaluated multiple climate variables simultaneously. Random Forest also emerged as the algorithm best able to optimize GDD thresholds, that is, the algorithm with the highest-accuracy predictions based on a single cumulative GDD variable. Several papers have pointed out the advantages of using decision trees and particularly Random Forest for ecological problems (Olden et al. 2008, Prasad et al. 2006). Due to its ability to evaluate multiple interacting variables, Random Forest can outperform classification by linear regression (Cutler et al. 2007). Decision trees have been used to predict phenology of aphids (Holloway et al. 2018), trees (LeBourgeois et al. 2010) and wheat (Liu et al. 2018). Though the identification of a decision rule (or set of decision rules) by decision trees can be very straightforward, this may also limit model performance when, for example, separate populations of a species are governed by different rules (Wiley et al. 2003). The butterfly observations were collected from several metapopulations (Milko et al. 2012) within a small area of Fort Bragg (less than 10 km^2), but no differentiation by site was incorporated into the analysis.

Machine learning is advantageous when it is not possible to individually determine thresholds empirically. Thresholds are known for only a handful of species. This is unsurprising because the process of obtaining critical thresholds requires growth chambers to test ranges of temperatures under which larval development can take place. These methods are costly, both in terms of funding and effort. In the case of endangered species like Saint Francis' Satyr, such methods are simply not possible.

Machine learning is a viable method in the many more instances when species presence/absence data are available, and it has already been applied in the field of niche modelling (e.g. Drake et al. 2006). Available datasets can include historical/ museum records and published survey data. For plants, remote sensing data to evaluate annual green up has emerged as a way to track vegetation response to climate change (Peng et al. 2017), and there exist examples where machine learning has been applied to detect phenological changes (Almeida et al. 2014). Another emerging source of data are large citizen science datasets where volunteers record observations of relevant species over a specified time period and location. For butterflies, there are multiple such monitoring schemes covering numerous species (Pollard et al. 1995, Ries & Oberhauser 2015).

TABLES

Table 4.1. Performance of three different classifiers using 66% split and 10-fold cross validation techniques to evaluate 1) the first historic (climate variable) dataset, and 2) the second historic (growing degree day) dataset.

1) Climate Variables						
Classifier	**SMO**		**MLP**		**Random Forest**	
Cross-Validation Method	66% Split	10-fold	66% Split	10-fold	66% Split	10-fold
% Correctly Classified Instances	84.83	84.74	96.20	96.12	96.81	97.54
Kappa Statistic	0.00	0.00	0.85	0.85	0.87	0.90
AUROC	0.50	0.50	0.99	0.98	0.99	1.00
2) Growing Degree Day Variables						
Classifier	**SMO**		**MLP**		**Random Forest**	
Cross-Validation Method	66% Split	10-fold	66% Split	10-fold	66% Split	10-fold
% Correctly Classified Instances	85.09	85.14	96.97	96.92	95.84	96.17
Kappa Statistic	0.00	0.00	0.88	0.87	0.83	0.85
AUROC	0.50	0.50	0.96	0.97	0.99	0.99

Table 4.2. All climate variables and cumulative GDD calculated using March 1st and January 1st start dates. On the left, variables ranked using InfoGainAttributeEval which evaluates information gained with respect to correct class assignment. On the right, variables ranked using ClassifierAttributeEval which evaluates variable importance specific to Random Forest as the specified classifier.

InfoGainAttributeEval		**ClassifierAttributeEval with Random Forest**	
p-value	**Variable (attribute)**	**p-value**	**Variable (attribute)**
0.0886	Cumulative GDD Mar1	0.46496	Cumulative GDD Mar1
0.0884	Cumulative GDD Jan1	0.46432	Cumulative GDD Jan1
0.0775	Ordinal Date	0.40241	Ordinal Date
0	Year	0.17733	Minimum Temperature
-0.0287	Adjusted Maximum Temperature	0.17719	Adjusted Minimum Temperature
-0.0389	Precipitation	0.17617	Daily GDD
-0.0466	Adjusted Minimum Temperature	0.16909	Specific Humidity
-0.0474	Minimum Temperature	0.1556	Maximum Temperature
-0.0516	Max Relative Humidity	0.1556	Adjusted Maximum Temperature
-0.0523	Maximum Temperature	0.10756	Downward Shortwave Radiation
-0.0532	Specific Humidity	0.04382	Max Relative Humidity
-0.0537	Daily GDD	0.02882	Minimum Relative Humidity
-0.07	Downward Shortwave Radiation	0.00657	Precipitation
-0.0929	Minimum Relative Humidity	0.00346	Year

Table 4.3. Top 10 growing degree day variables defined by separate upper (UT) and lower thresholds (LT). On the left, variables ranked using InfoGainAttributeEval which evaluates information gained with respect to correct class assignment. On the right, variables ranked using ClassifierAttributeEval which evaluates variable importance specific to Random Forest as the specified classifier.

InfoGainAttributeEval		**ClassifierAttributeEval with Random Forest**	
p-value	**Variable (attribute)**	**p-value**	**Variable (attribute)**
0.4461	Cumulative GDD (UT=33, LT=6)	0.0836	Cumulative GDD (UT=30, LT=8)
0.44504	Cumulative GDD (UT=32, LT=6)	0.0826	Cumulative GDD (UT=31, LT=5)
0.44456	Cumulative GDD (UT=31, LT=6)	0.081	Cumulative GDD (UT=32, LT=12)
0.44427	Cumulative GDD (UT=30, LT=11)	0.0803	Cumulative GDD (UT=29, LT=10)
0.44398	Cumulative GDD (UT=32, LT=9)	0.0793	Cumulative GDD (UT=27, LT=7)
0.44369	Cumulative GDD (UT=31, LT=10)	0.0792	Cumulative GDD (UT=31, LT=10)
0.44361	Cumulative GDD (UT=30, LT=6)	0.0791	Cumulative GDD (UT=33, LT=5)
0.44316	Cumulative GDD (UT=28, LT=11)	0.079	Cumulative GDD (UT=29, LT=14)
0.44303	Cumulative GDD (UT=30, LT=8)	0.079	Cumulative GDD (UT=34, LT=9)
0.44298	Cumulative GDD (UT=28, LT=10)	0.0789	Cumulative GDD (UT=30, LT=7)

FIGURES

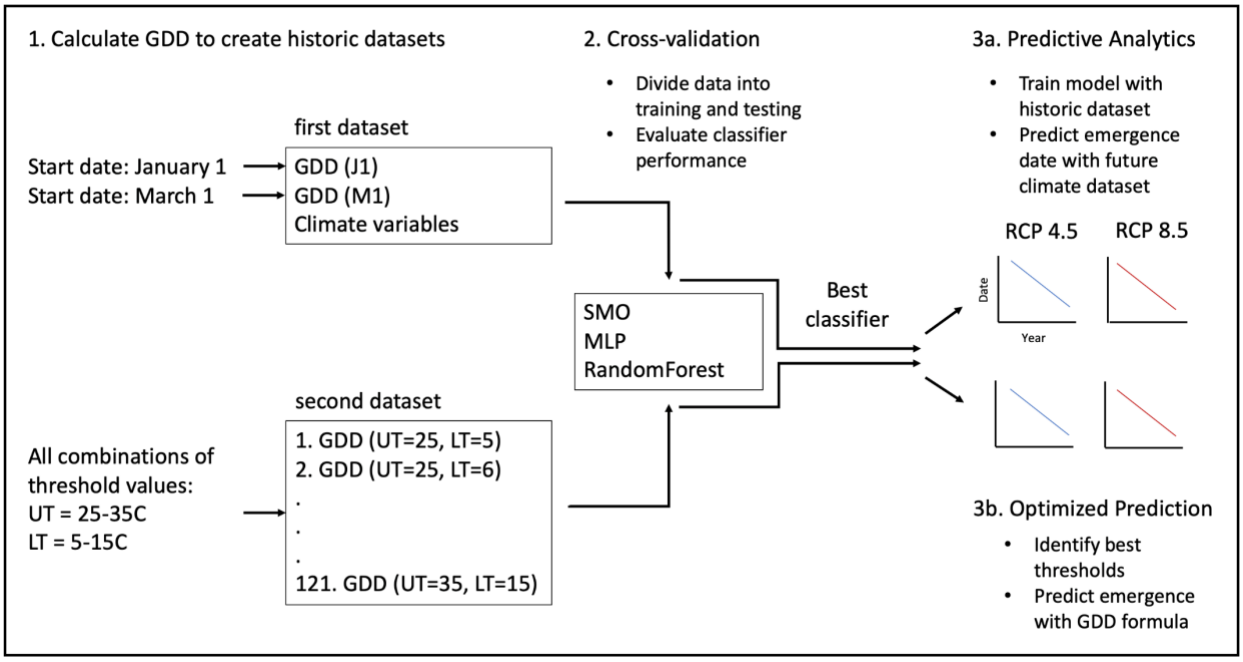

Figure 4.1. Workflow for evaluating the use of growing degree day models to predict future butterfly first emergence dates. The start date for GDD accumulation for the second dataset was March 1st.

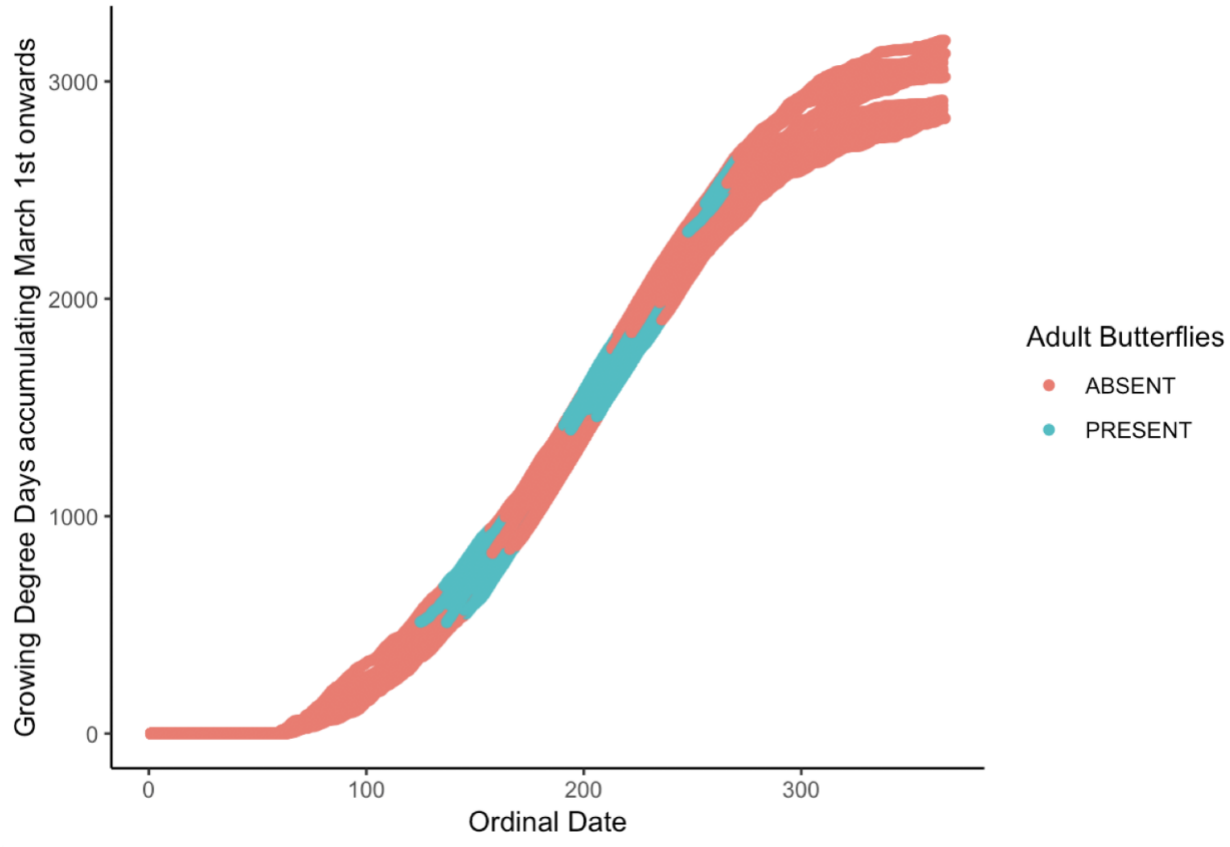

Figure 4.2. Cumulative growing degree days for each of 16 years (2003-2018) with daily observed presence (green) and absence (red) of adult Saint Francis' Satyr. Degree days accumulated from March 1st onwards.

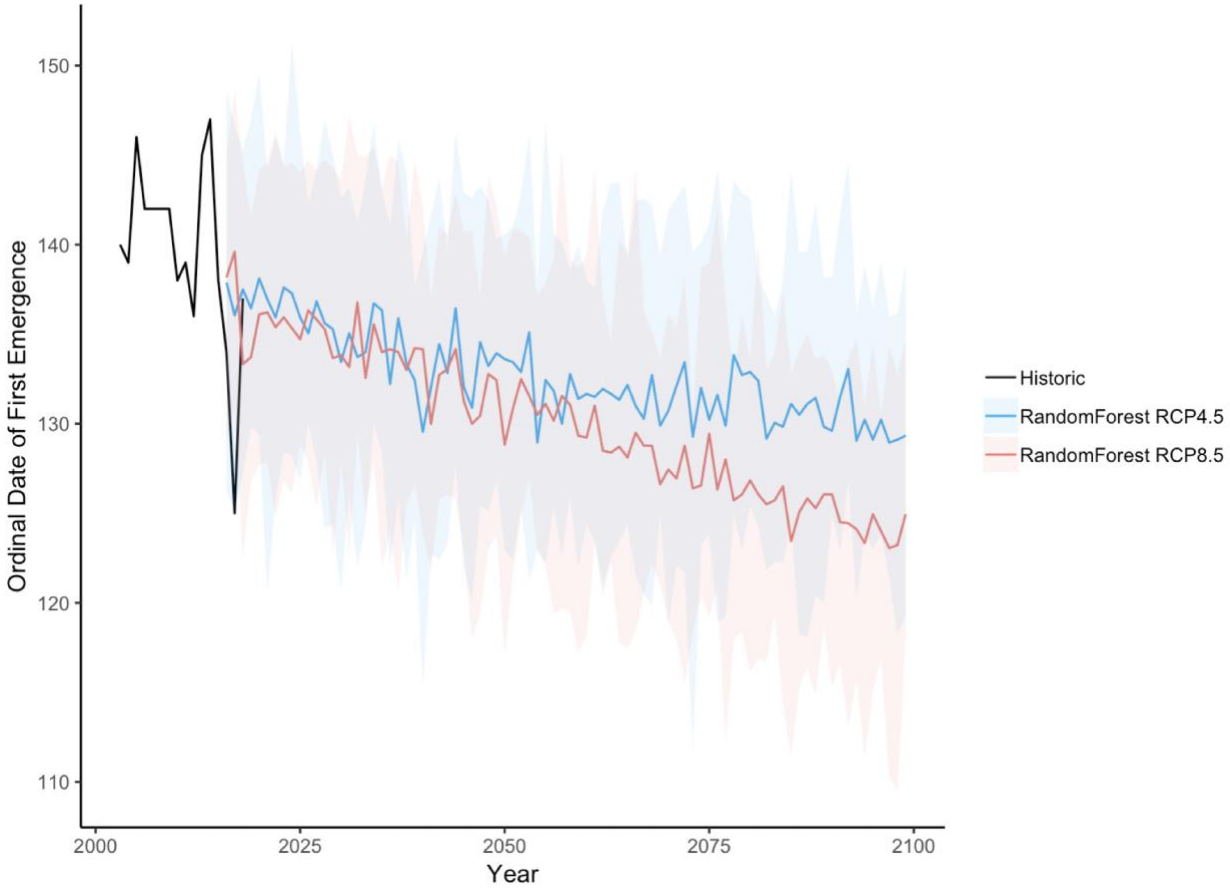

Figure 4.3. Saint Francis' Satyr first emergence ordinal date historically observed (2003-2018) and predicted (2016-2099) by the Random Forest classifier under two future climate scenarios (RCP 4.5 and RCP 8.5). Blue and red lines represent the mean of 18 predicted ordinal dates of first emergence based on each of 18 GCMs. Shadings represent the 5th to 95th percentile range.

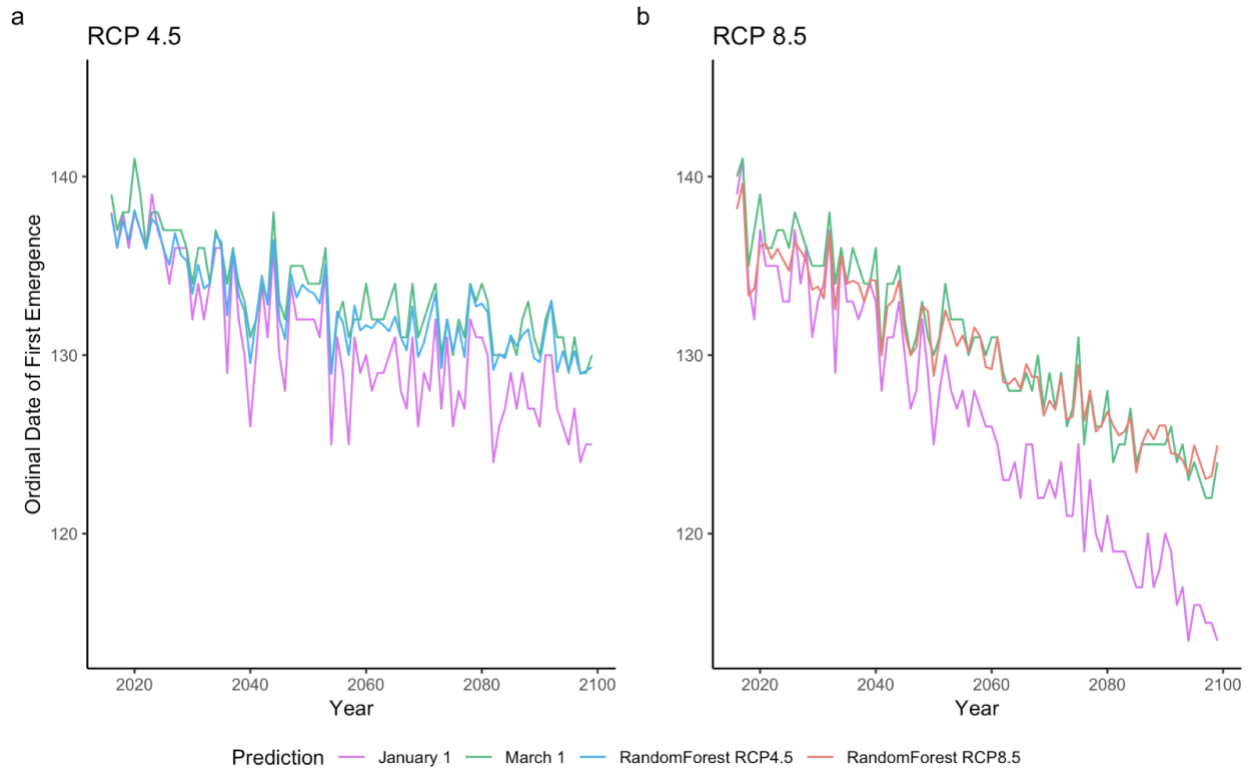

Figure 4.4. Comparison of predicted ordinal dates of annual first emergence using GDD (with March 1st and January 1st start dates, upper threshold = 30°C and lower threshold = 10°C) and Random Forest for a) RCP 4.5 and b) RCP 8.5 emissions scenarios. Random Forest predictions are comparable to both March 1 and January 1 GDD predictions up to ~2050, then mirror March 1 GDD predictions from that time onwards.

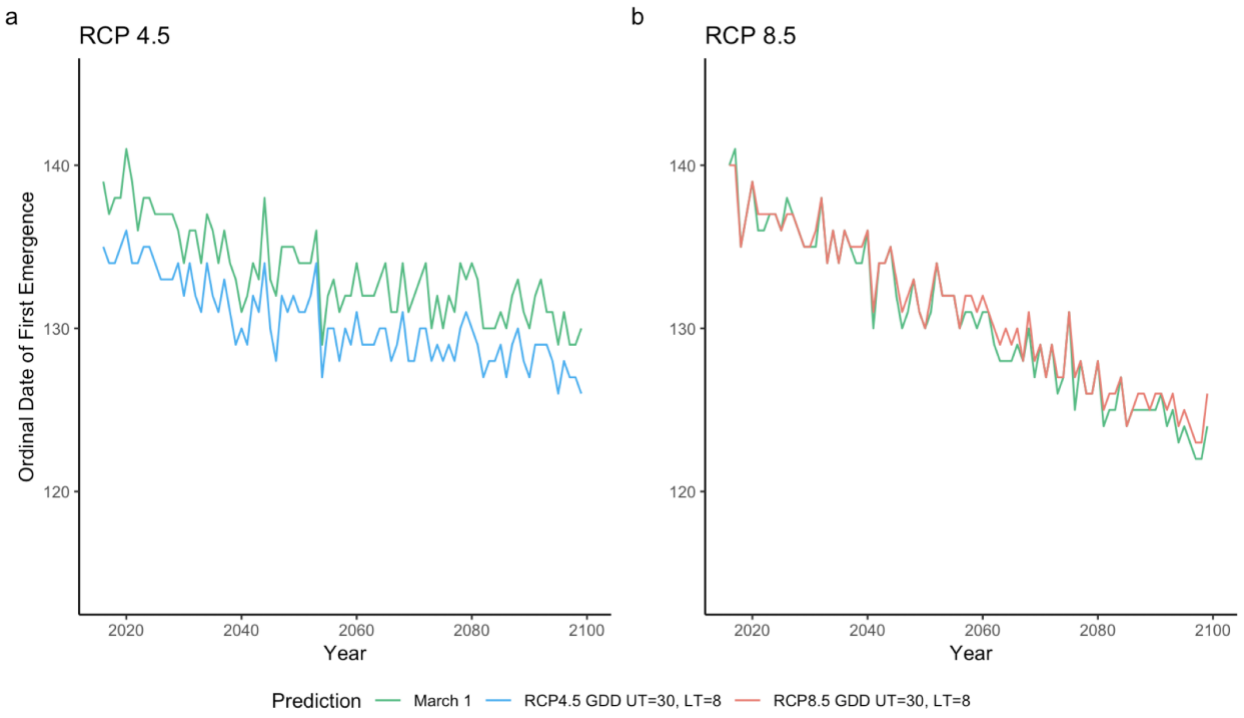

Figure 4.5. Comparison of predicted ordinal dates of annual first emergence using GDD (with March 1st start date, upper threshold = 30°C and lower threshold = 10°C) and GDD (with March 1st start date, upper threshold = 30°C and lower threshold = 8°C) for a) RCP 4.5 and b) RCP 8.5 emissions scenarios.

REFERENCES

1. Abatzoglou, J. T. (2011). Development of gridded surface meteorological data for ecological applications and modelling. International Journal of Climatology, 33(1), 121–131.

2. Abatzoglou John T., & Brown Timothy J. (2012). A comparison of statistical downscaling methods suited for wildfire applications. International Journal of Climatology, 32(5), 772–780.

3. Alexander, L. V., Zhang, X., Peterson, T. C., Caesar, J., Gleason, B., Tank, A. M. G. K., … Vazquez-Aguirre, J. L. (2006). Global observed changes in daily climate extremes of temperature and precipitation. Journal of Geophysical Research: Atmospheres, 111(D5).

4. Almeida, J., dos Santos, J. A., Alberton, B., Torres, R. da S., & Morellato, L. P. C. (2014). Applying machine learning based on multiscale classifiers to detect remote phenology patterns in Cerrado savanna trees. Ecological Informatics, 23, 49–61.

5. Anandhi, A. (2016). Growing degree days – Ecosystem indicator for changing diurnal temperatures and their impact on corn growth stages in Kansas. Ecological Indicators, 61, 149–158.

6. Augspurger, C. K. (2013). Reconstructing patterns of temperature, phenology, and frost damage over 124 years: Spring damage risk is increasing. Ecology, 94(1), 41–50.

7. Bryant, S. R., Bale, J. S., & Thomas, C. D. (1998). Modification of the triangle method of degree-day accumulation to allow for behavioural thermoregulation in insects. Journal of Applied Ecology, 35(6), 921–927.

8. Bryant, S. R., Thomas, C. D., & Bale, J. S. (2002). The influence of thermal ecology on the distribution of three nymphalid butterflies. Journal of Applied Ecology, 39(1), 43–55.

9. Cayton, H. L., Haddad, N. M., Gross, K., Diamond, S. E., & Ries, L. (2015). Do growing degree days predict phenology across butterfly species? Ecology, 96(6), 1473–1479.

10. Crozier, L., & Dwyer, G. (2006). Combining Population-Dynamic and Ecophysiological Models to Predict Climate-Induced Insect Range Shifts. The American Naturalist, 167(6), 853–866.

11. Cutler, D. R., Edwards, T. C., Beard, K. H., Cutler, A., Hess, K. T., Gibson, J., & Lawler, J. J. (2007). Random Forests for Classification in Ecology. Ecology, 88(11), 2783–2792.

12. Davis, P. M., Brenes, N., & Allee, L. L. (1996). Temperature Dependent Models To Predict Regional Differences in Corn Rootworm (Coleoptera: Chrysomelidae) Phenology. Environmental Entomology, 25(4), 767–775.

13. De'ath, G., & Fabricius, K. E. (2000). Classification and regression trees: A powerful yet simple technique for ecological data analysis. Ecology, 81(11), 3178–3192.

14. DeLucia, E. H., Nabity, P. D., Zavala, J. A., & Berenbaum, M. R. (2012). Climate Change: Resetting Plant-Insect Interactions. Plant Physiology, 160(4), 1677–1685.

15. Drake, J. M., Randin, C., & Guisan, A. (2006). Modelling ecological niches with support vector machines. Journal of Applied Ecology, 43(3), 424–432.

16. Easterling, D. R., Meehl, G. A., Parmesan, C., Changnon, S. A., Karl, T. R., & Mearns, L. O. (2000). Climate Extremes: Observations, Modeling, and Impacts. Science, 289(5487), 2068–2074.

17. Ehrlich, P. R., & Raven, P. H. (1964). Butterflies and Plants: A Study in Coevolution. Evolution, 18(4), 586.

18. Frank, E., Hall, M., Holmes, G., Kirkby, R., Pfahringer, B., Witten, I. H., & Trigg, L. (2010). Weka-A Machine Learning Workbench for Data Mining. In O. Maimon & L. Rokach (Eds.), Data Mining and Knowledge Discovery Handbook (pp. 1269–1277).

19. Girvetz, E. H., Zganjar, C., Raber, G. T., Maurer, E. P., Kareiva, P., & Lawler, J. J. (2009). Applied Climate-Change Analysis: The Climate Wizard Tool. PLOS ONE, 4(12), e8320.

20. Goebel, R. (2006). The effect of temperature on development and reproduction of the sugarcane stalk borer, Chilo sacchariphagus (Bojer 1856) (Lepidoptera: Crambidae). African Entomology, 14(1), 103–111.

21. Gregory, P. J., Johnson, S. N., Newton, A. C., & Ingram, J. S. I. (2009). Integrating pests and pathogens into the climate change/food security debate. Journal of Experimental Botany, 60(10), 2827–2838.

22. Haddad, N. M., Hudgens, B., Damiani, C., Gross, K., Kuefler, D., & Pollock, K. (2008). Determining optimal population monitoring for rare butterflies. Conservation Biology, 22(4), 929–940.

23. Holloway, P., Kudenko, D., & Bell, J. R. (2018). Dynamic selection of environmental variables to improve the prediction of aphid phenology: A machine learning approach. Ecological Indicators, 88, 512–521.

24. Holmes, G., Donkin, A., & Witten, I. H. (1994). WEKA: A machine learning workbench. Proceedings of ANZIIS '94 - Australian New Zealand Intelligent Information Systems Conference, 357–361.

25. Inouye, D. W. (2008). Effects of Climate Change on Phenology, Frost Damage, and Floral Abundance of Montane Wildflowers. Ecology, 89(2), 353–362.

26. Kharouba, H. M., Paquette, S. R., Kerr, J. T., & Vellend, M. (2014). Predicting the sensitivity of butterfly phenology to temperature over the past century. Global Change Biology, 20(2), 504–514.

27. Lebourgeois, F., Pierrat, J.-C., Perez, V., Piedallu, C., Cecchini, S., & Ulrich, E. (2010). Simulating phenological shifts in French temperate forests under two climatic change scenarios and four driving global circulation models. International Journal of Biometeorology, 54(5), 563–581.

28. Lek, S., Delacoste, M., Baran, P., Dimopoulos, I., Lauga, J., & Aulagnier, S. (1996). Application of neural networks to modelling nonlinear relationships in ecology. Ecological Modelling, 90(1), 39–52.

29. Lesica, P., & Kittelson, P. M. (2010). Precipitation and temperature are associated with advanced flowering phenology in a semi-arid grassland. Journal of Arid Environments, 74(9), 1013–1017.

30. Liu, J., Feng, Q., Gong, J., Zhou, J., Liang, J., & Li, Y. (2018). Winter wheat mapping using a random forest classifier combined with multi-temporal and multi-sensor data. International Journal of Digital Earth, 11(8), 783–802.

31. Liu, Y., Reich, P. B., Li, G., & Sun, S. (2011). Shifting phenology and abundance under experimental warming alters trophic relationships and plant reproductive capacity. Ecology, 92(6), 1201–1207.

32. McBrien, H. L., & Judd, G. J. R. (1998). Forecasting Emergence, Flight, and Oviposition of Spilonota ocellana (Lepidoptera: Tortricidae), in British Columbia. Environmental Entomology, 27(6), 1411–1417.

33. McMaster, G. S., & Wilhelm, W. W. (1997). Growing degree-days: One equation, two interpretations. Agricultural and Forest Meteorology, 87(4), 291–300.

34. Menzel, A. (2000). Trends in phenological phases in Europe between 1951 and 1996. International Journal of Biometeorology, 44(2), 76–81.

35. Milko, L. V., Haddad, N. M., & Lance, S. L. (2012). Dispersal via stream corridors structures populations of the endangered St. Francis' satyr butterfly (Neonympha mitchellii francisci). Journal of Insect Conservation, 16(2), 263–273.

36. Olden, J. D., Lawler, J. J., & Poff, N. L. (2008). Machine Learning Methods Without Tears: A Primer for Ecologists. The Quarterly Review of Biology, 83(2), 171–193.

37. Parmesan, C. (2007). Influences of species, latitudes and methodologies on estimates of phenological response to global warming. Global Change Biology, 13(9), 1860–1872.

38. Parmesan, C., & Yohe, G. (2003). A globally coherent fingerprint of climate change impacts across natural systems. Nature, 421(6918), 37–42.

39. Peng, D., Wu, C., Li, C., Zhang, X., Liu, Z., Ye, H., … Fang, B. (2017). Spring green-up phenology products derived from MODIS NDVI and EVI: Intercomparison, interpretation and validation using National Phenology Network and AmeriFlux observations. Ecological Indicators, 77, 323–336.

40. Peterson, R. K. D., & Meyer, S. J. (1995). Relating Degree–Day Accumulations to Calendar Dates: Alfalfa Weevil (Coleoptera: Curculionidae) Egg Hatch in the North Central United States. Environmental Entomology, 24(6), 1404–1407.

41. Pollard, E., Moss, D., & Yates, T. J. (1995). Population Trends of Common British Butterflies at Monitored Sites. Journal of Applied Ecology, 32(1), 9–16.

42. Powney, G. D., Roy, D. B., Chapman, D., & Oliver, T. H. (2010). Synchrony of butterfly populations across species' geographic ranges. Oikos, 119(10), 1690–1696.

43. Prasad, A. M., Iverson, L. R., & Liaw, A. (2006). Newer Classification and Regression Tree Techniques: Bagging and Random Forests for Ecological Prediction. Ecosystems, 9(2), 181–199.

44. Riahi, K., Rao, S., Krey, V., Cho, C., Chirkov, V., Fischer, G., … Rafaj, P. (2011). RCP 8.5—A scenario of comparatively high greenhouse gas emissions. Climatic Change, 109(1), 33.

45. Ries, L., & Oberhauser, K. (2015). A Citizen Army for Science: Quantifying the Contributions of Citizen Scientists to our Understanding of Monarch Butterfly Biology. BioScience, 65(4), 419–430.

46. Root, T. L., Price, J. T., Hall, K. R., Schneider, S. H., Rosenzweig, C., & Pounds, J. A. (2003). Fingerprints of global warming on wild animals and plants. Nature, 421(6918), 57–60.

47. Roy, D. B., & Sparks, T. H. (2000). Phenology of British butterflies and climate change. Global Change Biology, 6(4), 407–416.

48. Stefanescu, C., Peñuelas, J., & Filella, I. (2003). Effects of climatic change on the phenology of butterflies in the northwest Mediterranean Basin. Global Change Biology, 9(10), 1494–1506.

49. Thomson, A. M., Calvin, K. V., Smith, S. J., Kyle, G. P., Volke, A., Patel, P., … Edmonds, J. A. (2011). RCP4.5: A pathway for stabilization of radiative forcing by 2100. Climatic Change, 109(1), 77.

50. Van ASCH, M., Van TIENDEREN, P. H., Holleman, L. J. M., & Visser, M. E. (2007). Predicting adaptation of phenology in response to climate change, an insect herbivore example. Global Change Biology, 13(8), 1596–1604.

51. Wepprich, T., Adrion, J. R., Ries, L., Wiedmann, J., & Haddad, N. M. (2019). Butterfly abundance declines over 20 years of systematic monitoring in Ohio, USA. BioRxiv, 613786.

52. Wiley, E. O., McNyset, K. M., Peterson, A. T., Robins, C. R., & Stewart, A. M. (n.d.). Niche Modeling and Geographic Range Predictions in the Marine Environment Using a Machine-learning Algorithm. 16(3), 8.

53. Wilson, L., & Barnett, W. (1983). Degree-days: An aid in crop and pest management. California Agriculture, 37(1), 4–7.

54. Witten, I., Frank, E., & Hall, M. (2011). Data Mining: Practical machine learning tools and techniques, 3rd Ed. Morgan Kauffmann.

55. Witter, L. A., Johnson, C. J., Croft, B., Gunn, A., & Poirier, L. M. (2012). Gauging climate change effects at local scales: Weather-based indices to monitor insect harassment in caribou. Ecological Applications, 22(6), 1838–1851.

APPENDICES

Appendix 1

Table 1.A1. Coefficient test results and random effect variances from highest ranked model of egg survival, larval survival and daily fecundity. Bolded values indicate p<0.05.

Vital Rate	Fixed Effect	Estimate	Std Error	z or t value	p	Random Effect	N	Variance	Standard Deviation
Egg Daily Survival	Intercept	2.4527	0.3463	7.083	**<0.001**	Plot:Site	9	0.10086	0.3176
	Maximum Temperature	-0.2591	0.1442	-1.797	0.0723	Site	3	0.08217	0.2867
	Second Generation	-0.0466	0.3704	-0.126	0.8999				
	Third Generation	0.6216	0.3602	1.726	0.0844				
Larval Survival	Intercept	-0.6365	0.5051	-1.260	0.208	Plot:Site	9	0.15481	0.3935
	Maximum Temperature	-2.8077	0.5457	-5.145	**2.68e-07**	Site	3	0.04738	0.2177
	Second Generation	0.2832	0.4359	0.650	0.516				
	Third Generation	-4.6265	1.1057	-4.184	**2.86e-05**				
Eggs Laid Per Day	Intercept	-30.98196	24.31430	-1.274	0.211				
	Maximum Temperature	2.47835	1.66169	1.491	0.145				
	Maximum Temperature ^2	-0.04569	0.02834	-1.613	0.116				

Table 1.A2. Top 10 models predicting egg daily survival.

Fixed Effects	Random Effect	df	logLik	AICc	delta	weight
Maximum Temperature + Generation	Plot nested in Site	6	-94.97	203.38	0.00	0.09
Maximum Temperature + Generation + Treatment	Plot nested in Site	8	-92.45	203.47	0.09	0.09
Maximum Temperature + Generation + Maximum Temperature * Generation	Plot nested in Site	8	-92.73	204.03	0.65	0.07
Maximum Temperature + Generation + Treatment + Dam	Plot nested in Site	9	-91.40	204.07	0.69	0.07
Generation	Plot nested in Site	5	-96.56	204.15	0.77	0.06
Maximum Temperature + Generation + Dam	Plot nested in Site	6	-95.39	204.22	0.84	0.06
Maximum Temperature + Generation + Dam + Maximum Temperature * Generation	Plot nested in Site	7	-94.17	204.30	0.91	0.06
Maximum Temperature + Treatment + Dam	Plot nested in Site	9	-91.58	204.44	1.06	0.05
Minimum Temperature + Generation	Plot nested in Site	7	-94.27	204.50	1.12	0.05
Maximum Temperature + Generation + Treatment + Dam + Maximum Temperature * Generation	Plot nested in Site	6	-95.59	204.62	1.24	0.05

Table 1.A3. Top 10 models predicting larval survival.

Fixed Effects	Random Effect	df	logLik	AICc	delta	weight
Maximum Temperature + Generation	Plot nested in Site	6	-122.18	258.15	0.00	0.77
Maximum Temperature + Generation + Dam	Plot nested in Site	7	-122.16	260.74	2.59	0.21
Maximum Temperature + Treatment	Plot nested in Site	6	-126.05	265.89	7.73	0.02
Maximum Temperature + Treatment + Dam	Plot nested in Site	7	-125.95	268.34	10.18	0.00
Mean Temperature + Generation + Treatment + Mean Temperature * Generation	Plot nested in Site	10	-121.86	268.84	10.68	0.00
Mean Temperature + Generation + Treatment + Dam + Mean Temperature * Generation	Plot nested in Site	11	-121.86	272.01	13.85	0.00
Mean Temperature + Treatment	Plot nested in Site	6	-131.17	276.14	17.98	0.00
Maximum Temperature	Plot nested in Site	4	-133.74	276.31	18.15	0.00
Generation + Treatment	Plot nested in Site	7	-130.79	278.01	19.86	0.00
Minimum Temperature +Treatment	Plot nested in Site	6	-132.18	278.14	19.98	0.00

Table 1.A4. Larval survival was significantly different in the third (winter) generation compared to the first and second generations. Table shows Tukey posthoc comparing means and standard deviations of larval survival across generations.

Generation	N	Least Squared Mean	Standard Error	Tukey p-value	
				First	Second
First	90	0.34604	0.62364		
Second	214	0.41257	0.59709	0.79	
Third	282	0.00515	0.69202	0.001	<0.001

Table 1.A5. Ranked models comparing covariates of adult transition probability (Psi).

Variables in Model	Number of Parameters	AICc	DeltaAICc	weight	Deviance
Distance	5	387.909895	0	0.99996524	300.43939
Constant	4	410.273386	22.363491	1.39E-05	324.93983
Maximum Temperature	5	410.738315	22.82842	1.10E-05	323.26781
Mean Temperature	5	412.326405	24.41651	4.99E-06	324.8559
Minimum Temperature	5	412.398875	24.48898	4.81E-06	324.92837

Table 1.A6. Ranked models comparing covariates of adult detection probability (p).

Variables in Model	Number of Parameters	AICc	DeltaAICc	weight	Deviance
Cut	5	387.909895	0	0.99937224	300.43939
Plot	18	402.655337	14.7454413	0.00062776	284.52357

Table 1.A7. Ranked models of effects of temperatures on eggs laid per day.

Model	**df**	**logLik**	**QAICc**	**delta**	**weight**
Maximum Temperature + Maximum Temperature ^2	3	-150.6558	61.60589	0	0.325018126
Maximum Temperature	2	-159.5394	62.17040	0.5645089	0.245090249
Mean Temperature	2	-162.8112	63.30743	1.7015413	0.138810586
Minimum Temperature	2	-164.1148	63.82743	2.1545350	0.110676710
Mean Temperature + Mean Temperature ^2	3	-157.0483	64.65783	2.2215360	0.107030403
Minimum Temperature + Minimum Temperature ^2	3	-159.4378	64.65783	3.0519407	0.070662188
Global model	7	-143.9791	71.17847	9.5725820	0.002711739

Table 1.A8. Vital rate estimates under a range of increased maximum temperatures in the absence of predation. The +0 °C column refers to the lowest average maximum temperatures experienced by each life stage measured under field conditions during the 2016-17 warming experiments. Final row shows the annual growth rate estimated (following the population model formula) as the product of egg survival, the larval survival and the fecundity from all three generations.

Vital Rate	**Generation**	**+0 °C**	**+1 °C**	**+2 °C**	**+3 °C**	**+4 °C**	**+5 °C**
Egg Survival (e_1)	First	0.735	0.711	0.685	0.658	0.629	0.599
Larval Survival (l_1)	First	0.203	0.136	0.088	0.056	0.035	0.022
Daily Fecundity (f_1)	First	4.209	5.429	6.392	6.868	6.735	6.028
Adult Lifespan (a)	ALL	11.747	11.747	11.747	11.747	11.747	11.747
Fecundity (af_1)	First	49.445	58.457	58.457	58.457	58.457	58.457
Egg Survival (e_2)	Second	0.601	0.569	0.536	0.502	0.468	0.432
Larval Survival (l_2)	Second	0.297	0.206	0.138	0.090	0.057	0.036
Daily Fecundity (f_2)	Second	6.445	5.511	4.300	3.063	1.991	1.181
Fecundity (af_2)	Second	58.457	58.457	50.519	35.980	23.387	13.874
Egg Survival (e_3)	Third	0.808	0.790	0.770	0.749	0.726	0.701
Larval Survival (l_3)	Third	0.360	0.257	0.176	0.116	0.075	0.047
Daily Fecundity (f_3)	Third	6.614	6.893	6.557	5.693	4.510	3.262
Fecundity (af_3)	Third	58.457	58.457	58.457	58.457	52.986	38.316
Annual Growth Rate	--	1310.598	459.368	104.085	17.690	2.319	0.210

Table 1.A9. Annual growth rate estimates under a range of increased maximum temperatures with larval survival adjusted to incorporate predation as measured by Aschehoug et al. (2015).

Vital Rate	**Generation**	**+0 °C**	**+1 °C**	**+2 °C**	**+3 °C**	**+4 °C**	**+5 °C**
Larval Survival (l_1)	First	0.033	0.022	0.014	0.009	0.006	0.004
Larval Survival (l_2)	Second	0.048	0.033	0.022	0.014	0.009	0.006
Larval Survival (l_3)	Third	0.058	0.042	0.028	0.019	0.012	0.008
Annual Growth Rate	--	5.544	1.943	0.440	0.075	0.010	0.001

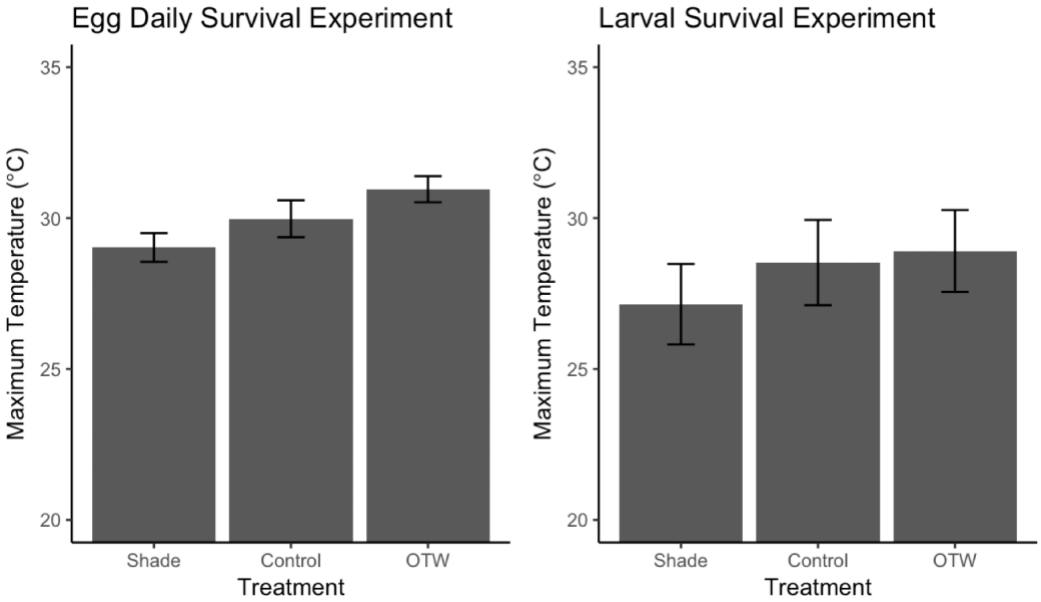

Figure 1.A1. The effect of Open Top Warming (OTW) treatments on maximum temperature was significantly greater than Shade treatments during the egg survival experiments. Error bars represent means ± standard error.

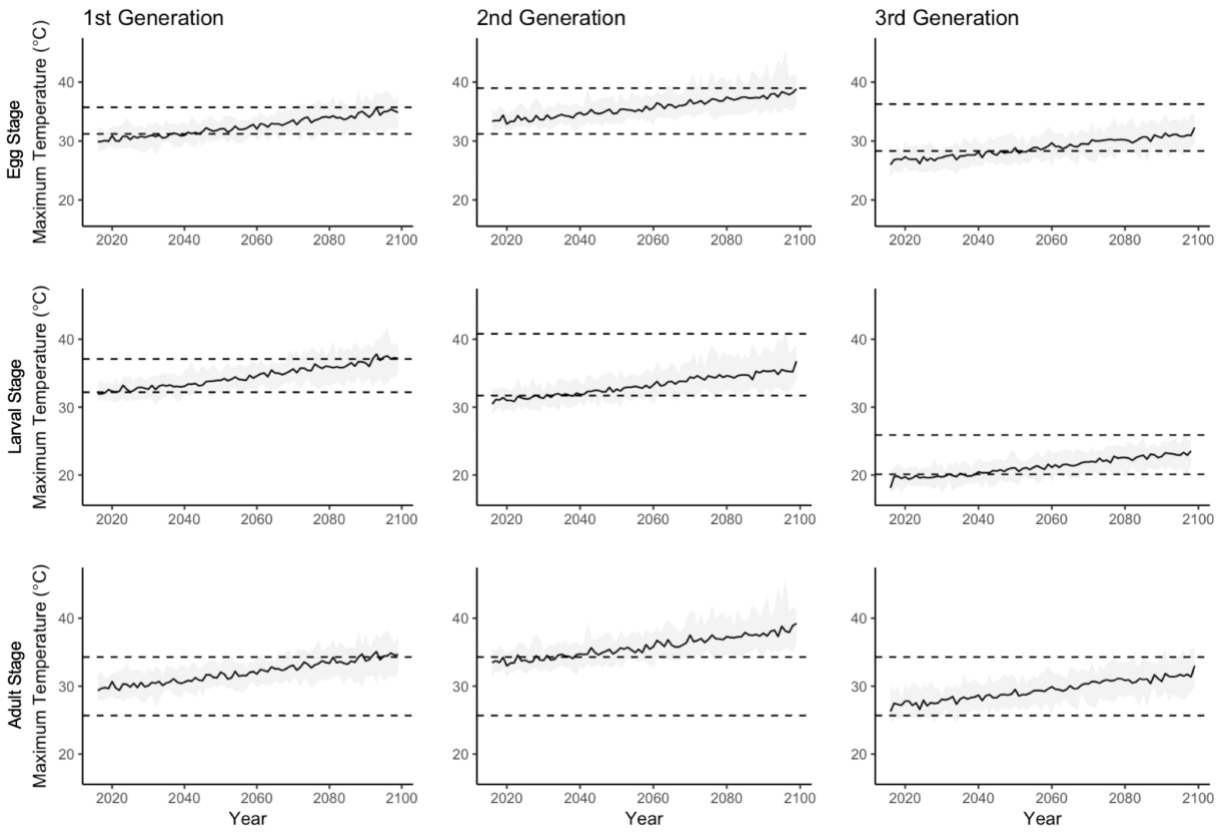

Figure 1.A2. Projected average of maximum temperatures predicted using the MACA downscaled climate dataset by butterfly life stage and generation. Line represents median and shading represents 5th to 95th percentile range estimated from 20 GCMs. Temperatures within the dashed lines were tested during warming experiments. Field temperatures that were recorded using iButtons were converted to the corresponding METDATA values for this comparison. Experimental temperatures during the adult stage correspond to directly to those measured in the fecundity experiment.

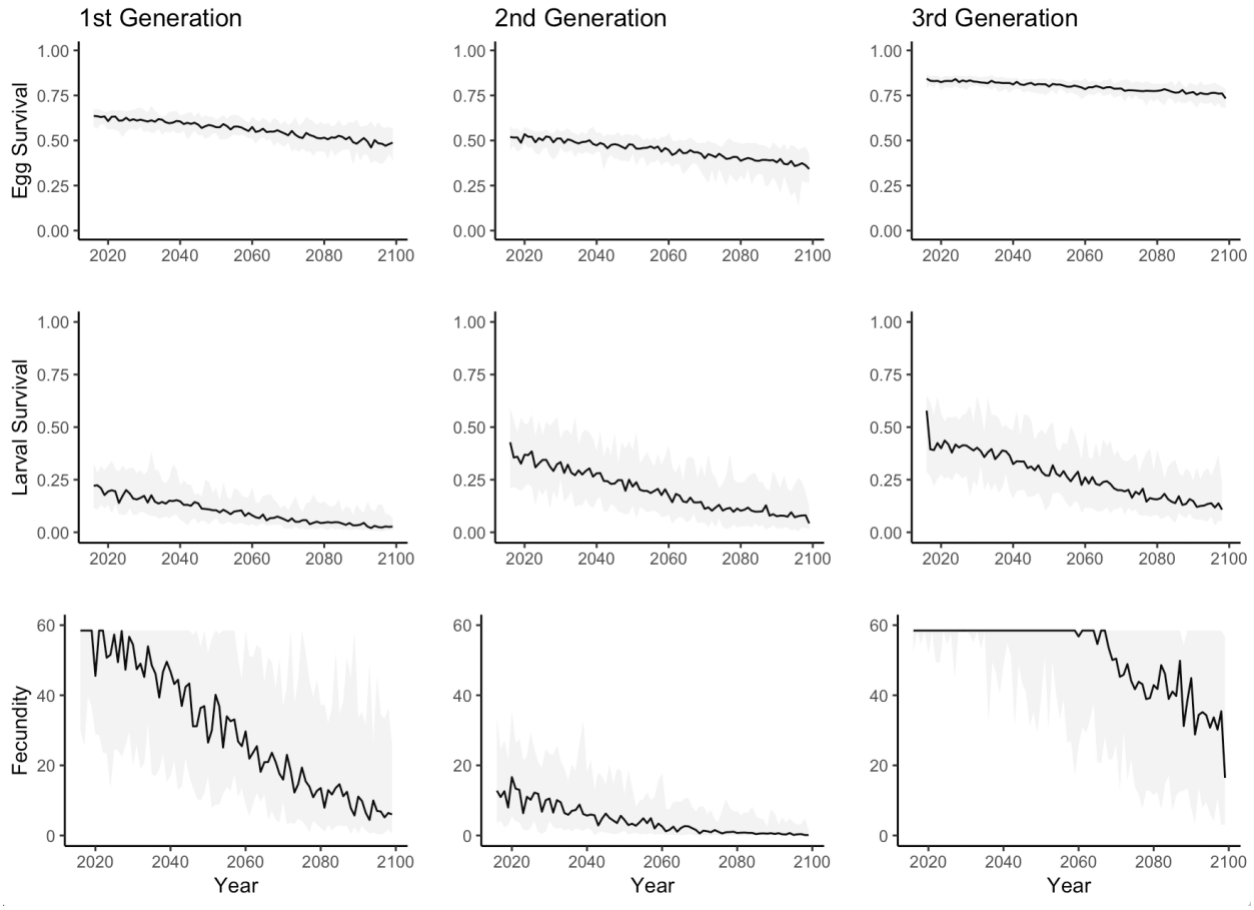

Figure 1.A3. Projected changing vital rates by life stage and generation in response to increasing temperatures over the course of the 21st century. Line represents median and shading represents 5th to 95th percentile range estimated from 20 GCMs.

Appendix 2

Table 2.A1. Critical photoperiod experiment results from generalized linear model (binomial) linking ordinal date and proportion of second generation larvae developing directly into adults. Bolded values indicate p<0.001.

Fixed Effect	Estimate	Standard Error	z value	p
Intercept	49.967	11.892	4.202	**2.65E-05**
Ordinal Date	-0.232	0.055	-4.188	**2.82E-05**

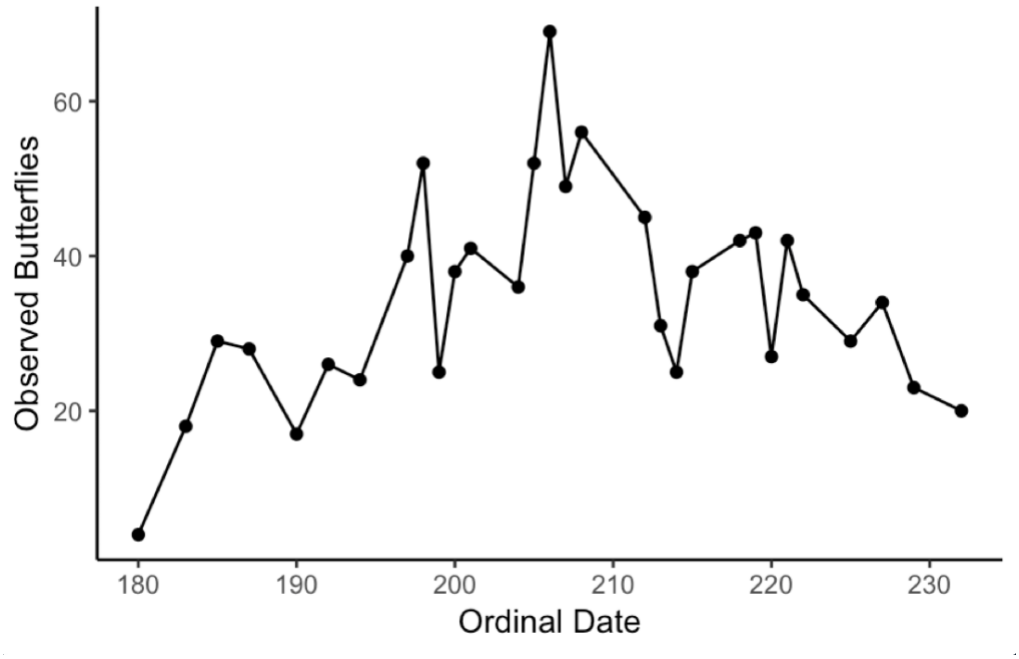

Figure 2.A1. Observed transect counts from surveys (N=1038).

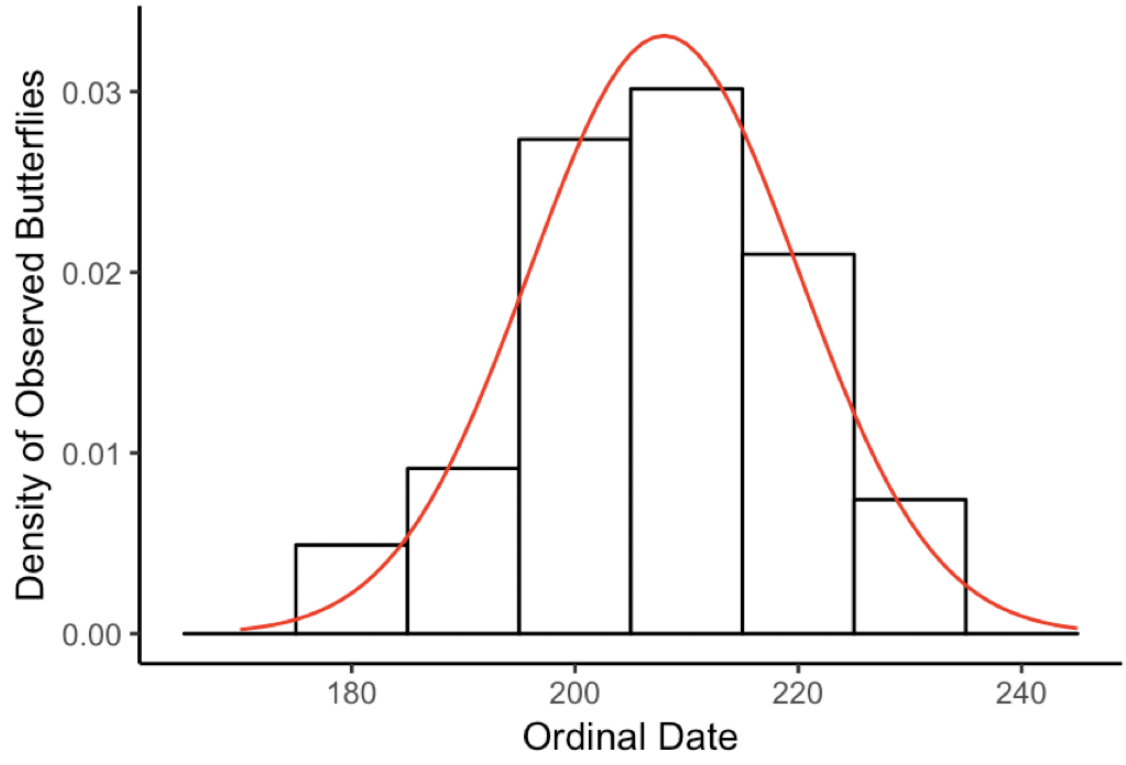

Figure 2.A2. Histogram of second flight period transect counts with fitted normal curve (red line, mean = 207.97, standard deviation = 12.05).

Appendix 3

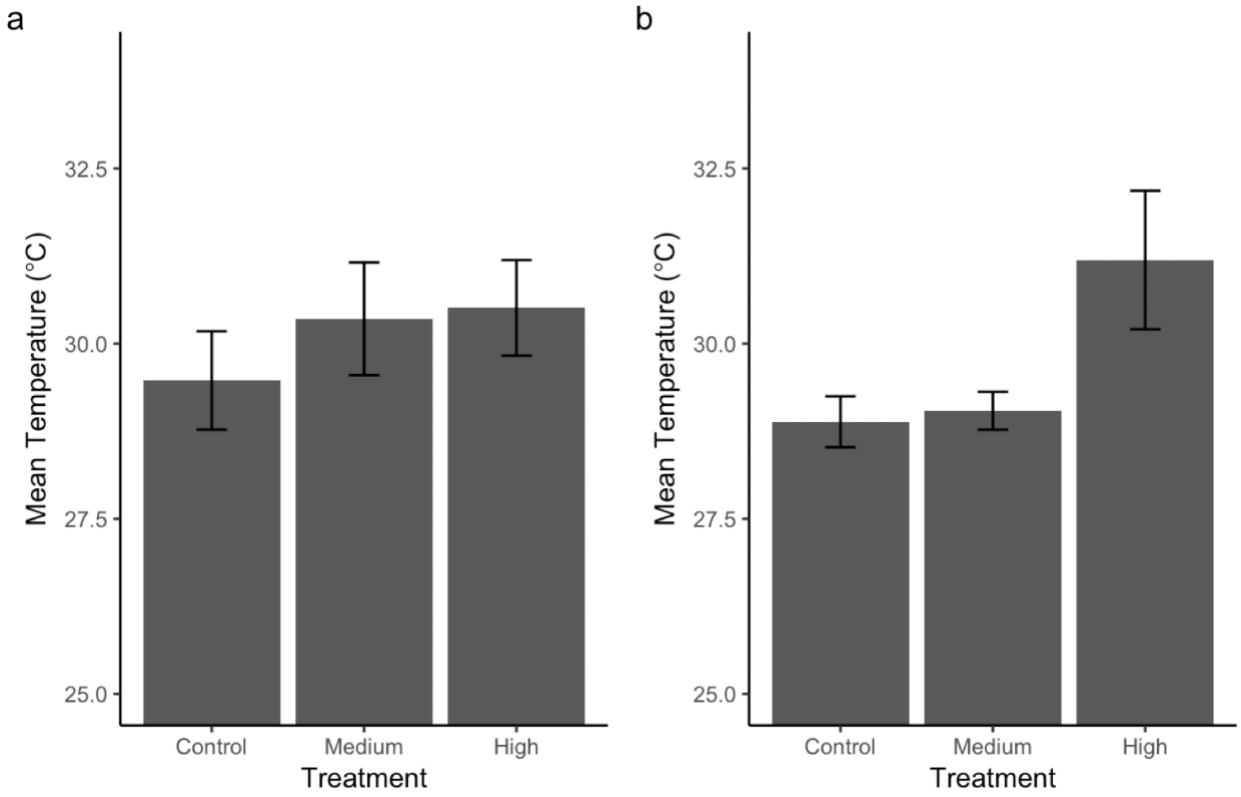

Figure 3.A1. Effect of infrared lamp intensity (treatment) on mean temperatures during the egg (a) and larval (b) range extremes experiments. Error bars represent means ± standard error.

Appendix 4

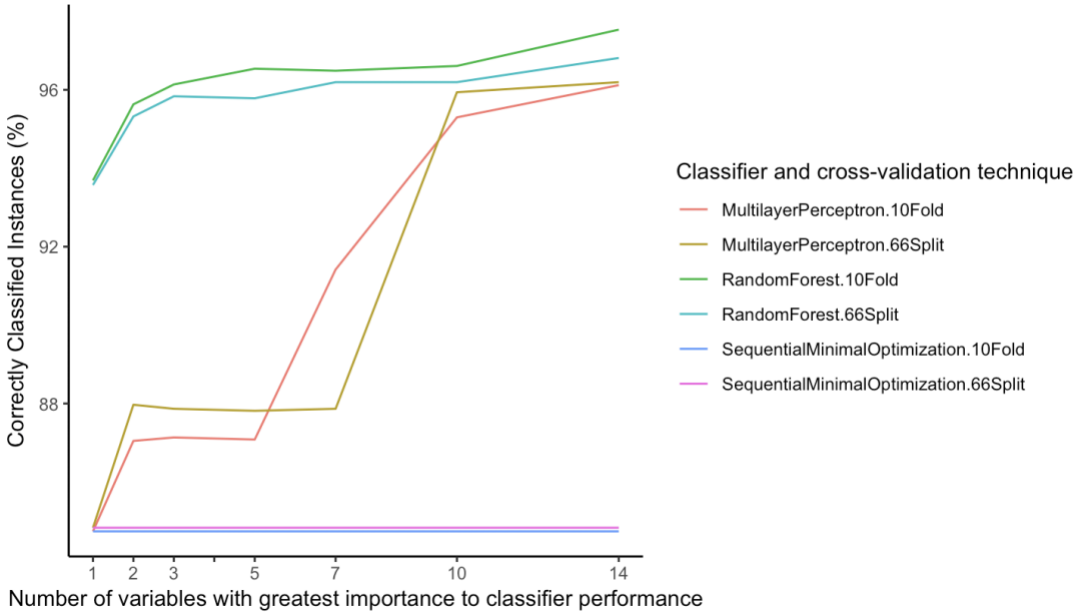

Figure 4.A1. Using up to 14 climate variables to carry out model fitting for 3 classifiers (Sequential Minimal Optimization, Multilayer Perceptron, and Random Forest) using 2 cross-validation techniques (66% Split, 10-Fold).

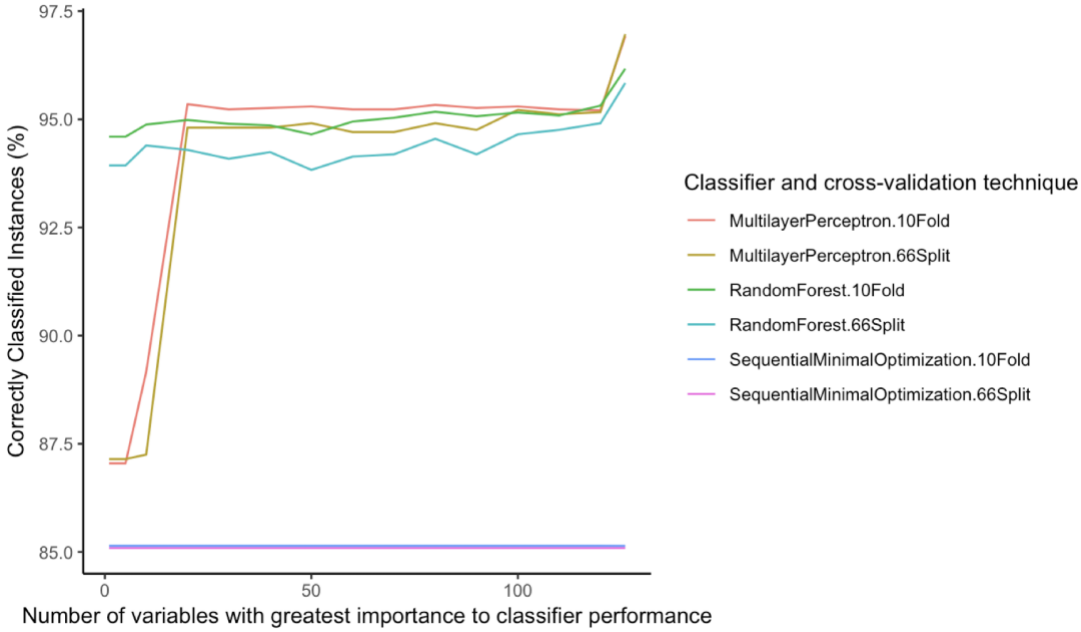

Figure 4.A2. Using up to 121 Growing Degree Day variables to carry out model fitting for 3 classifiers (Sequential Minimal Optimization, Multilayer Perceptron, and Random Forest) using 2 cross-validation techniques (66% Split, 10-Fold).